universität wien

DIPLOMARBEIT / DIPLOMA THESIS

Titel der Diplomarbeit / Title of the Diploma Thesis

„Search for a DNA methylation based biomarker for early diagnosis of late-onset Alzheimer's disease“

verfasst von / submitted by

Alexandra Scheichel

angestrebter akademischer Grad / in partial fulfilment of the requirements for the degree of

Magistra der Naturwissenschaften (Mag. rer. nat.)

Wien, 2016 / Vienna, 2016

Studienkennzahl lt. Studienblatt / degree programme code as it appears on the student record sheet	A 190 423 482
Studienrichtung lt. Studienblatt / degree programme as it appears on the student record sheet	Lehramtsstudium UF Chemie UF Bewegung und Sport
Betreut von / Supervisor	ao. Univ.-Prof. Mag. Dr. Margit Cichna-Markl

ACKNOWLEDGEMENT

My sincere gratitude goes to ao. Univ.-Prof. Mag. Dr. Margit Cichna-Markl, who continuously supervised me before, during and after my laboratory work. Thanks for being constantly supporting, patient and motivating, for an excellent mentoring and for the many things I was able to learn during my thesis.

Secondly, I would like to express my deep thanks to Dipl.-Ing. Melanie Spitzwieser for her patience in explaining and for her support.

I am thankful to Mag. Dr. Ellen Umlauf and Ass.-Prof. Dipl.-Ing. Dr. Maria Zellner, Medical University of Vienna, for providing the samples as well as to Univ.-Prof. Dr. Doris Marko and Univ.-Prof. Dr. Christopher Gerner, University of Vienna, for sharing their laboratory facilities.

I am very thankful to my colleagues for a motivating, critical and cheerful environment and for the extremely affectionate acceptance.

Deep thanks to my father who encouraged me during my whole course of studies and who supports me in every situation in life. Thanks dad!

Last but not least I would like to thank my core family including my deepest friends and my partner for patient listening and for motivating and critical talks.

Special thanks go to my mother for making me the woman I am.

I am thinking of you all the time.

Table of contents

1 INTRODUCTION 1

1.1 ALZHEIMER'S DISEASE 1

1.1.1 Clinical facts about AD 1

1.1.2 Pathophysiology of AD 2

1.1.3 Diagnosis of AD 4

1.2 EPIGENETICS 4

1.2.1 DNA methylation 6

1.3 PRESENILIN 1 9

1.4 ABC TRANSPORTERS 10

1.4.1 ABCA7 10

1.4.2 ABCB1 and ABCC1 11

1.5 LINE-1 11

2 AIM OF THE THESIS 12

3 THEORETICAL BACKGROUND 13

3.1 BISULFITE CONVERSION 13

3.2 POLYMERASE CHAIN REACTION 14

3.2.1 Principle of PCR 15

3.2.2 Temperature profile of PCR 17

3.2.3 Reagents for PCR 18

3.2.4 Touchdown PCR 18

3.3 PYROSEQUENCING 19

3.3.1 Enzymatic cascade 20

3.3.2 Pyrogram 21

3.4 METHYLATION-SENSITIVE HIGH RESOLUTION MELTING ANALYSIS 21

3.4.1 MS-HRM workflow 23

3.5 PRIMER DESIGN 23

3.5.1 Primer design for PCR 24

3.5.2 Primer design for PSQ 25

3.5.3 Primer design for HRM 25

3.6 AGAROSE GEL ELECTROPHORESIS 25

4 EXPERIMENTAL PART 27

4.1 DNA ISOLATION 27

4.2 BISULFITE CONVERSION 28

4.3 PRIMER DESIGN 30

4.4 OPTIMIZATION OF PCR 30

4.5 POLYMERASE CHAIN REACTION FOR PYROSEQUENCING 31

4.6 PYROSEQUENCING 32

4.7 METHYLATION-SENSITIVE HIGH RESOLUTION MELTING ANALYSIS 34

4.8 STATISTICAL CALCULATIONS 36

5 METHOD DEVELOPMENT 37
5.1 PSEN1 37
5.2 ABCA7 42
5.2.1 Primer set 1 43
5.2.2 Primer set 2 47
5.2.3 Primer set 3 52
6 RESULTS AND DISCUSSION 56
6.1 PROBLEMS CONCERNING THE BISULFITE CONVERSION 56
6.2 DETERMINATION OF THE DNA METHYLATION STATUS OF PSEN1 59
6.3 DETERMINATION OF THE DNA METHYLATION STATUS OF ABCA7 62
6.3.1 DNA methylation of ABCA7 analyzed with primer set 1 62
6.3.2 DNA methylation of ABCA7 analyzed with primer set 2 64
6.3.3 DNA methylation of ABCA7 analyzed with primer set 3 65
6.4 DETERMINATION OF THE DNA METHYLATION STATUS OF ABCB1 67
6.5 DETERMINATION OF THE DNA METHYLATION STATUS OF ABCC1 68
6.6 HRM ANALYSIS OF LINE-1 69
6.7 ANALYSIS OF CANCER CELL LINES 73
6.8 DISCUSSION AND CONCLUSION 74
7 APPENDIX 78
7.1 LIST OF UTENSILS 78
7.1.1 Chemicals and kits 78
7.1.2 Consumables 78
7.1.3 Equipment 79
7.1.4 Webservers and databases 79
7.1.5 Software 80
7.2 ABSTRACT 81
7.3 KURZZUSAMMENFASSUNG 82
7.4 LIST OF ABBREVIATIONS 84
7.5 LIST OF TABLES 86
7.6 LIST OF FIGURES 87
7.7 LIST OF EQUATIONS 88
7.8 OVERVIEW OF METHODS 89
7.9 POOLED DNA EXTRACTS FROM AD PATIENTS AND CONTROLS 90
7.10 RAW DATA 92
8 REFERENCES 111

1 Introduction

Alzheimer's disease (AD) is a polygenic, complex and the most common neurodegenerative disorder which inevitably leads to need for long-term care and death. Not only genetic factors are involved in AD but also environmental factors (e.g. nutrition), cerebrovascular dysfunction and epigenetic changes [1].

1.1 Alzheimer's disease

AD is the most common type of age-related dementia. According to the World Alzheimer Report 2015, 46 million people worldwide suffer from dementia [2]. Due to the increasing life expectancy and the ongoing improvement of medical care, the proportion of people high in age grows steadily. Prince *et al.* (2015) predicted that 131.5 million people will suffer from dementia by 2050 [2], most of them (71%) living in developing countries [2, 3]. It is estimated that numbers of patients suffering from AD double every 20 years [1]. This affects not only patients suffering from AD but also the society in terms of a social and economic burden. In 2005 the costs for AD were estimated to be 248 billion dollars a year [3]. Today, the costs are estimated 818 billion dollars worldwide [2].
AD is among the top three causes of death, right behind cardiovascular diseases and cancer [4] and it lasts about 8.5 years from onset of AD (including clinical symptoms) until death [5].

More than 100 years ago, in 1907, the German psychiatrist and neuropathologist Alois Alzheimer described AD for the first time. His 51-year old patient Auguste D. suffered from an "Unusual Illness of the Cerebral Cortex" (German: "eigenartige Erkrankung der Hirnrinde"). This illness went along with progressive cognitive decline and neuropsychiatric dysfunctions. As a consequence, symptoms like disorientation and memory impairment occurred. After her death Alzheimer investigated her brain and found changes in form of plaques and neurofibrillary tangles. From these findings Alzheimer inferred that he had discovered a previously unknown disease [6].

1.1.1 Clinical facts about AD

Different forms of AD exist. First, the patients can be divided in either early or late AD where the threshold value is set at about 65 years. Secondly, patients can be divided in two groups according to putative syndromes, namely early- or late-onset type. One has to consider that there is no sharp distinction between early- (EOAD) and late-onset (LOAD) type [7].

In general, symptoms of AD are [7]:

- Memory impairment present for at least six months
- Decline in other cognitive abilities characterized by deterioration in judgement and thinking
- Preserved awareness of the environment
- Decline in emotional control or motivation or a change in social behavior

The listed symptoms describe dementia. To ensure that the patient does not suffer from another form of dementia, dementia in AD is described, provided that “there is no evidence […] for any other possible cause of dementia (e.g. cerebrovascular disease, Parkinson's disease, Huntington's disease, normal pressure hydrocephalus), a systemic disorder (e.g. hypothyroidism, vitamin B12 or folic acid deficiency, hypercalcemia), or alcohol- or drug-abuse” [7].
Dementia in AD with late onset must occur at the age of 65 or more and meet either an “evidence of a very slow, gradual onset and progression” or a “predominance of memory impairment […] over intellectual impairment” [7].

The greatest risk factor for LOAD is age [3]. Due to progressive neurodegeneration in selected brain regions, memory loss and changes of behavior and personality occur as results and affect the daily life of patients [1]. Orientation, abstract thinking and decision-making are affected by AD, as well as calculating, speaking and writing [8].

AD is a serious health problem because no sufficient treatment is available. The available treatment aims at slowing down disease progression [1].

1.1.2 Pathophysiology of AD

In AD neurons are facing a progressive loss which finally leads to death of neurons. As a consequence, the brain shows typical morphological abnormalities as shown in Figure 1, visible as shrinkage of the brain. Especially the hippocampus, an area that plays a key role in the formation of memories, is affected by this shrinkage.

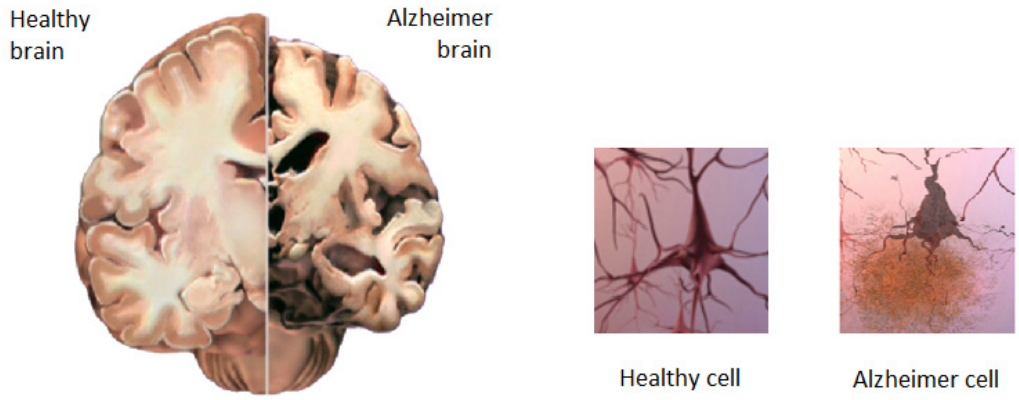

Figure 1: Macroscopical and microscopical changes in AD; modified from [9, 10]

Even if intensive research is ongoing and methods have improved a lot during the last decades, the pathological mechanisms of AD have not been deciphered completely [11].

In 1992 Hardy and Higgins assumed that the generation of neurotoxic amyloid-β-protein (Aβ) by β-secretase and γ-secretase is responsible for the pathophysiology of AD. This includes developing of senile plaques (SP), neurofibrillary tangles (NFT), cell loss, vascular damage and dementia as a consequence of the deposition of Aβ [12]. This theory is still relevant [13] as pathological alterations in AD are still characterized by SP and NFT. SP consist of extracellular - normally soluble - Aβ with a length of either 40 (Aβ40) or 42 (Aβ42) amino acids [14]. The longer Aβ42 enhances the formation of amyloid fibrils from soluble Aβ and is thus more neurotoxic than Aβ40 [15]. Wang *et al.* (2006) and Kim *et al.* (2007) showed that increased levels of Aβ40 might even protect patients from amyloid deposition in brain regions [16, 17].

More than 150 years ago amyloid was defined as a tissue deposit. These deposits could be detected using microscopy. In severe cases they were visible even macroscopically. The occurrence of Aβ is not only related to AD and the brain, but Aβ is present in different organs in various human diseases, for example in type II diabetes [18]. Aβ is produced by proteolysis of amyloid precursor protein (APP) by β-secretase and γ-secretase. The γ-secretase consists of four different integral membrane proteins. Presenilin 1 (PSEN1) is one of the proteins in the γ-secretase complex [19] and is described in detail in section 1.3.

Formation of tau protein, which leads to the second histopathological characteristic of AD, namely NFT, occurs as a result of Aβ imbalance. This imbalance is the result of the discrepancy between Aβ production and Aβ clearance [13].

1.1.3 Diagnosis of AD

Diagnosing AD is one of the major problems scientists are currently struggling with. As long as five years before the onset of dementia, mild cognitive impairment occurs. The likelihood of diagnosing AD correctly in this phase could be raised to above 80% but still no definite diagnosis of AD is possible [20].

Apart from imaging techniques like PET (positron emission tomography), CT (computed tomography) and MRI (magnetic resonance imaging), different psychological tests are used to diagnose AD. The only way to prove that a patient suffered from AD is to examine the brain post mortem [21].

AD research aimed at the discovery of biomarkers but the search is still at the beginning. Especially for LOAD no accurate biomarkers are available [14]. Biomarkers are crucial in case of diagnosis because the pre-clinical stages of AD could be detected, even when no symptoms are apparent. This fact is based on the onset of pathological mechanisms before the occurrence of symptoms. If AD is diagnosed in early stages, preventive strategies can be applied and the progression of the disease can be slowed down. In addition, the establishment of biomarkers gives information about the processes and mechanisms of the disease. This leads to a better understanding and to the development of treatments designated to these special processes and mechanisms. Moreover biomarkers could monitor the success of medical treatment [22].

1.2 Epigenetics

Cells store, retrieve, translate and pass on genetic information. This genetic information is stored in genes which are regions of deoxyribonucleic acid (DNA) and passed on millions of times during a human's life with hardly any changes. DNA consists of a sugar-phosphate backbone and four bases called cytosine (C), adenine (A), guanine (G) and thymine (T). These bases, shown in Figure 2, also occur in ribonucleic acid (RNA) except thymine which is replaced by uracil (U) [23].

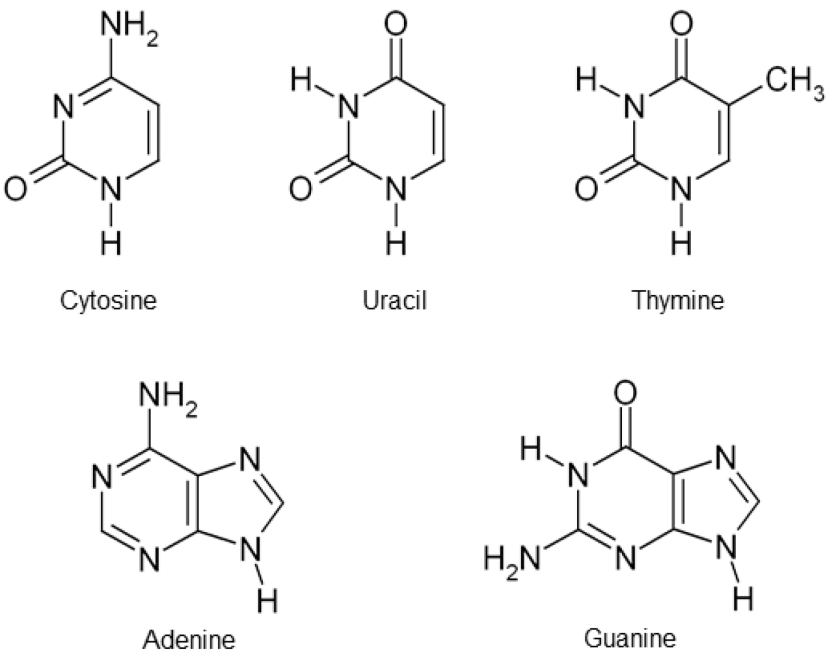

Figure 2: Bases of DNA and RNA; cytosine, uracil, thymine, adenine and guanine

DNA is preserved as a double strand in which the bases pair according to a specific rule [24]: thymine pairs with adenine and cytosine pairs with guanine as shown in Figure 3. This complementary base pairing is characterized by the formation of hydrogen bonds between two bases. A and T form two hydrogen bonds and G and C form three hydrogen bonds [23].

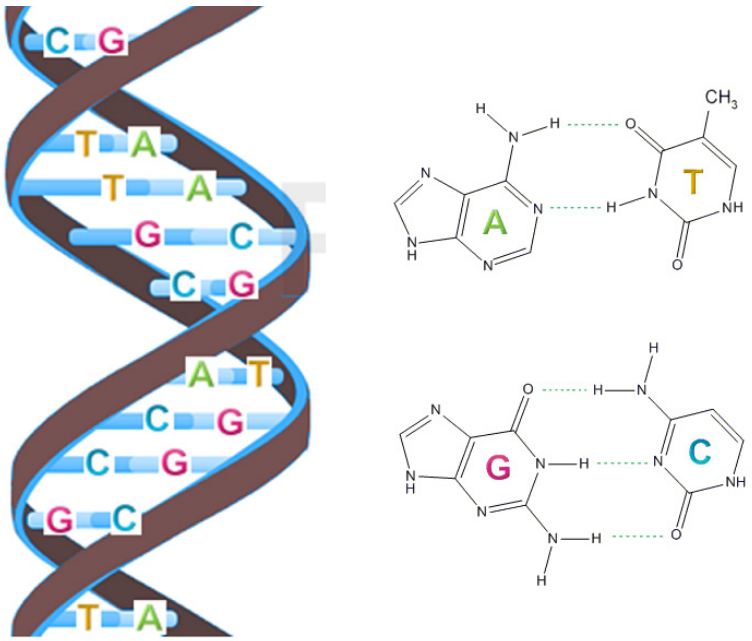

Figure 3: Base pair rules; modified from [25, 26]

The human genome contains not only genetic information - the information to manufacture all proteins indispensable to life - but also epigenetic information, which influences how, where and when proteins are transcribed [27].

In 1942 Conrad Hal Waddington introduced the term epigenetics, literally meaning “above genetics”, for studies of causal mechanisms that underlie developmental processes. This refers to all molecular pathways controlling the expression of a genotype into a particular phenotype [28]. Wu and Morris defined the term epigenetics as “the study of changes in gene function that are mitotically and/or meiotically heritable and that do not entail a change in DNA sequence” [29]. Epigenetic changes especially occur in adulthood because of environmental influences during lifetime [30]. As a result, epigenetics represents the link between inheritance and environmental influences [31].

Epigenetic modifications include histone variants, posttranslational modifications of amino acids on the amino-terminal tail of histones, and covalent modifications of DNA bases. Their impact is not limited to coding regions, but also non-coding sequences can be modified [32].

In 1969 Griffith and Mahler suggested that epigenetic modifications may modulate gene expression [33]. In multi-cellular organisms gene expression of many genes is partly or permanently repressed. Repression occurs for example in tissue-specific and embryonic genes [34].

AD is a polygenic and complex disease in which epigenetic modifications play a key role. Epigenetic modifications stabilize gene expression and may contribute to AD pathology by hypermethylation as well as hypomethylation.
However, epigenetics in AD is still in its infancy and new research has to be done to decipher whether epigenetic modifications are a primary mechanism or occur as a consequence of AD. Epigenetic modifications are a promising field for diagnosis as well as potential pharmacological and dietary treatment because epigenetic modifications are reversible [35]. AD can be a result of accumulation of epigenetic effects throughout life especially when a critical threshold is reached, but also a result of embryonal stages or epigenetic alterations in the parents [36].

1.2.1 DNA methylation

DNA methylation is the most relevant [27] and thus widely studied epigenetic mechanism and is involved in many human diseases including cancer and neurodegenerative disorders like AD [37].

Even if the term epigenetics refers to changes in gene expression (phenotypic changes) which are independent of changes in structural DNA, the sequence still has an impact on how gene expression is influenced by DNA methylation [31].

Methylation of cytosine is the most prevalent modification in mammalian DNA [37]. If cytosine is methylated, this methylation occurs at carbon number five in cytosine-phosphate-guanine (CpG) dinucleotides. CpG means that cytosine is followed by guanine with a linking phosphate [38]. Figure 4 shows the DNA methylation on position five of the pyrimidine ring of cytosine.

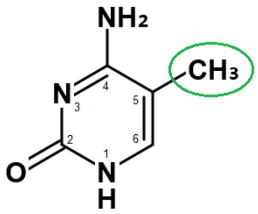

Figure 4: 5-methylcytosine

Methylated cytosine accounts for about 1% of all DNA bases in human somatic cells [39]. Three different DNA methylation states are observed as shown in Figure 5. Most regions are fully methylated (FMR). Within CpG-dense regions (so-called CpG islands) unmethylated regions (UMR) are predominant. Low methylated regions (LMR) occur aloof from UMR. Gene regulatory elements and transcription factor binding sites are frequently found within LMR [31].

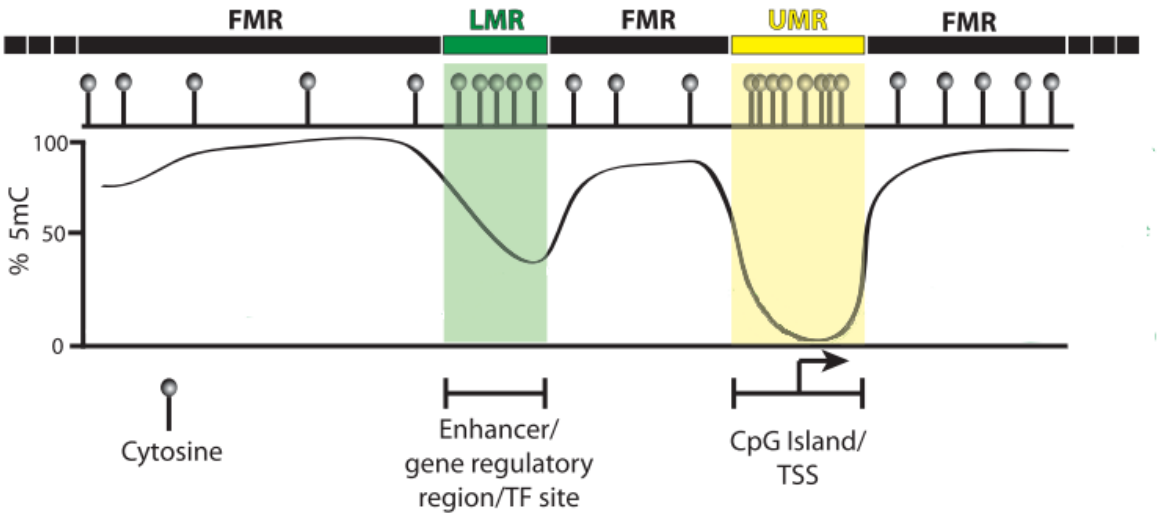

Figure 5: DNA methylation patterns in fully methylated regions (FRM), low methylated regions (LMR) and unmethylated regions (UMR); TF… transcription factor, TSS… transcription start site, 5mC… 5-methylcytosine; modified from [31]

DNA methylation has a regulatory function that is based on changed gene expression [31, 38]. These regulatory effects especially occur if CpG islands (CGIs) are involved. These CGIs often occur in the promoter region of genes [40]. The binding of specific transcription factors may be prevented by methylation of cytosine. As a consequence, gene expression may be repressed by this hypermethylation [27, 41]. Proteins can have specific binding sites, called methyl-CpG-specific binding domains (MBDs), by which transcription can be repressed. The exact function and effects of MBD proteins need to be investigated in detail in further research [31, 38].

It is assumed that DNA methylation stabilizes already silenced genes, but it is not responsible for silencing genes that are actively transcribed [38].

Sado *et al.* (2000) suggested that DNA methylation is important for the maintenance of the inactive state of randomly inactivated X chromosomes [42]. Bradley-Whitman and Lovell (2013) showed that the methylation status of genomic DNA is altered not only in the development of LOAD but also early in the disease progression [43].

1.2.1.1 Mechanism of DNA methylation

Cytosine is methylated by transferring a methyl group from S-adenosylmethionine (SAM) to the carbon five of cytosine by DNA methyltransferases [44]. The mechanism was investigated by Wu and Santi (1987) [45]. DNA methylation states are not irrevocable but can be modified and removed [31].

1.2.1.2 Global and gene-specific DNA methylation

In epigenomics global methylation patterns and also gene-specific methylation patterns can be investigated. The long interspersed nuclear element 1 (LINE-1) is a repetitive element and contains numerous CpGs. Therefore it can be analyzed to examine global methylation patterns (see section 1.5 for details) [46].

In this thesis global methylation was assessed by analyzing LINE-1, whereas gene-specific methylation was determined for the genes encoding presenilin 1 (*PSEN1*; see section 1.3) and various ATP-binding cassette (ABC) transporters (see section 1.4).

1.3 Presenilin 1 (PSEN1)

PSEN1 encodes a protein called presenilin 1 which is, as presenilin 2 (PSEN2), a multi-pass transmembrane protein being part of the gamma secretase complex. The gamma secretase complex is involved in the cleavage of transmembrane proteins, e.g. APP, and thus an important player in the pathophysiology of AD [19, 47]. By proteolysis of APP, Aβ is produced which can accumulate to form SP, one of the histopathological characteristics of AD [19]. PSEN1 is expressed in peripheral tissue (including blood cells) as well as in brain tissue [48] but a difference in protein expression was observed. This difference could lead to different effects on the processing of APP in blood and in the brain [49].

Mutations in *PSEN1* [50] and *PSEN2* [51] are associated with EOAD. Lleó *et al.* (2002) explained about 50% of autosomal dominant EOAD cases by mutations in *PSEN1*. Furthermore they described that mutations in familial and sporadic EOAD cases are rare [52]. So far, more than 160 known mutations in *PSEN1* and *PSEN2* have been detected [53].

Aberrant methylation levels in *PSEN1* led to an altered promoter activity and thus an altered expression of PSEN1 [54]. It is not possible to turn off the gene completely because PSEN1 has an important physiological function and blocking could lead to severe side effects. Wong *et al.* (1997) found a deficiency of PSEN1 being lethal in mice [55]. According to Scarpa *et al.* (2003) a better approach would be the prevention of Aβ overproduction. It is unclear if Aβ accumulates due to a defect in clearance or a defective (over-) production. The reduction of Aβ production would be a mild intervention. Due to downregulation of *PSEN1,* Aβ production could be decreased. This reduction should be achieved by S-adenosylmethionine (SAM) treatment [56]. Fuso *et al.* (2008, 2011) showed that vitamin B deficiency can have an impact on the methylation status of specific CpGs in the *PSEN1* 5'-flanking promoter region. They investigated neuroblastoma cells cultivated on vitamin B deficient medium and found two regions which became demethylated. As a result PSEN1 was expressed in higher amounts. This effect could be reverted by addition of SAM which prevents both DNA demethylation and gene overexpression. Fuso *et al.* (2008, 2011) stated that further investigations are needed to evaluate SAM as a possible approach in LOAD treatment [57, 58].

1.4 ABC transporters

Cells interact with the extracellular milieu by substance exchange via the cell membrane. Cell membranes are selectively permeable for various substances. This permeability is crucial for maintaining special chemical conditions. The importance of selective transport is represented by the fact that proteins that contribute to this machinery are encoded by about 10% of all genes. These include ion channels and facilitators and also active transporters. The largest group of active transporters – 48 transcriptionally active genes exist in the human genome - are the physiologically diverse ABC transporters [59]. Active transporters use energy to move substances against their concentration gradients. The required energy is derived from adenosine triphosphate (ATP) hydrolysis [60]. ABC transporters occur in all cells of all species and consist of two transmembrane domains (TMD) and two nucleotide-binding domains (NBD) [59]. ABC transporters are grouped into seven subfamilies, ranging from A-G. Classification is based on homology in sequence and organization of NBDs. ABC transporters occur in cellular membranes of mammals including plasma membranes and also in intracellular membranes. Many ABC transporters show a substrate specificity and tissue-specific expression [61].

ABC transporters play an important role in multidrug resistance [62] and in lipid transport across membranes. These transport mechanisms were examined in peripheral tissue but the role of ABC transporters in the central nervous system (CNS) has not been understood so far [61].

1.4.1 ABCA7

Genes that are certainly associated with AD are *APP* and *PSEN* in EOAD and apolipoprotein E (*apoE*) in LOAD. Recent genome-wide association studies have shown an association of ATP-binding cassette sub-family A member 7 (ABCA7) with LOAD. ABCA7 is mainly expressed in brain microglia cells [63]. Vasquez *et al.* (2013) suggested a model in which increased expression of ABCA7 reduces the risk of AD. Increased expression of ABCA7 in AD could be a compensatory effect [64]. ABCA7 shows 54% homology (based on amino acid identity) to ATP-binding cassette sub-family A member 1 (ABCA1). ABCA7 plays a major role in phagocytosis of neuronal debris [65] and is involved in the transport of phospholipids and thus could influence Aβ accumulation and lipid metabolism [63, 66].

Satoh *et al.* (2015) showed that a decrease in expression or a loss of function of ABCA7 could result in Aβ accumulation [67]. Karch *et al.* (2012) reported altered expression of ABCA7 in AD patients. Cognitive decline was increased as more ABCA7 was expressed [68]. Yu *et al.* (2015) showed that higher expression of ABCA7 in dorsolateral prefrontal

cortex tissues is associated with tau tangle pathology [69].
Humphries *et al.* (2015) identified differences in the DNA methylation status of *ABCA7* between LOAD and control post mortem human brain samples. A CGI shore was hypomethylated in LOAD patients compared to both healthy controls and disease controls [70].

Further studies are needed to confirm the possible roles of *ABCA7* in AD and to establish new possible treatment schemes [63].

1.4.2 ABCB1 and ABCC1

ABCB1 is an important transporter with a broad specificity for various drugs [71] as well as lipids. Therefore it is characterized as a drug pump and associated with multidrug resistance. Currently, there is no direct evidence for special pathways by which AD could be influenced by ABCB1 [61]. Despite the low expression of ABCB1 in the brain [72] this protein plays a role in the transport across the blood-brain barrier, including Aβ clearance [73, 74]. More studies are needed to confirm and describe suggested pathways related to AD [61] and to develop possible methods for prevention and treatment [61, 75].

The *ABCC1* gene is also associated with multidrug resistance [76]. Krohn *et al.* (2011) showed that Aβ accumulated with a deficiency of ABCC1 in a mouse model for AD. Moreover the activation of *ABCC1* led to reduced Aβ levels [77]. ABCC1, like ABCB1, plays a role in the blood-brain barrier and is expressed in neural stem cells and progenitor cells [78].

1.5 LINE-1

In the human genome less than 5% of the DNA are genes that encode proteins. The genome contains repetitive sequences that sum up to minimum 50% of the whole genome. As passive markers, these repetitive elements can provide useful information for example about mutation and selection [79]. Information is, however, obtained not only about mutation and selection but also about epigenetic modification as about 85% of all CpGs are found in repetitive elements and are hypermethylated and thus these elements are silenced [80].
Long interspersed elements (LINEs) are 6-8 kb (kilo bases) long, repetitive sequences and divided into 3 classes from LINE-1 to LINE-3. LINEs account for about 20% of the human genome and LINE-1 is the major representative with a fraction of approximately 17% [79]. Therefore it can be analyzed to estimate the extent of global DNA methylation [46].

Bollati *et al.* (2011) showed an increased methylation degree in LINE-1 in blood DNA from AD patients compared to a control group [81]. These findings are not in line with Hernández *et al.* (2014) who did not observe any difference in methylation degree of LINE-1 between AD samples and control samples [125].

2 Aim of the thesis

Alzheimer's disease (AD) is a polygenic, complex disease and the most common neurodegenerative disorder. It inevitably leads to need for long-term care and death. Even if methods for diagnosis improved over the past decades, a definite diagnosis is possible only after examination of the brain post mortem.

The aim of the project "Development of a late-onset-Alzheimer´s disease (LOAD) profile for accurate diagnosis and identification of potential therapeutic approaches" [82] is to develop a kit that enables an early diagnosis of LOAD. Furthermore potential therapeutic targets should be identified.

This thesis is part of the project mentioned above. The primary objective is to find potential biomarkers for correct and early diagnosis of LOAD. To test loci for their potential suitability as a biomarker, 39 samples from female patients suffering from AD and 40 samples from healthy female controls should be analyzed. Moreover, nine AD and nine control pooled blood DNA extracts should be analyzed. DNA extracts from whole blood were provided by Mag. Dr. Ellen Umlauf and Ass.-Prof. Dipl.-Ing. Dr. Maria Zellner, Institute of Physiology, Medical University of Vienna.

The DNA extracts should be converted in a bisulfite reaction where unmethylated cytosine is converted into thymine. The converted DNA should then be amplified by polymerase chain reaction (PCR) to obtain a sufficient DNA amount for methylation analysis. Global DNA methylation should be assessed by determining the methylation status of the repetitive long interspersed element number 1 (LINE-1) by methylation-sensitive high resolution melting (MS-HRM) analysis. MS-HRM analysis is based on the different melting behavior of bisulfite treated methylated and unmethylated DNA.
Gene-specific methylation analysis should be performed by pyrosequencing (PSQ) analysis. Methods for the genes presenilin 1 (*PSEN1*) and ATP-binding cassette, subfamily A, member 7 (*ABCA7*) should be developed by finding a target region and designing appropriate primers, followed by optimization of PCR conditions regarding to annealing temperature and primer concentration. Methylation levels of ATP-binding cassette, subfamily B member 1 (*ABCB1*) and ATP-binding cassette, subfamily C, member 1 (*ABCC1*) should be determined using in-house developed methods.

3 Theoretical background

This section gives an overview of the theoretical aspects of the applied methods.

3.1 Bisulfite conversion

In order to be able to determine the DNA methylation status by MS-HRM or pyrosequencing, the DNA has to be treated with bisulfite. After extracting and purifying DNA, the next important step is to differentiate between cytosine and 5-methylcytosine. With bisulfite cytosine is converted to uracil whereas 5-methylcytosine is not affected by this treatment as shown in Figure 6. A heating step is included in the procedure. This step is necessary to denature the DNA because the bisulfite reaction is specific for single stranded DNA. During the first step bisulfite (HSO_3^-) is added to the 5-6 double bond of cytosine. The second step is a hydrolytic deamination which converts cytosine sulfonate into uracil sulfonate. In the last step the sulfonate group is removed from uracil sulfonate by alkali treatment and uracil is obtained [83, 84].

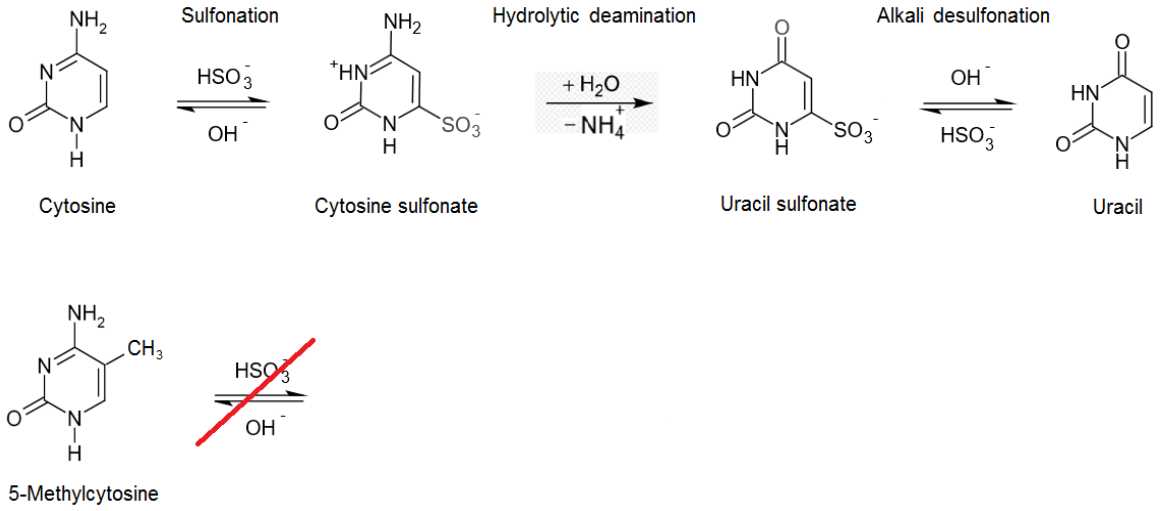

Figure 6: Bisulfite conversion of cytosine and 5-methylcytosine; modified from [83]

In the next step - the polymerase chain reaction (PCR) - only 5-methylcytosine is amplified as cytosine because all cytosines were converted to uracil. Uracil is the demethylated form of thymine and is thus amplified as thymine as shown in Figure 7 [83].

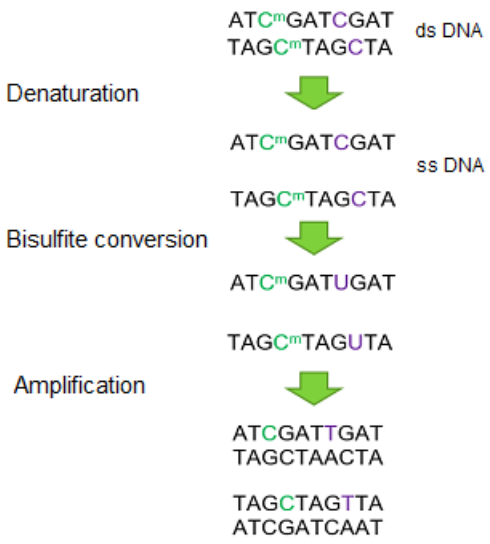

Figure 7: Bisulfite conversion and amplification; ds… double stranded; ss… single stranded; modified from [83]

3.2 Polymerase chain reaction

The polymerase chain reaction (PCR) is a method to amplify, which means copy, DNA *in vitro*. It is used in various settings in molecular biology, cell biology and for example in forensic science. Kary Banks Mullis was awarded the Nobel Prize in Chemistry (1993) for his invention of this technique in 1983. The first publication was released 30 years ago by Saiki *et al.* The scientific interest increased since this time and still many improvements are achieved but the basic principle remained the same [24, 85].

3.2.1 Principle of PCR

The principle of PCR is based on three steps as shown in Figure 8.

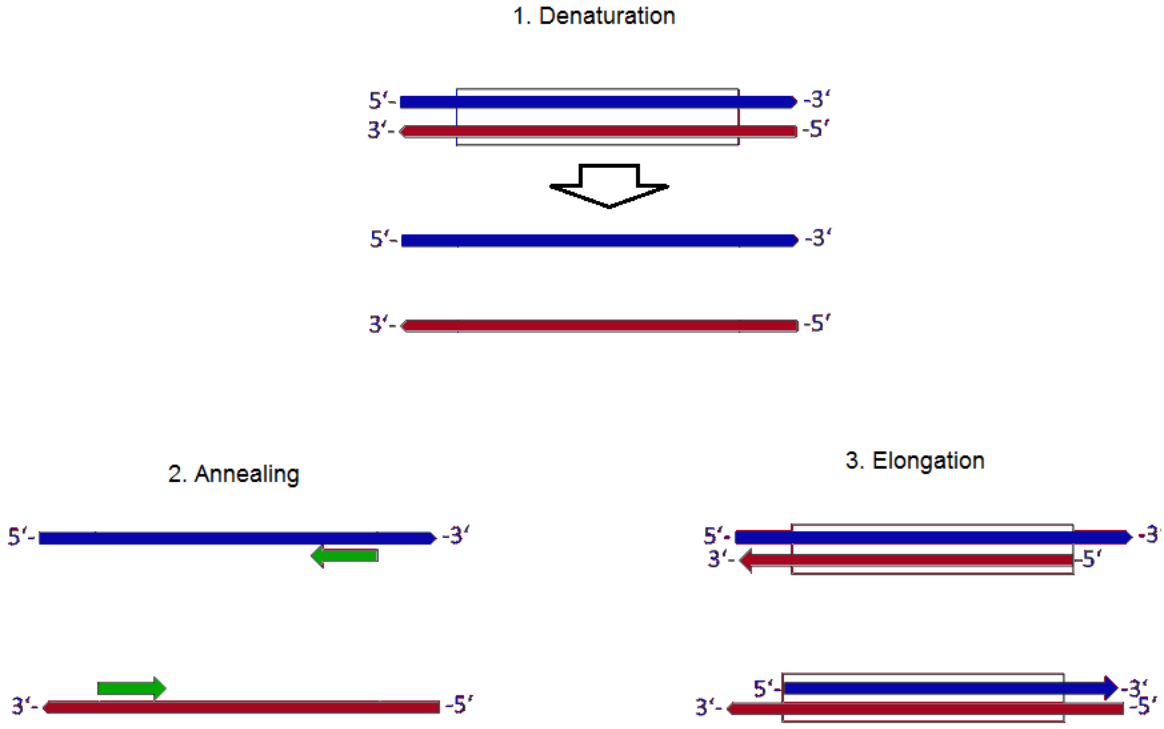

Figure 8: Principle of PCR; DNA strands colored blue and red, primers colored green, target region framed; modified from [85]

- The first step is denaturation, which means separation of double stranded DNA.
- In the next step oligodeoxynucleotides, so-called primers, bind to the single stranded DNA. This process is called annealing [24].

  The polymerase catalyzes the addition of a new nucleotide to an existing 3'-OH group. Therefore a primer which provides this 3'-OH group is needed [85]. Primers define the target region by binding to the complementary bases in the DNA strand.
- In the last step, the so-called elongation, the DNA polymerase extends the complementary strand [24].

These three steps are repeated until the required number of copies is achieved. In theory just one molecule of DNA is sufficient and the number of DNA copies should double after each cycle of PCR which includes denaturation, annealing and elongation. Therefore, the theoretical amplification is 2^n where n is the number of cycles. However, this is just a theoretical approach because in practice less than 2^n copies are obtained. The actual amplification efficiency is about 60-80% and the PCR can be divided into three phases as shown in Figure 9 [24].

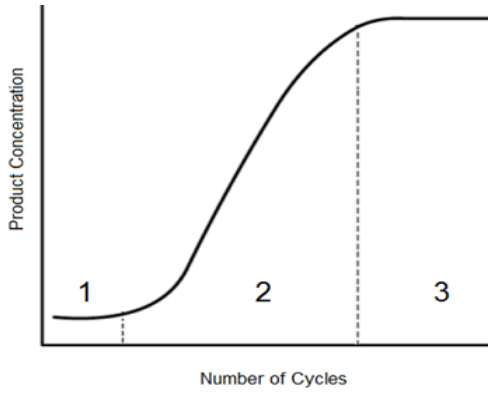

Figure 9: Kinetics of PCR; modified from [24]

In the first phase (1) there is a relatively small amount of DNA and the primers “are searching” for the complementary sequence. In the next phase (2) the accumulation is exponential due to good reaction conditions. In the late cycles (3) the polymerase does not work as efficiently as in the beginning because the number of amplicons exceeds the number of available polymerase molecules or already obtained products inhibit the reaction by re-annealing. Another interfering factor can be the accumulation of non-specific products that serve as alternative templates. This phase is also called plateau phase [24].

Product formation can be observed in real-time if intercalating dyes, for example *EvaGreen,* are used. Intercalating dyes are embedded between the strands of double stranded DNA. In the beginning the fluorescence signal increases slowly although the product formation is almost exponential. The cycle number at which the measured fluorescence signal exceeds the background fluorescence is called the C_T value or threshold cycle value as shown in Figure 10.

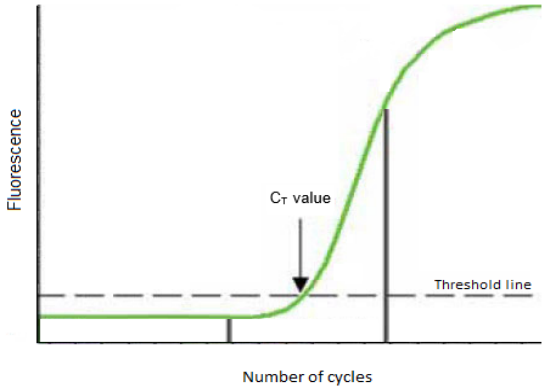

Figure 10: C_T value; modified from [86]

To compare the C_T values of different samples, the same threshold line value must be applied to all samples [87].

3.2.2 Temperature profile of PCR

The temperature profile of PCR is shown in Figure 11.

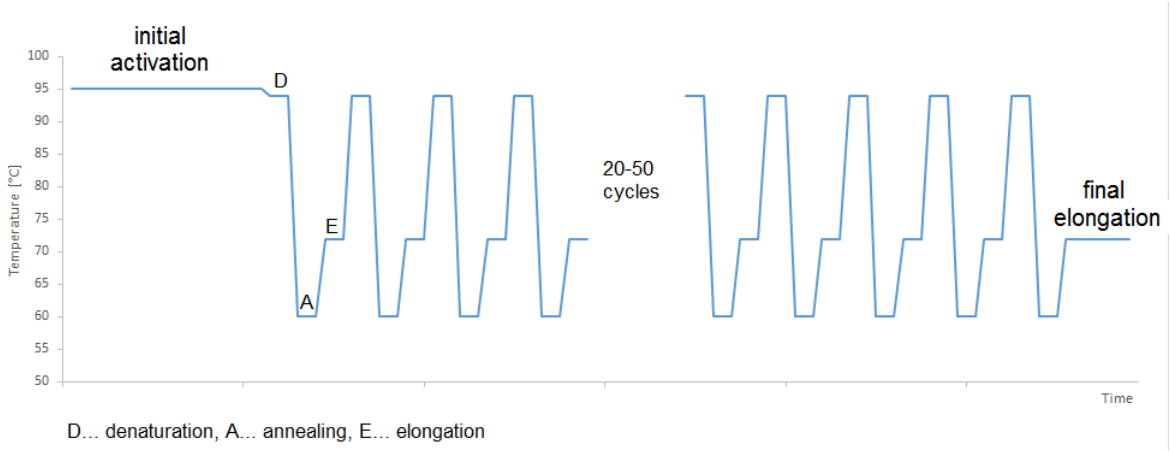

Figure 11: PCR temperature profile; modified from [24]

Denaturation of DNA is achieved by subjecting it to a temperature of 94°C. At 94°C, the hydrogen bonds between the base pairs break and the DNA is separated into two single strands. The initial heating step should be longer than the heating step in the following cycles because the initial DNA template is longer than the amplicons obtained during the following steps and to ensure the activation of the polymerase [85].

After cooling to a special temperature, the so-called annealing temperature (T_a), the primers bind to the complementary sequence. The annealing temperature is primer specific and is about 5°C below the melting temperature (T_m). Typical values for annealing temperatures are between 40°C and 60°C. If T_a is too high annealing cannot take place but if T_a is too low false PCR products could be generated because of mispriming [85].

The DNA polymerase catalyzes the synthesis of the complementary strand by extending the oligodeoxynucleotides until the reaction is stopped by either the end of the DNA strand or by heat. Elongation usually takes place at 72°C. It requires the availability of free nucleoside triphosphates containing deoxyribose (dNTPs) of which the new strand is synthesized.

The DNA polymerase activity decreases with the number of cycles. Therefore the final elongation step should be longer than the elongation step in the previous cycles to ensure complete synthesis of all complementary strands [85].

Even if the principle of PCR seems to be relatively simple, the formation of unspecific side products is not excluded. The probability of formation of primer dimers can be reduced to a minimum by using appropriate algorithms to calculate the risk of dimer formation and possible secondary structures (see section 3.5 for details). Primer design software can be used to calculate the binding probability to the DNA strand. The region for which binding probabilities are calculated is often limited, for example to 10000 bases when using the primer design software *PyroMark Assay Design 2.0* (Qiagen) for a methylation assay.
Thermally stable DNA polymerases start to elongate the DNA strand directly after annealing of the primers even at sub-optimal temperatures (<70°C). If the primers bind to unspecific regions of DNA, elongation of unspecific products can occur during the reaction setup, even when the components are brought together on ice. To avoid the formation of unspecific side products, a modified thermally stable DNA polymerase is used which gains its elongation activity after an initial heating step at 95°C for 5-15 min [85].

3.2.3 Reagents for PCR

Although the replication process is highly complex in a living cell, a PCR reaction needs few components to work in a test tube: a buffer system, a DNA polymerase, deoxynucleotides (dATP, dGTP, dCTP, dTTP) and specific primers [24]. All components are mixed in one test tube and the whole reaction takes place in a thermocycler [85].

Because the DNA polymerase is added just once and passes through all heating steps, a thermally stable polymerase is required. This thermostable polymerase can be derived from the thermophilic bacterium *Thermus aquaticus* and is used in about 90% of all PCRs.

Common buffers contain Cl^- and Mg^{2+} ions because most polymerases need $MgCl_2$ as a metabolic cofactor. Mg^{2+} ions form a soluble complex with the deoxynucleotides which works as substrate for the polymerase. In most commercial kits a separate $MgCl_2$ solution is provided to adjust optimal reaction conditions [85].

The DNA template should be intact and free from inhibitors like EDTA. All components should be pure because little amounts of contaminating DNA could lead to false (positive) results. Therefore, all components should be stored in aliquots [85].

3.2.4 Touchdown PCR

Touchdown PCR is also used for avoiding the mispriming of one or both oligodeoxynucleotides at lower temperatures during the first PCR cycles. This mispriming is crucial especially during the first cycles because shorter misprimed products are favored compared to the longer target product. This effect would multiply in course of the PCR reaction.

The annealing temperature is gradually decreased during the first cycles to ensure optimal binding to the target region and an accumulation of the correct product during the first cycles [88]. A standard protocol for a touchdown PCR would be a gradual decrease of 1°C each cycle over the course of 15 cycles. Therefore the initial annealing temperature should be 14°C higher than the optimal annealing temperature. This protocol can be modified to ensure an optimal touchdown PCR [85, 89].

3.3 Pyrosequencing

Pyrosequencing (PSQ) was invented in Stockholm in the 1990s by Ronaghi and Nyrén as the first real-time DNA sequencing technique without electrophoresis. PSQ is a special kind of DNA sequencing and is based on the first sequencing invention of Sanger *et al.* published in 1977 [90]. PSQ is based on the sequence by synthesis principle which means incorporation of one deoxynucleotide after another [91]. Thus, pyrosequencing allows to determine the methylation status of individual CpGs [92]. The DNA polymerase catalyzes the synthesis of the complementary strand and whenever a deoxynucleotide is incorporated, light is released and detected. PSQ uses an enzymatic reaction cascade to detect the incorporation of a deoxynucleotide [91]. The only drawback compared to Sanger sequencing is the shorter read length because it is limited to a maximum of about 100 [93] to 400 bases [94].

When PSQ is used for methylation analysis, the DNA section of interest must be treated with bisulfite and amplified via PCR. One PCR primer (either forward or reverse) must be biotinylated ([btn]-) at the 5' end to ensure biotin-streptavidin binding. Most commonly the reverse primer is biotinylated but also the inverted way is possible. This is called a "reverse assay" because the ratio of dGTP to dATP-α-S (deoxyadenosine α-thio triphosphate) instead of dCTP to dTTP is used to calculate the methylation status. The nucleotide dATP-α-S is used because dATP would result in false light signals due to a reaction with one of the used enzymes, namely luciferase [91].

The following steps are preparing for the actual PSQ analysis. This preparation includes binding of biotinylated templates to *Streptavidin Sepharose High Performance* beads which are coated with streptavidin. The next step is the denaturation of DNA to obtain single stranded DNA. In the subsequent washing step the DNA strand without biotin is washed away. After obtaining the single stranded PCR product a sequencing primer is annealed and after a heating step for 5 min at 80°C the template DNA is ready for sequencing [92].

3.3.1 Enzymatic cascade

During each cycle of PSQ, solutions (dNTPs, enzyme and substrate) are added in a specific order. The deoxynucleotides are dispensed into the chamber which contains the template DNA and the sequencing primer. The nucleotides dATP-α-S, dCTP, dGTP and dTTP are added in the so-called dispensation order, which is programmed beforehand [92]. The fitting nucleotide is incorporated by the DNA polymerase. To ensure that no "out of phase" sequencing takes place, a polymerase without proofreading activity is used. This means that the polymerase used is lacking an exonuclease activity. As a deoxynucleotide is incorporated, inorganic pyrophosphate (PPi) is released. PPi serves as substrate for ATP sulfurylase. ATP is generated from adenosine 5´ phosphosulfate (APS) by ATP sulfurylase. Oxyluciferin and light are generated as ATP is used by luciferase. In addition to ATP, luciferase also needs D-luciferin and oxygen for synthesizing oxyluciferin and emitting light. The emitted signal is proportional to the number of incorporated nucleotides. Up to three dATP-α-S and up to five dGTPs, dCTPs and dTTPs can be detected because of a linear correlation between the amount of dNTPs and the height of the light signal. One has to consider the limits of this correlation when setting up the assay and even when selecting the target region and designing the primers.

After the light signal has been detected all the remaining nucleotides as well as remaining ATP are hydrolyzed by the fourth enzyme in this luciferase-based enzymatic system, namely apyrase [92]. The whole process of PSQ analysis after PCR amplification including the enzymatic cascade is shown in Figure 12.

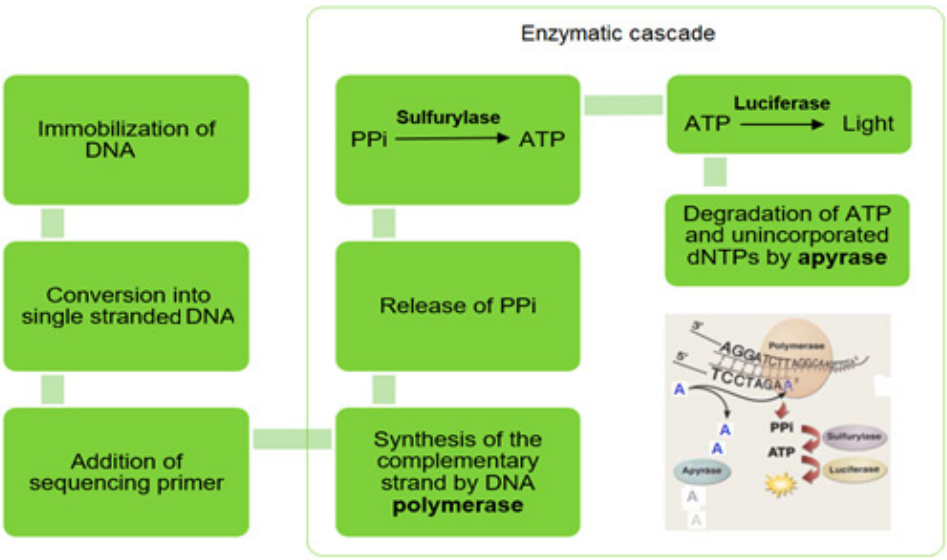

Figure 12: Luciferase-based enzymatic PSQ system; modified from [95, 96]

3.3.2 Pyrogram

A pyrogram is the visualization of the PSQ analysis results. It is compared to the theoretical peak pattern which is shown in the histogram. The calculated DNA methylation status is shown above each variable position, highlighted in grey. Figure 13 shows an example of a pyrogram and the corresponding histogram.

A color code works as an internal control. The values highlighted in blue can be taken without further consideration. Yellow highlighted values can be used but need an accurate inspection. Red highlighted values should be excluded from any further calculations. The position highlighted in orange shows the bisulfite control and is part of every pyrogram in DNA methylation analysis. No C should be incorporated at this position and thus no peak should be visible. The limit of quantification (LOQ) of PSQ is estimated to be 5% (Qiagen). The upper limit of quantification (ULOQ) of PSQ is estimated to be 95% (Qiagen) [97].

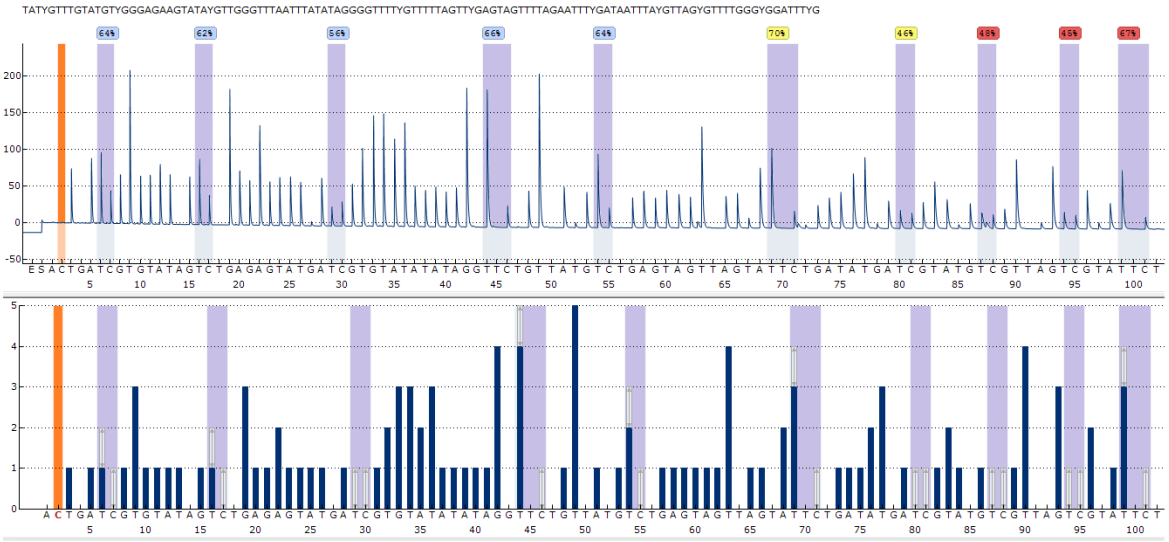

Figure 13: Example of a pyrogram and the corresponding histogram; x-axis shows the dispensation order; y-axis shows the obtained light signal in the pyrogram and the expected light signal in the histogram

3.4 Methylation-sensitive high resolution melting analysis

Methylation-sensitive high resolution melting analysis (MS-HRM) is a technique for DNA methylation analysis of double stranded DNA. It is a highly reproducible and cost effective method that was first introduced in 1997 with the LightCycler. MS-HRM analysis is based on fluorescence measurement [98].

The complementary base pairing of DNA is characterized by the formation of hydrogen bonds between two bases. A and T form two hydrogen bonds and G and C form three

hydrogen bonds. These hydrogen bonds are binding forces between the two DNA strands [23]. As there is a difference in the strength of these binding forces, the bonds between A and T break earlier than the bonds between G and C when DNA is exposed to heat. MS-HRM utilizes bisulfite treatment and PCR amplification of DNA. Due to bisulfite conversion all unmethylated Cs are converted into Ts and thus form two hydrogen bonds instead of three. As a consequence, denaturation of unmethylated DNA occurs at lower temperatures than denaturation of methylated DNA as shown in Figure 14. As a result, different melting profiles are obtained. This fact is used for distinguishing between methylated and unmethylated DNA [99, 100].

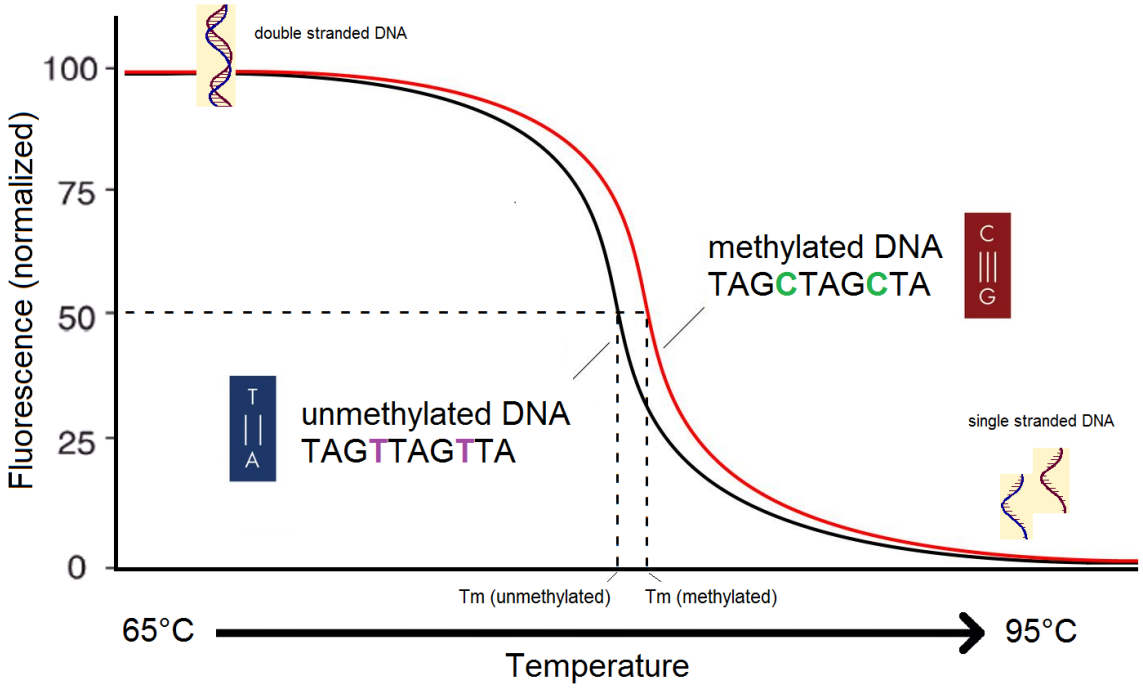

Figure 14: MS-HRM methylation profile of methylated and unmethylated DNA; modified from [98, 99]

MS-HRM analysis is an in-tube method as it is performed directly after the amplification in the PCR tube. Therefore, a dye is needed that does not inhibit the DNA polymerase. This in-tube performance is advantageous because of rapidity and the decreased contamination risk. The major differences compared to PSQ are that one cannot obtain information about the methylation status of a single CpG and standards are needed for quantification. MS-HRM could serve as a first screening method for a region of interest [98, 100].

3.4.1 MS-HRM workflow

After bisulfite treatment and PCR the samples are exposed to a raising temperature gradient of 0,1-1°C/s [98]. If DNA is double stranded, an intercalating fluorescent dye – for example *EvaGreen* in the *EpiTect HRM™ Kit* by Qiagen [101] – binds to the DNA. *EvaGreen* binds equally to CG-rich and AT-rich regions and can be used in higher concentrations compared to *SYBR Green I* [101]. As the temperature rises, the DNA denatures into single stranded DNA, the dye is no longer bound to DNA and thus the fluorescence signal decreases as shown in Figure 14. T_m of a DNA double strand depends on its amount of CG, length and sequence. T_m is defined as the temperature at which 50% of the DNA occurs as a double strand and 50% as a single strand and thus the normalized fluorescence is 50%. The obtained methylation profiles are separated from distracting background, normalized and the first negative derivative is calculated to obtain peaks as shown in Figure 15 [85, 98, 100].

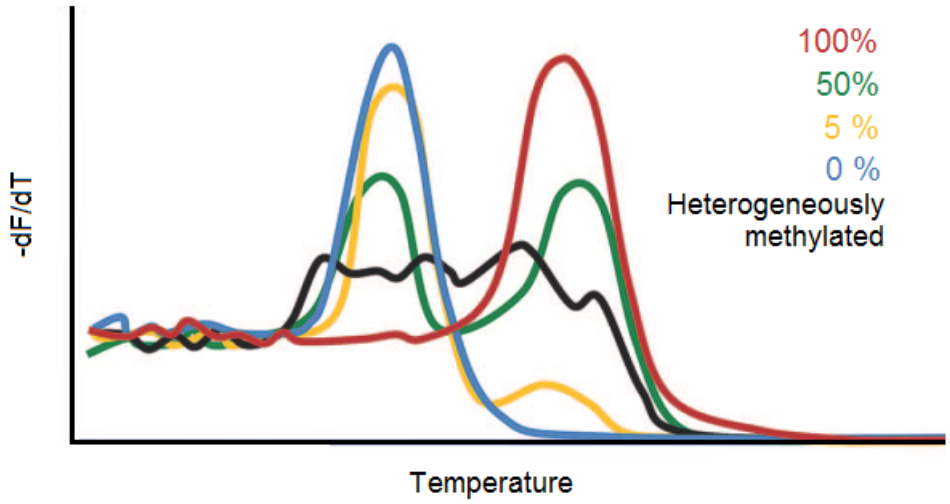

Figure 15: MS-HRM; first negative derivative of the normalized fluorescence over temperature for differently methylated samples; modified from [102]

The methylation status in samples can be obtained by comparison of the methylation profiles obtained for the unknown sample and those of standardized references with different methylation status [98–100].

3.5 Primer design

Primer design is an important step for the functionality of different approaches. Therefore some general rules are recommended to ensure specific binding and optimal performance [24, 85, 100]:

- Ideally the ratio A/T to G/C should be similar

- Secondary structures should be avoided and tested *in silico*
- The difference in T_m of the primers should be less than 1°C
- Homo- and heterodimer formation of the primers should be avoided and checked *in silico*
- Sequence comparison between primers should prevent mispriming especially on the 3' end because this is the starting point for extension of the DNA polymerase
- Primers should not contain more than five equal nucleotides in a row

3.5.1 Primer design for PCR

For PCR two primers are needed; one forward primer (F) and one reverse primer (R). The length should be about 16-28 nucleotides. If the length is too short, annealing temperatures (T_a) are too low and unspecific binding is more likely. On the other hand, if the primer sequence is too long, secondary structures and dimer formation become more likely. Especially the last four nucleotides at the 3' end should not pair as a homo- or heterodimer. The CG content should be between 35% and 65%, leading to optimal efficiency without stable mispriming [24].

The optimal temperature at which the primers bind to the template DNA should be tested for each primer pair. In general, this temperature (T_a) is about 5°C lower than T_m. Different formulas and methods of calculation are available, for example Equation 1, where G, C, A and T are the number of bases in the corresponding primer.

$$T_m = 4 * (G + C) + 2 * (A + T)$$

Equation 1: Standard calculation of T_m; based on [85, 103]

OligoCalc [103] can be used to calculate the salt adjusted melting temperature using Equation 2 for sequences longer than 13 nucleotides, where G, C, A and T are the number of bases in the corresponding primer.

$$T_m = 100.5 + (41 * \frac{G + C}{A + T + G + C} - \frac{820}{A + T + G + C} + 16.6 * log10([Na^+])$$

Equation 2: Salt adjusted T_m calculation; based on [103]

The optimum T_m is about 60°C but a range from 50 to 69°C is possible [104]. The reaction setup should not only be tested for the optimal annealing temperature, but also for the optimum primer concentration. If the concentration is too high, unspecific side

products can be formed. If the concentration is too low, too little product can be obtained for further analysis [85].
The optimum amplicon size is smaller than 250 bp because longer amplicons lead to a decrease in PCR efficiency [24].

3.5.2 Primer design for PSQ

One PCR primer has to be labeled with biotin at the 5' end to allow streptavidin-biotin binding. Primers for PCR should not contain any CpGs to avoid PCR bias [92]. The amplicon obtained by PCR should be 100-200 bp long. Nevertheless fragments up to 300-500 bp can be amplified [104].

For PSQ one additional primer, namely the sequencing primer (S), is needed. The sequencing primer should be close to the target region. It should be complementary to the amplicon (to the biotin-labeled strand) at only one position. Sequencing primers should be 16-24 bp long [92].

3.5.3 Primer design for HRM

For MS-HRM, as for PCR, two primers are needed; one forward primer and one reverse primer. The optimum length of the amplicon is around 100 bp.
One or more Ts (former non-CpG Cs) can be incorporated at the 3' end of the primer to ensure that only bisulfite converted DNA is amplified [100].
PCR bias, the preferred amplification of either methylated or unmethylated DNA, has to be considered when designing primers [83, 100, 105].

3.6 Agarose gel electrophoresis

Agarose gel electrophoresis is a simple method to separate and identify DNA fragments between 0.1 kb and 25 kb in length. The amount of agarose and thus the agarose concentration in the gel depends on the expected length of the DNA fragments [106].
The separation of DNA fragments is based on the fact that the sugar-phosphate backbone of DNA is negatively charged and therefore DNA migrates when an electric field is applied. When the electric current is applied, the negatively charged DNA migrates toward the positively charged anode. The value of mobility depends on the molecular weight and therefore the length of a DNA fragment [107]. By comparison of the samples with a molecular size marker, a so-called DNA ladder, the size of the product can be estimated. A DNA ladder contains standards to identify the size of the DNA samples. The DNA ladder shown in Figure 16 is suitable for sizing samples from 25 bp to 500 bp [106].

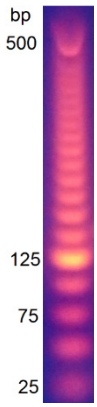

Figure 16: 25 bp DNA ladder

4 Experimental part

Methylation levels of *PSEN1*, *ABCA7*, *ABCB1 and ABCC1* were determined by PSQ whereas LINE-1 methylation status was analyzed using MS-HRM analysis.

Figure 17 summarizes the workflow for methylation analysis using PCR and either PSQ or MS-HRM analysis.

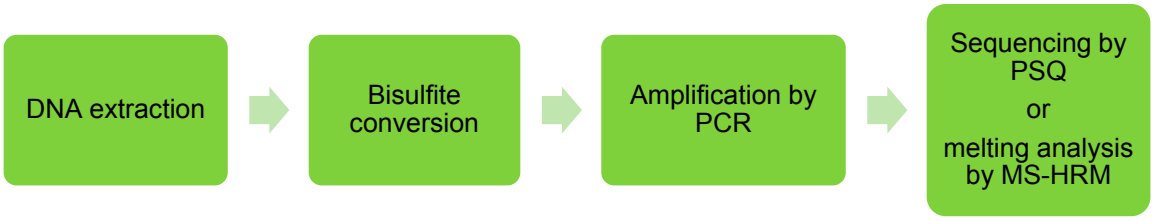

Figure 17: Summary of PSQ and MS-HRM workflow

As handling with DNA always goes hand-in-hand with contamination risk, all surfaces were cleaned using decontamination solution *DNA-Exitus Plus™ IF* (AppliChem). Moreover, the reaction setup was divided in parts handling with and without DNA. All master mixes were pipetted in workstation A. Adding of DNA to a master mix was performed in workstation B (in a different room) to avoid contamination. All tubes containing amplicons were stored and opened in rooms where no other reagents were stored to avoid contamination.

4.1 DNA isolation

The isolation of DNA from blood samples was performed by Mag. Dr. Ellen Umlauf, Institute of Physiology, Medical University of Vienna.

Blood samples were collected from patients suffering from Alzheimer's disease (AD) and healthy controls. DNA was isolated with a column-based *PerfectPure DNA Blood Kit 0.4 ml* (5prime). DNA was checked for purity and concentration was determined using a *NanoDrop* (Thermo Scientific) spectrophotometer and diluted by adding RNase-free water to obtain a concentration of 500 ng / 40 µL (12.5 ng/µL).

Blood DNA extracts from 39 AD patients and 40 healthy controls were analyzed. Moreover, the DNA methylation levels of nine pooled DNA extracts from AD patients and nine pooled DNA extracts from controls were analyzed.

Pools were prepared by Mag. Dr. Ellen Umlauf using equal amounts of DNA from either AD patients or controls to obtain a final concentration of 500 ng / 40 µL (12.5 ng/µL). Nine

pools of AD DNA extracts were prepared by mixing individual extracts from 10 AD patients for each pool. Eight of nine pools of DNA extracts from controls were obtained by mixing DNA extracts from 10 individual control persons whereas pool nine contained DNA from six control persons. Pooled DNA extracts from AD patients and controls were matched according to the age of the patients. A detailed list of the compositions of each pool is given in section 7.9.

4.2 Bisulfite conversion

CpGenome universal methylated DNA (c=100 ng/µL, Millipore), *EpiTect human unmethylated control DNA* (c=50 ng/µL, Qiagen) and DNA extracts (individual and pooled ones; c=12.5 ng/µL) were converted using the *EpiTect Fast DNA Bisulfite Kit* (Qiagen) according to the manufacturer's protocol [109]. The centrifuge 5424 (Eppendorf) was used for all centrifugation steps.

The bisulfite conversion procedure is shown in Figure 18. The bisulfite reaction was carried out at room temperature and the reaction was set up in 200 µL PCR tubes according to Table 1.

Table 1: Bisulfite reaction setup; modified from [109]

Component	**High concentration samples (1 ng – 2 µg) Volume per reaction [µL]**	**Low concentration samples (1-500 ng) Volume per reaction [µL]**
DNA	X (maximum 20 µL)	Y (maximum 40 µL)
RNase-free water	20-X	40-Y
Bisulfite Solution	85	85
DNA Protect Buffer	35	15
Total volume	140	140

The components were added in the order given by the producer to achieve repeatable results.

The PCR tube was placed in the *Rotor-Gene Q* thermocycler (Qiagen) and the temperature program given in Table 2 was applied.

Table 2: Temperature program for bisulfite reaction; modified from [109]

Step	Time [min]	Temperature [°C]
Denaturation	5	95
Incubation	10	60
Denaturation	5	95
Incubation	10	60
Hold	1	25

After the bisulfite reaction the PCR tube was centrifuged briefly (up to about 2000 rpm) and the solution was transferred to a clean 1.5 mL tube. 310 µL *Buffer BL* were added and the tube was vortexed for 5 s and centrifuged briefly (up to about 5000 rpm). 250 µL ethanol (96%) were added and the tube was vortexed (pulse vortexing, 15 s) and centrifuged briefly (up to about 2000 rpm). The solution including the denatured DNA pellet was transferred into a *MinElute DNA spin column* which was placed in a collection tube. The column was centrifuged for 1 min at 14000 rpm, the flow-through was discarded and 500 µL *Buffer BW* were added. The column was centrifuged for 1 min at 14000 rpm, the flow-through was discarded and 500 µL *Buffer BD* were added. *Buffer BD* was stored at 4°C and the lid was closed as fast as possible to prevent *Buffer BD* from acidification. The mixture was incubated for 15 min at room temperature. The column was centrifuged for 1 min at 14000 rpm, the flow-through was discarded and 500 µL *Buffer BW* were added. The column was centrifuged for 1 min at 14000 rpm, the flow-through was discarded and again 500 µL *Buffer BW* were added. The column was centrifuged for 1 min at 14000 rpm and the flow-through was discarded. After adding 250 µL ethanol (96%) the column was centrifuged for 1 min at 14000 rpm and the flow-through was discarded. The column was placed into a new 2 mL collection tube and centrifuged for 1 min at 14000 rpm. The mixture was incubated at 60°C for 5 min with open lid and the column was placed into a clean 1.5 mL tube afterwards. 15 µL *Buffer EB* were added directly onto the center of the column and the mixture was incubated for 1 min at room temperature. The column was centrifuged for 1 min at 12000 rpm.

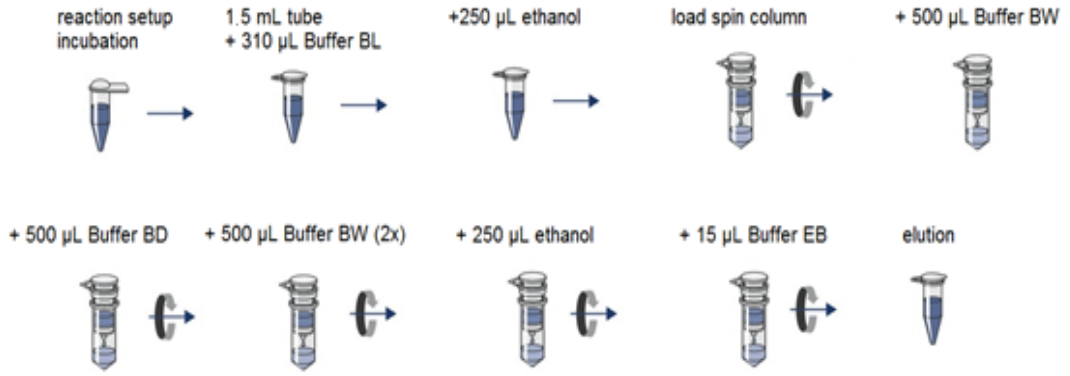

Figure 18: Bisufite reaction procedure; modified from [110]

A final DNA concentration of 5 ng/µL was adjusted by adding RNase-free water. Bisulfite treated DNA was aliquoted in 9 µL and stored at -20°C until further analysis.

4.3 Primer design

Primers for *PSEN1* and *ABCA7* were designed using the *PyroMark Assay Design Software 2.0* (Qiagen). Various settings were tested to obtain primers in compliance with the rules for primer design as described in section 3.5. The software listed primer sets according to their fitting to the settings. Primer sets with the highest score were tested for secondary structures using *RNAfold* [111], for their differences in T_m using *OligoCalc* [103] and for the formation of hetero- and homodimers using *OligoAnalyzer* [112].

4.4 Optimization of PCR

PCR methods were optimized using four different annealing temperatures and two different primer concentrations, namely 0.2 µM and 0.4 µM. Bisulfite converted *CpGenome universal methylated DNA* (Millipore), bisulfite converted *EpiTect human unmethylated control DNA* (Qiagen) and RNase free water as no template control (NTC) were amplified using the *iQ 5 Cycler* (Bio-Rad) thermal cycler to apply a temperature gradient.

Afterwards the PCR products were analyzed using agarose gel electrophoresis. Gel electrophoresis was performed using a two percent agarose gel matrix. 2 g agarose were diluted and heated in a TAE (tris-acetate-EDTA) buffer solution and stained with the fluorescent nucleic acid gel dye *GelRed* (Biotium). Then the solution was casted in the *Wide Mini-Sub Cell GT Cell* (Bio-Rad) electrophoresis unit with a well comb to create wells for adding the samples. After cooling of the agarose and thus solidifying, the *Wide Mini-Sub Cell GT Cell* was filled with TAE buffer. The wells were loaded with a *25 bp DNA*

ladder (Thermo Fisher Scientific) including a *DNA Electrophoresis Sample Loading Dye* (Bio-Rad) and the amplicons. An electric potential of 80 V was applied via a power supply. The final step was to visualize the separated fragments under UV light using the *Transilluminator UVT-20 M* (Herolab) and compare the bands to the DNA ladder.

Annealing temperatures and primer concentrations resulting in the highest amount of specific product and the lowest amount of unspecific products were considered as optimal.

4.5 Polymerase chain reaction for pyrosequencing

A commercial kit, *PyroMark PCR Kit* (Qiagen), was used. Reagents used for PCR were a *PyroMark PCR Master Mix, 2x* (Qiagen; component of the kit; containing *HotStarTaq DNA Polymerase*, 3 mM $MgCl_2$ and dNTPs), *CoralLoad* concentrate (Qiagen; component of the kit) as a dye, RNase-free water and a forward and reverse primer synthesized by Sigma-Aldrich. One primer was biotinylated at its 5' end for PSQ analysis. Section 7.8 lists the primers used. All reagents were stored at -20°C until use.

PCR was performed according to the manufacturer's protocol (Qiagen) [114]. All required reagents were thawed but the reaction was set up on ice. To avoid contamination, the PCR reaction setup was performed in three different rooms using two workstations A and B (Peqlab). In workstation A all reagents (except DNA) were mixed thoroughly and set up according to Table 3. The lyophilized primers were dissolved and diluted to a concentration of 10 µM using RNase-free water and stored in 9 µL aliquots at -20°C for re-use. The master mix was prepared for DNA extracts, a no template control (NTC) and typically two tolerance samples. The master mix was vortexed briefly (about 5 s) and pipetted in 200 µL PCR tubes (Qiagen) or 200 µL PCR strip tubes (Thermo Fisher Scientific) depending on the thermocycler used for amplification.

Table 3: General scheme for PCR reaction setup; modified from [114]

Component	Volume per reaction [µL]	Final concentration
PyroMark PCR Master Mix, 2x	12.5	1x
CoralLoad concentrate, 10x	2.5	1x
Forward primer (initial concentration 10 µM)	0.5/1*	0.2 µM/0.4 µM*
Reverse primer (initial concentration 10 µM)	0.5/1*	0.2 µM/0.4 µM*
RNase-free water	8/6*	
Template DNA	2 (c=5 ng/µL)	10 ng in 25 µL
Total volume	25	

* depending on the optimal PCR conditions

In workstation B the DNA or respectively RNase-free water for the NTC was added. The DNA extract was mixed with the master mix by gently pipetting up and down.
A thermal cycler, either *Rotor-Gene Q* (Qiagen) or *iQ 5 Cycler* (Bio-Rad), was programmed according to Table 4 and the cycling program was started.

Table 4: PCR temperature program; modified from [114]

Step	Time	Temperature [°C]	
Activation	15 min	95	
Denaturation	30 s	94	3 step cycling
Annealing	30 s	X*	
Extension	30 s	72	
Final extension	10 min	72	
Number of cycles	50		

* Annealing temperature depended on the analyzed region

Amplicons were either used directly for PSQ analysis or stored at –20°C until use.

4.6 Pyrosequencing

PSQ was performed according to the manufacturer's protocol using the *PyroMark Q24 Advanced CpG Reagents* (Qiagen) [97] and *Streptavidin Sepharose High Performance* beads (GE Healthcare). The assays were designed using the *PyroMark Q24 Advanced 3.0.0 Software* (Qiagen) as described in detail for each analyzed region in section 5.

The *PyroMark Q24 Advanced instrument* (Qiagen) was switched on at least 30 min before starting PSQ analysis. A heating block (*Thermomixer comfort*, Eppendorf) was pre-heated to 80°C, the *PyroMark Q24 Plate Holder* (Qiagen) was placed on it and the *PyroMark Q24*

Vacuum Workstation (Qiagen) was prepared as follows: the vacuum tool was tested and washed by flushing with about 70 mL *Milli-Q* water and dried by raising the tool to beyond 90° vertical for 5 s.

In workstation A a master mix was prepared according to Table 5, briefly vortexed for about 5 s and pipetted into a 24-well PCR plate. The lyophilized sequencing primer was dissolved and diluted to a concentration of 10 µM using *Milli-Q* water and briefly vortexed for about 5 s. It was further diluted to 0.375 µM with *PyroMark Advanced Annealing Buffer* (Qiagen) and again briefly vortexed. The master mix and the primer were prepared for the DNA immobilization reaction including two tolerance samples.

Table 5: PSQ reaction setup; modified from [97]

Component	**Volume per reaction [µL]**
Streptavidin *Sepharose High Performance*	1
Milli-Q water	24
PyroMark Binding Buffer	40
Total volume	65

The *PyroMark Q24 Cartridge* (Qiagen) was also loaded in workstation A. Enzyme and substrate mixtures of the *PyroMark Q24 Advanced CpG Reagents* were dissolved in 660 µL *Milli-Q* water and mixed by swirling (not by vortexing).
The nucleotide solutions provided in the *PyroMark Q24 Advanced CpG Reagents* were vortexed briefly for about 5 s and the cartridge was loaded according to the pre run information obtained by the *PyroMark Q24 Advanced 3.0.0 Software*. The cartridge was placed in the *PyroMark Q24 Advanced Instrument*.

15 µL of the biotinylated PCR product were pipetted to the master mix. The components were mixed by sealing the plate with adhesive foil and agitating for 7-10 min at 1400 rpm at room temperature. Meanwhile 20 µL of the sequencing primer were added to each well of a *PyroMark Q24 Plate*.
After shaking the plate containing the master mix and the biotinylated PCR product, the foil was removed carefully but quickly and the plate was placed on the vacuum workstation. The vacuum was switched on and the filter probes were lowered into the PCR plate to capture the *Streptavidin Sepharose High Performance* beads containing the immobilized template. The vacuum tool was hold in place for 15 s. The vacuum tool was transferred to a trough containing 70% ethanol for 5 s, to a trough containing *Denaturation Solution* for 5 s, to a trough containing *Wash Buffer* for 10 s and was dried for 5 s by raising the tool to beyond 90° vertical. Finally, the vacuum was switched off while holding the tool over the *PyroMark Q24 Plate* and the filter probes were lowered into the

sequencing primer and slewed gently. The *PyroMark Q24 Plate* was placed on the pre-warmed *PyroMark Q24 Plate Holder* for 5 min at 80°C.
After incubation the plate was placed on the heating block of the *PyroMark Q24 Advanced instrument* and the PSQ analysis was started.

After the run had finished, the results were analyzed using *PyroMark Q24 Advanced 3.0.0 Software* and exported to *Excel* (Microsoft)*, SPSS 21* (IBM) and *SigmaPlot 11* (Systat) for calculations. Red highlighted values in the pyrogram were excluded from any further computation. All statistic calculations were performed using *SPSS 21* (IBM). Methylation levels below 5% were set as <LOQ (limit of quantification) and values above 95% were set as >ULOQ (upper limit of quantification) as suggested by the manufacturer (Qiagen). For statistical calculations all values <LOQ were treated as $\frac{\mathrm{LOQ}}{2} = 2.5\%$ and all values >ULOQ were treated as 97.5% [115].

4.7 Methylation-sensitive high resolution melting analysis

MS-HRM was performed for the repetitive element LINE-1 to assess the global methylation status. The analysis was performed using the *EpiTect HRM PCR Kit* (Qiagen) according to manufacturer's protocol [101].
Reagents used for PCR were the *2x EpiTect HRM PCR Master Mix* (Qiagen; containing *HotStarTaq Plus DNA Polymerase, EpiTect PCR Buffer* with *EvaGreen* dye and dNTPs), RNase-free water and a forward and reverse primer.

The reagents were thawed completely but the reaction was set up on ice. MS-HRM analysis was carried out in duplicates. A master mix was prepared in workstation A. All reagents (except DNA) were mixed thoroughly and set up according to Table 6. The lyophilized primers were dissolved and diluted to a concentration of 10 µM using RNase-free water and stored in 9 µL aliquots at -20°C for re-use. The master mix was prepared for the respective number of DNA samples, two NTCs and four tolerance samples. The master mix was vortexed briefly (about 5 s) and pipetted in the prepared 100 µL PCR strip tubes (Qiagen).

Table 6: MS-HRM analysis setup for LINE-1; modified from [101]

Component	**Volume per reaction [µL]**
EpiTect HRM PCR Master Mix, 2x	10
Forward primer (initial concentration 10 µM)	0.5
Reverse primer (initial concentration 10 µM)	0.5
RNase-free water	7
Template DNA (c=5 ng/µL)	2
Total volume	20

In workstation B the DNA or respectively RNase-free water for the NTC was added. The DNA was mixed with the master mix by gently pipetting up and down.

Bisulfite converted *CpGenome Universal methylated DNA* and bisulfite converted *EpiTect human unmethylated control DNA* were pipetted in workstation B according to Table 7 to obtain a total volume of 5 µL.

Table 7: Pipetting scheme for MS-HRM standards using bisulfite converted commercial standards

Methylation status [%]	Methylated standard [µL]	Unmethylated standard [µL]
0	0	5
10	0.5	4.5
25	1.25	3.75
50	2.5	2.5
75	3.75	1.25
100	5	0

The *Rotor-Gene Q* (Qiagen) thermal cycler was programmed according to Table 8.

Table 8: General scheme for the MS-HRM temperature program; modified from [114]

Step	Time	Temperature [°C]	
Activation	5 min	95	
Denaturation	10 s	95	
Annealing	30 s	63-57 Touchdown, 7 cycles	3 step cycling, 50 cycles
Extension	10 s	72	
Hold 1	1 min	95	
Hold 2	1 min	40	
MS-HRM	2 s	67-86 0.1 increments	

Raw data was analyzed using *Rotor-Gene Q Series Software 2.3.1* (Qiagen). After obtaining amplification curves, the DNA methylation values were scaled automatically and the NTC was checked. Regions of normalization were adjusted to obtain representative baseline data for the pre-melt and post-melt phases [116]. Data was exported to *Excel* (Microsoft) and mean values for normalized fluorescence were calculated.

To standardize the obtained data, the standardized fluorescence (SF) was calculated using Equation 3 where x is the obtained value, min is the value obtained for the 0% standard and max is the obtained value for the 100% standard.

$$SF\ [\%] = \frac{x - min}{max - min} * 100$$

Equation 3: Standard fluorescence calculation

Therefore, all values for standards were standardized to a range of 0-100%. Data was transferred to *SigmaPlot 11.0* (Systat) and a calibration curve was created.

4.8 Statistical calculations

To evaluate a significant difference in the DNA methylation status between AD and control samples, either Mann–Whitney U test or Student's t-test was performed depending on the distribution of the obtained values using *SPSS 21* (IBM). For a narrow distribution Levene's test for equality of variances and subsequently Student's t-test was performed, which is based on the comparison of mean values. For a broad distribution Mann–Whitney U test was performed, which is based on the comparison of median values [117]. The null hypothesis was that there is no difference in DNA methylation levels between AD patients and controls. The alternative hypothesis was that there is a difference between the analyzed groups. The null hypothesis was rejected at p-value (two-sided) of $p \leq 0.050$ which indicated a significant difference between the two groups. The significance was divided in three groups according to the level of significance. P-values of ≤ 0.050 were considered as significant (*), $p \leq 0.010$ was considered as very significant (**) and $p \leq 0.001$ as highly significant (***).

5 Method development

Methylation patterns of *PSEN1*, *ABCA7*, *ABCB1* and *ABCC1* were determined using PSQ whereas the LINE-1 methylation status was analyzed using MS-HRM. All methods were developed in-house. Methods for *ABCB1*, *ABCC1* and LINE-1 were developed by Dipl.-Ing. Melanie Spitzwieser in course of her PhD thesis. Methods for *PSEN1* and *ABCA7* were developed in course of this thesis. An overview of the methods is given in section 7.8.

5.1 *PSEN1*

The target region of *PSEN1* was selected based on a paper by Fuso *et al.* (2011) [57], who reported a difference in DNA methylation pattern in few CpG moieties due to a metabolic stimuli, namely vitamin B deficiency. Neuroblastoma cells cultivated on vitamin B deficient medium showed hypomethylation at few CpG sites compared to cells cultivated on control medium.
Vitamin B is an essential cofactor in the DNA methylation metabolism and low levels of vitamin B have been associated with LOAD [118].

A new method was developed to determine the DNA methylation pattern of four CpGs (CG^1-CG^4 in Figure 19) analyzed by Fuso *et al.* (2011). These CpGs are located in the promoter region. The DNA sequence of *PSEN1* was taken from the *National Center for Biotechnology Information* (NCBI) [119] database and the promoter region was taken from the *Transcriptional Regulatory Element Database* (TRED) [120]. The gene accession number from NCBI is NG_007386.2 (Homo sapiens presenilin 1 (*PSEN1*), RefSeqGene on chromosome 14). A section of the *PSEN1* promoter region including the 261 bp (base pairs) long PCR product and the 118 bp long target region is shown in Figure 19.

>gi|213511787:4276-5335 Homo sapiens presenilin 1 (PSEN1), RefSeqGene on chromosome 14

GTTTTTTGAATACCCATGTTTGACATTTCTCCGTTCACCTTGATTAAATAAGGTAGTATTCATTTTTTAGTTTTA
GCTTTTGGATATATGTGTAAGTGTGGTATGCTGTCTAATGAATTAGACATTGGTACTGTCTTTACCAAAACTGG
ACAAAGAGCAGGCAGATGCAAAAATCAAGTGACCCAGCAAACCAGACACATTTTCTGCTCTCAGCTAGCTTG
CCACCTAGAAAGACTGGTTGTCAAAGTTGGAGTCCAAGAATCGCGGAGGATGTTTAAAATGCAGTTTCTCAG
GTTCTCGCCACCCACCAGAAGTTTTGATTCATTGAGTGGTGGGAGAGGGCAGAGATATTTGCGATTTTAACA
GCATTCTCTTGATTGTGATGCAGCTGGTTCGCAAATAGGTACCCTAAAGAAATGACAGGTGTTAAATTTAGGA
TGGCCATCG[1]CTTGTATGCCG[2]GGAGAAGCACACG[3]CTGGGCCCAATTTATATAGGGGCTTTCG[4]TCCTCAGC
TCG[5]AGCAGCCTCAGAACCCCG[6]ACAACCCACG[7]CCAGCG[8]CTCTGGGCG[9]GATTCCG[10]TCAGGTGGGGAAG
GCCAGGTGGAGCTCTGGGTTCTCCCCGCAATCGTTTCTCCAGGCCGGAGGCCCCGCCCCCTTCCTCCTGGC
TCCTCCCCTCCTCCGTGGGCCGGCCGCCAACGACGCCAGAGCCGGAAATGACGACAACGGTGAGGGTTCT
CGGGCGGGGCCTGGGACAGGCAGCTCCGGGGTCCGCGGTTTCACATCGGAAACAAAACAGCGGCTGGTCT
GGAAGGAACCTGAGCTACGAGCCGCGGCGGCAGCGGGGCGGCGGGGAAGCGTATGTGCGTGATGGGGAG
TCCGGGCAAGCCAGGAAGGCACCGCGGACATGGGCGGCCGCGGGCAGGGCCCGGCCCTTTGTGGCCGCC
CGGGCCGCGAAGCCGGTGTCCTAAAAGATGAGGGGCGGGGCGCGGCCGGTTGGGGCTGGGGAACCCCGT
GTGGGAAACCAGGAGGGGCGGCCCGTTTCTCGGGCTTCGGGCGCGGCCGGGTGGAGAGAGATTCCGGGG

Figure 19: Section of the promoter region of *PSEN1*; target region for PSQ DNA methylation analysis is highlighted yellow, binding sites for forward and reverse primers are highlighted blue, binding site for the sequencing primer is highlighted blue and underlined twice, exon 1 is highlighted grey, CpGs are highlighted green and the analyzed CpGs are numbered according to their order in the corresponding pyrogram.

Primers for *PSEN1* were designed using the *PyroMark Assay Design Software 2.0* (Qiagen) as described in section 4.3 and according to primer design rules as given in section 3.5. Figure 20 shows the applied settings for *PSEN1* primer design.

PCR Primer	
Min Primer Length [nt]	18
Max Primer Length [nt]	30
Optimal Amplicon Length From [nt]	50
Optimal Amplicon Length To [nt]	250
Max Amplicon Length [nt]	400
Allow Primer Over Variable Position	☐
Melting Temperature Algorithm	NN Mismatch
Primer Concentration [µM]	0.2
Min Melting Temperature [°C]	50.0
Max Melting Temperature [°C]	72.0
Max Allowed Tm Difference [°C]	10.0
Max GC Difference [%]	50

Sequencing Primer	
Min Primer Length [nt]	15
Max Primer Length [nt]	25
Min Distance From Target [nt]	0
Max Distance From Target [nt]	5
Allow Primer Over Variable Position	☐
Generate Forward Primers	☑
Generate Reverse Primers	☑
Melting Temperature Algorithm	NN Mismatch
Min Melting Temperature [°C]	29.0
Max Melting Temperature [°C]	59.0

Figure 20: Settings for designing *PSEN1* primers

The software listed primer sets according to their fitting to the settings. The primers with the highest scores were tested for secondary structures, for their differences in T_m and for the formation of hetero- and homodimers as given in section 4.3.

Table 9 lists the sequences of the primers that were used in the current work, their predicted secondary structures and T_m. None of the primers showed the tendency to form secondary structures.

Table 9: Characteristics of the *PSEN1* primers; F... forward primer, R… reverse primer, S… sequencing primer, [btn]-… biotin

Primer sequence [5'-3']	**Secondary structure**	**T_m [°C]**
F: TGGTGGGAGAGGGTAGAGA	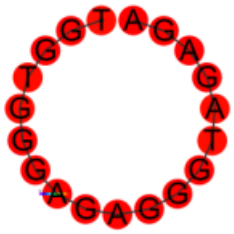	59.5
R: [btn]-CCAAAACTCCACCTAACCTTC		59.5
S: GTGTTAAATTTAGGATGGT	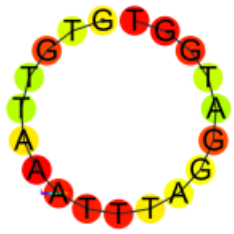	48.9

PCR was optimized using four different annealing temperatures (55.2, 57.6, 59.5 and 61.9°C) and two different primer concentrations, namely 0.2 µM and 0.4 µM as described in detail in section 4.3.

Figure 21 and Figure 22 show the results obtained by subjecting the PCR products to agarose gel electrophoresis.

Figure 21 indicates that a PCR product of 261 bp was obtained for the 100% standard, independent of the annealing temperature and the primer concentration. However, for the 0% standard most conditions did not result in the formation of the correct amplicon.

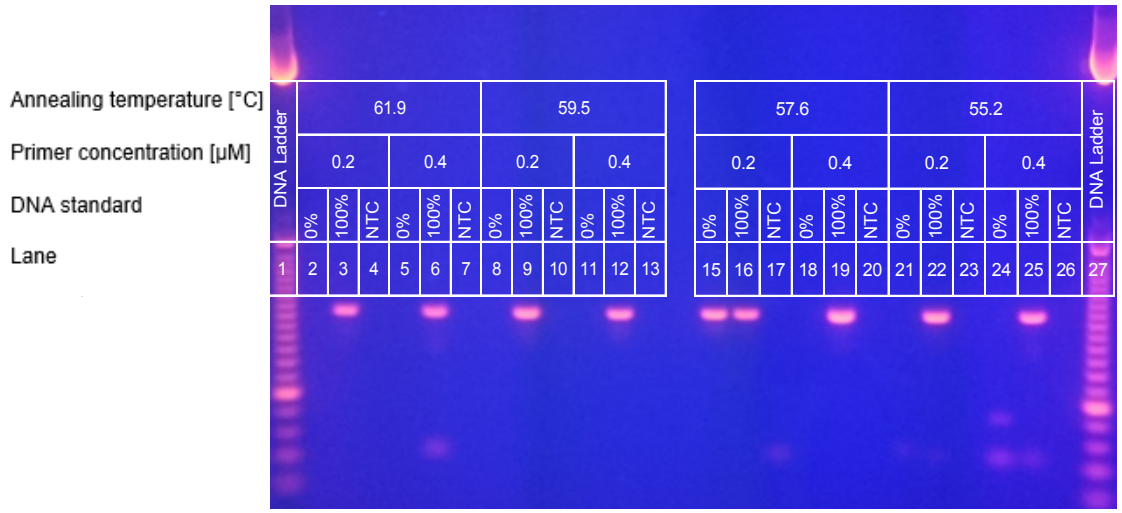

Figure 21: Agarose gel showing the results of PCR optimization for *PSEN1*; NTC… no template control, 0%... *EpiTect human unmethylated control DNA* (failed bisulfite conversion), 100%... *CpGenome universal methylated DNA*

Since it turned out that the bisulfite conversion of the 0% standard had failed (see discussion section 6.1), the optimization experiment was repeated with a freshly converted aliquot of the standards. In the second PCR optimization experiment, the annealing temperature was narrowed to a range from 55.6°C to 58.9°C. The primer concentration was fixed to 0.2 µM to minimize the formation of unspecific products. Figure 22 indicates that amplicons were obtained for both the 0% and the 100% standard.

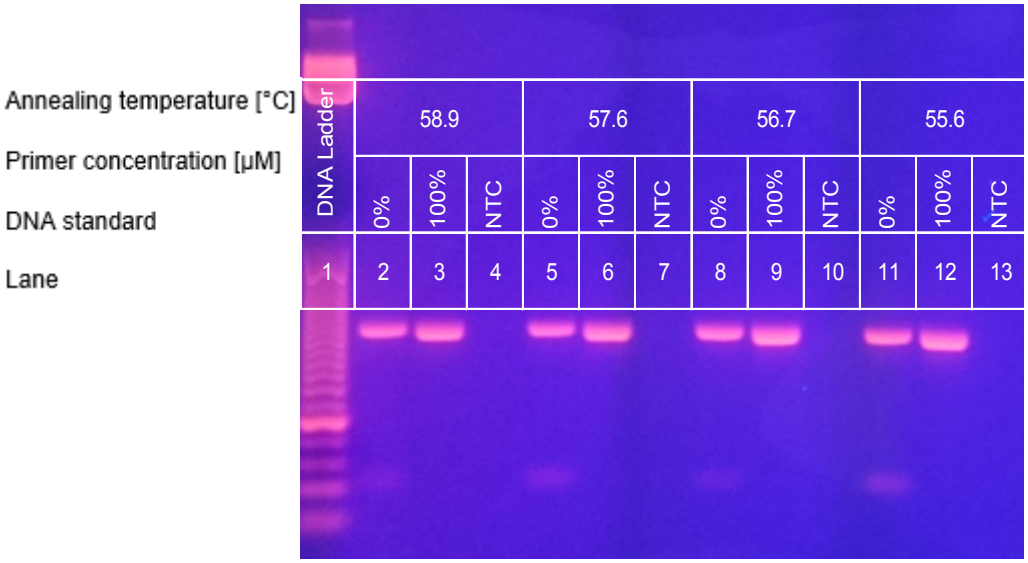

Figure 22: Agarose gel showing the results of the second PCR optimization for *PSEN1*; NTC… no template control, 0%... bisulfite converted *EpiTect human unmethylated control DNA*, 100%... bisulfite converted *CpGenome universal methylated DNA*

As the intensity of the fluorescence signal and thus the amount of product did not vary between the different annealing temperatures, the highest annealing temperature was selected to minimize the formation of unspecific products.

PCR amplification with an annealing temperature of 58.9°C and a primer concentration of 0.2 µM led, however, to low peak heights (low fluorescence signals) in PSQ analysis. As a consequence, a primer concentration of 0.4 µM was considered as optimal because the higher primer concentration led to an increase in the fluorescence signal in PSQ analysis. Table 10 lists the PCR reaction setup and Table 11 the temperature program for *PSEN1* amplification.

Table 10: PCR reaction setup for *PSEN1*; modified from [114]

Component	**Volume per reaction [µL]**
PyroMark PCR Master Mix, 2x	12.5
CoralLoad concentrate, 10x	2.5
Forward primer (initial concentration 10 µM)	1
Reverse primer (initial concentration 10 µM)	1
RNase-free water	6
Template DNA (c=5 ng/µL)	2
Total volume	25

Table 11: PCR temperature program for *PSEN1*; modified from [114]

Step	**Time**	**Temperature [°C]**	
Activation	15 min	95	
Denaturation	30 s	94	3 step cycling
Annealing	30 s	58.9	
Extension	30 s	72	
Final extension	10 min	72	
Number of cycles	50		

Figure 23 shows a representative pyrogram. The analyzed sequence before bisulfite treatment was CAT**YG**CTTGTATGC**YG**GGAGAAGCACA**YG**CTGGGCCCAATTTATATA GGGGCTTT**YG**TCCTCAGCT**YG**AGCAGCCTCAGAACCC**YG**ACAACCCA**YG**CCAG**YG**C TCTGGG**YG**GATTC**YG**. All CpGs are marked as **YG** (Y… variable position; either TG or

CG after bisulfite treatment). The length of the analyzed region was 118 bases and contained 10 CpGs. The methylation levels obtained for the last 5-6 CpGs were frequently highlighted in yellow (or even red), most frequently due to “high peak height deviation” at dispensations 52, 63, 67, 75 or due to “high peak height deviation in variable position”, indicating that the methylation status given was inaccurate. The pyrogram shown in Figure 23 indicates that, starting from about position 55 (CpG 5), the peak pattern does not correspond to the expected pattern.

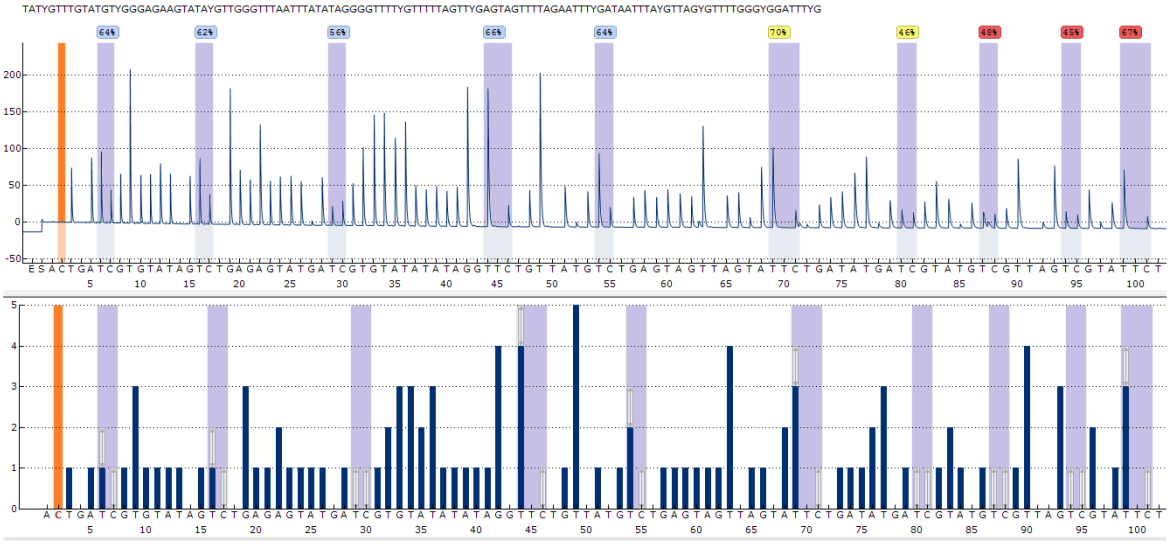

Figure 23: Representative pyrogram for *PSEN1* in comparison to the histogram showing the expected peak pattern; variable positions are highlighted in grey, position highlighted in orange shows the bisulfite control

5.2 *ABCA7*

Two different primer sets were designed for *ABCA7* based on regions analyzed by Yu *et al.* (2015) [69] and Humphries *et al.* (2015) [70].

Yu *et al.* (2015) [69] determined the DNA methylation status at loci that had previously been associated with AD. They analyzed DNA extracts from grey matter of the dorsolateral prefrontal cortex in 740 patients, 60.4% suffering from AD. Three CpGs were found to be associated with AD and two of them were close to the 3’ untranslated region of *ABCA7*.

Humphries *et al.* (2015) [70] investigated DNA methylation in post mortem human brain samples. CpGs in a CpG shore, located in a non-coding region of ABCA7, were found to be hypomethylated in samples from LOAD patients.

Another primer set was designed during this thesis to analyze the methylation status of the promoter region in *ABCA7*.

The region analyzed with primer set 2 is located 2818 bp downstream from the analyzed region in the promoter (analyzed with primer set 3) of *ABCA7*. The region analyzed with primer set 1 is located 26046 bp downstream of the region analyzed with primer set 2.

The DNA sequence for designing the three primer sets for *ABCA7* was taken from NCBI [119]. The gene accession number is NC_000019.10 (1040103-1071693). The promoter region was taken from TRED [120].

5.2.1 Primer set 1

Figure 24 shows the analyzed region of *ABCA7* including the CpG "cg02308560" (CG^4) which had been associated with AD by Yu *et al.* (2015) [69]. Yu *et al.* found the CpG to be higher methylated in samples from AD patients than in controls. The analyzed region is close to the 3' untranslated region of *ABCA7*.

The length of the PCR product was 381 bp and eight CpGs were analyzed by the PSQ reaction.

>gi|568815579:1070693-1071693 Homo sapiens chromosome 19, GRCh38.p2 Primary Assembly

GGCTGGTCTAGAACTCCCGAGCTAAAAACCGTTCTCCCGGCTCCGCCTCCCAAAGTGCTGGGATAACAGGC
CTGATCCACCGCGCCCGGCTGGGGGCGCCTTCTGTGCGTCTCGGGGCCGCCCCAGGCCAGAGAAGACCCT
GGCGGCTAGGATGTGGGCTCTAGTCCCGATGTTTCTCAGCTGCTGAGACCCTGGCAAGCCCCTTCCCTCTC
TAGGTGTCAGGTGACTTATCTATAAAATGGGGCCACCTGCATGCAGCGATGGTTGTGGGGTCCACCCCACA
GCTTGGGGACCCGCGTTCAGGAAGGAAGGCAGCTAGGAGGGGACCCACATGGACGGTGCCACCCCGACAC
TTCCCGGGCTTCCTCGTTCCCGGGCTTCAGGTCTGGGCCTCAGTTTCCCTGCCCGTCCTCGACCCTCCCCA
CCTCGAAGCTCTGCGGTTAAGGAAGGACCCAGGCTGGGGCG[1]AACG[2]GGACCCCAGGGCG[3]GGGTTTCCCT
CG[4]CG[5]GGGGCG[6]GGGCCTCCTGACCG[7]GCCG[8]GAGCCGGTTTGGCCACCGGAGACCCCCATCGGTCAGCT
GCCAGGCCCCACGCGCTCGCGGTCTCCGCGCCCCGACGGCTGCGCCATGTGTATCTGCGGGACGGCGCCA
CCCGGTGCTGGACGAGGGCCCCGTGCGCTGCCGGGCGGGCCCCCGAGGTGAGGGGACAGGTGCCGGGC
GCTGGGTCCCGCCGCGTCCGGGAGCACGTGGCGCTCGGGCCGTTTGCCGCCCGCGGTGGGGGAGCAGCG
GCTGCCGCGCGCCTGGCCTGGCCGTGCGCACCTGGGCATCCCTGCGCTGCGCAGGGGTCGCGCCGGCCG
CCGGCTTCCCGGGTAGGGGGTGTGCGGGGACAGCCGGGGGTCCGTGCGCCGGCCGCGCGCGGAGTGCC
GGGTGCCCGGCTGGAAGGTCCCGAGAAGGGGCGTGGCCGGGGCCTCCCAGCGGCTTCCCGGAGCTCCTG
GAGCCCCAATCCCATTCCCGGAGTCCGCCTCGCATCCAG

Figure 24: Section of the sequence of *ABCA7* targeted by primer set 1; target region for PSQ DNA methylation analysis with primer set 1 is highlighted yellow, binding sites for forward and reverse primers are highlighted blue, binding site for the sequencing primer is highlighted blue and underlined twice, CpGs are highlighted green and the analyzed CpGs are numbered according to their order in the corresponding pyrogram.

Figure 25 shows the applied settings for the design of primer set 1 for *ABCA7*.

PCR Primer	
Min Primer Length [nt]	18
Max Primer Length [nt]	30
Optimal Amplicon Length From [nt]	50
Optimal Amplicon Length To [nt]	200
Max Amplicon Length [nt]	400
Allow Primer Over Variable Position	☐
Melting Temperature Algorithm	NN Mismatch
Primer Concentration [µM]	0.2
Min Melting Temperature [°C]	50.0
Max Melting Temperature [°C]	72.0
Max Allowed Tm Difference [°C]	15
Max GC Difference [%]	60

Sequencing Primer	
Min Primer Length [nt]	15
Max Primer Length [nt]	25
Min Distance From Target [nt]	0
Max Distance From Target [nt]	20
Allow Primer Over Variable Position	☐
Generate Forward Primers	☑
Generate Reverse Primers	☑
Melting Temperature Algorithm	NN Mismatch
Min Melting Temperature [°C]	29.0
Max Melting Temperature [°C]	59.0

Figure 25: Primer design settings for *ABCA7* primer set 1

Table 12 lists the primer sequences including their secondary structures and T_m. Table 12 indicates that none of the primers showed the tendency to form secondary structures and that the difference in the melting temperature (T_m) between forward and reverse primer is 0.8°C.

Table 12: Characteristics of the *ABCA7* primer set 1; F... forward primer, R… reverse primer, S… sequencing primer, [btn]-… biotin

Primer sequence [5'-3']	**Secondary structure**	**T_m [°C]**
F: AGGTAGTTAGGAGGGGATTTATAT	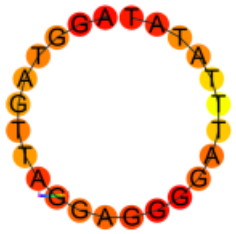	60.3
R: [btn]- ACACCTATCCCCTCACCTC	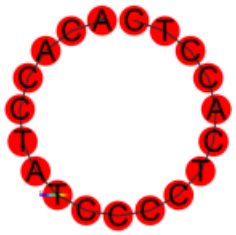	59.5
S: AGGAAGGATTTAGGTTG		47.5

PCR was optimized applying four different annealing temperatures (53.1, 56.4, 58.6, 60.2°C) and two different primer concentrations (0.2 µM and 0.4 µM).

Figure 26 shows the result obtained by verifying the identity of the PCR products by gel electrophoresis.

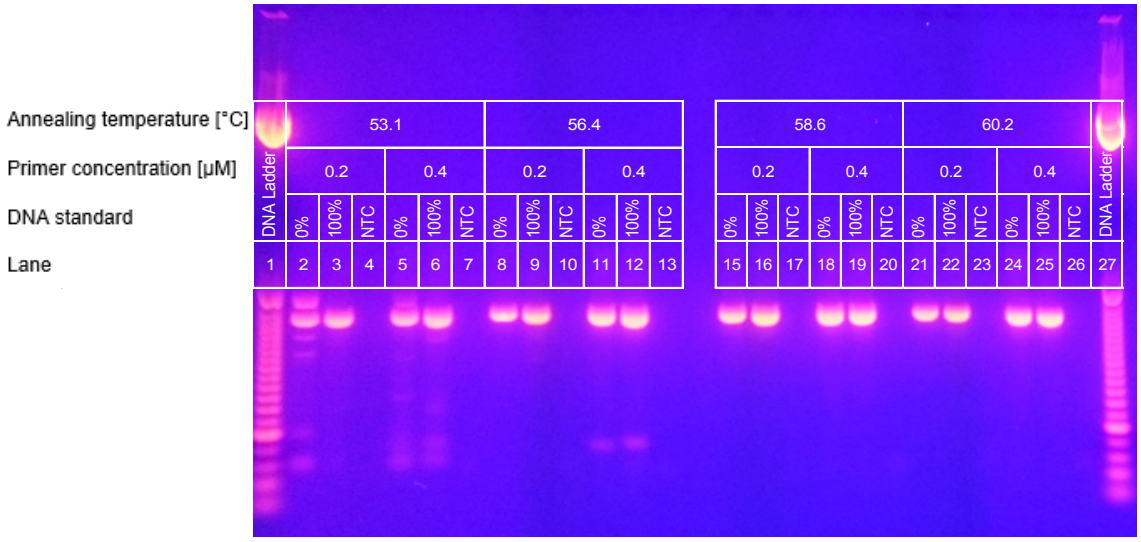

Figure 26: Agarose gel showing the results of the PCR optimization experiments for *ABCA7* primer set 1; NTC… no template control, 0%... bisulfite converted *EpiTect human unmethylated control DNA*, 100%... bisulfite converted *CpGenome universal methylated DNA*

Comparison of the obtained bands with the DNA ladder revealed that the PCR product had the correct length of 381 bp. The presence of additional bands indicated that unspecific products were formed at low annealing temperatures (lane 2, 3, 5, 6 at an annealing temperature of 53.1°C and lane 11, 12 at an annealing temperature of 56.4°C in Figure 26). With a primer concentration of 0.4 µM, more unspecific products were obtained than with a primer concentration of 0.2 µM. Thus, all further PCR runs were carried out at an annealing temperature of 60.2°C and with a primer concentration of 0.2 µM. Table 13 and Table 14 list the PCR reaction setup and the temperature program for *ABCA7* primer set 1, respectively.

Table 13: PCR reaction setup for *ABCA7* primer set 1; modified from [114]

Component	Volume per reaction [µL]
PyroMark PCR Master Mix, 2x	12.5
CoralLoad concentrate, 10x	2.5
Forward primer (initial concentration 10 µM)	0.5
Reverse primer (initial concentration 10 µM)	0.5
RNase-free water	7
Template DNA (c=5 ng/µL)	2
Total volume	25

Table 14: PCR temperature program for *ABCA7* primer set 1; modified from [114]

Step	Time	Temperature [°C]	
Activation	15 min	95	
Denaturation	30 s	94	3 step cycling
Annealing	30 s	60.2	
Extension	30 s	72	
Final extension	10 min	72	
Number of cycles	50		

Figure 27 shows an example of a pyrogram. The analyzed sequence before bisulfite treatment was GGG**YG**AA**YG**GGACCCCAGGG**YG**GGGTTTCCCT**YGYG**GGGGG**YG**GGG CCTCCTGAC**YG**GC**YG**. All CpGs are marked as **YG** (Y… variable position; either TG or CG after bisulfite treatment). The analyzed region consisted of 60 bp and contained 8 CpGs.

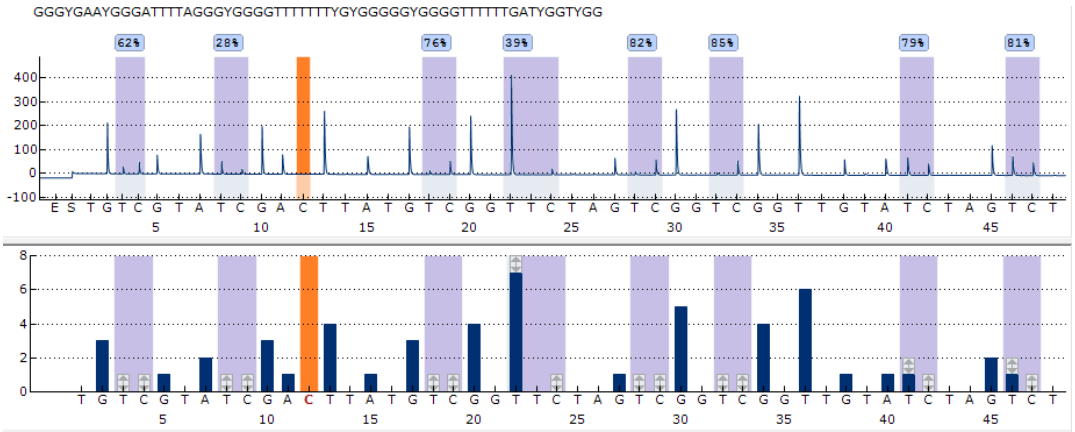

Figure 27: Representative pyrogram for *ABCA7* primer set 1 in comparison to the histogram showing the expected peak pattern; variable positions are highlighted in grey, position highlighted in orange shows the bisulfite control

5.2.2 Primer set 2

Figure 28 shows a section of the *ABCA7* gene including the 164 bp long PCR product and the region analyzed by PSQ with the method using primer set 2. The target region for DNA methylation analysis by PSQ is located 26046 bp upstream of the target region analyzed using primer set 1.

>gi|568815579:1044766-1045766 Homo sapiens chromosome 19, GRCh38.p2 Primary Assembly

GGGTCTGTTTCAGTGGGGAGGGCAGGTCCCATCCTAGTGTTCCCACCCTGGTGTTCCCAGGGGGAGGCGG
GCCCGGCCCTAGTAAGAGCCTGGGATTTGTAGAGATCTCAGGAGGGAGCCGGCCGTGGGCCTACGAGGGG
AAAACATGGCCCAGCCCCGAGGTCCAGGGGGAGGAGCGGAGTGGTCTAGGAGGCAGGCGGACCCCAGCG
CCTAGGACTCACCCCGCATCCCACAGTGCCTGTCCTTGGACAAGCTGGAGGCGGCACCCTCAGAGGCAG
CCCTGGTGTCG¹CG²GGCCCTGCAACTGCTCG³CG⁴GAACATCG⁵ATTCTGGGCCG⁶GCG⁷TCG⁸TCTTCTTGG
GACCTGAGGACTCTTCAGACCCCACAGAGCACCCAACCCCAGACCTGGGCCCCGGCCACGTGCGCATCAAA
ATCCGCATGGACATTGACGTGGTCACGAGGACCAATAAGATCAGGGACAGGTCAGGCGAGGGAGGGGGCG
GGGGGATGAGGGACTGGGCGGGGCCAAGAGCGTGGTGGGTGGGGCCAGGCAGCATTCAGCCTATTGGAG
ACCATGATAGACAGGATCTGGGCTGTATCAACAGTGGTATGGTAGCCAGAGCCCGGGGCTCCTTAGACCAA
TAGGGGCCCGTGATGGGCGGGGCCTAGGTGCATGAGGGGCGTGGCCATGGGCCTGAGATAAGATGAGAG
CAGGTATAGGTTGAGGGCAATGGTGGGCGGAGCCAGGTGTATTATTAGGTCCCTGGAATAAGGGTGGAGCT
AAAATTGCACCGGGTGCTGAGCGCAGTAGATCTTGCCTGTTATCTCAGAACTTTGGGAGGCCAAAGTGGGAG
AATCTCTTGAGGACAGGTATTCGAGACTAGCCTGGGCAACATAGTGAGACCGCCTCCCCCCCGCCCCCCTC
CCCCACCAACCTCACGAAAATATCTTTAAAAATTAGCCAGGTGAGGCCGGGCACAGTGGCTCACGCCTGTAA
TCCCAGCACTTTGGGAGGCT

Figure 28: Section of the sequence of *ABCA7* targeted by primer set 2; target region for PSQ DNA methylation analysis with primer set 2 is highlighted yellow, binding sites for forward and reverse primers are highlighted blue, binding site for the sequencing primer is highlighted blue and underlined twice, CpGs are highlighted green and the analyzed CpGs are numbered according to their order in the corresponding pyrogram

Primers for *ABCA7* primer set 2 were designed using the *PyroMark Assay Design Software 2.0* (Qiagen) and Figure 29 shows the applied settings.

PCR Primer	
Min Primer Length [nt]	18
Max Primer Length [nt]	30
Optimal Amplicon Length From [nt]	50
Optimal Amplicon Length To [nt]	100
Max Amplicon Length [nt]	250
Allow Primer Over Variable Position	☐
Melting Temperature Algorithm	NN Mismatch
Primer Concentration [µM]	0.2
Min Melting Temperature [°C]	50.0
Max Melting Temperature [°C]	72.0
Max Allowed Tm Difference [°C]	10.0
Max GC Difference [%]	50

Sequencing Primer	
Min Primer Length [nt]	15
Max Primer Length [nt]	25
Min Distance From Target [nt]	0
Max Distance From Target [nt]	10
Allow Primer Over Variable Position	☐
Generate Forward Primers	☑
Generate Reverse Primers	☑
Melting Temperature Algorithm	NN Mismatch
Min Melting Temperature [°C]	29.0
Max Melting Temperature [°C]	59.0

Figure 29: Primer design settings for *ABCA7* primer set 2

Table 15, summarizing the primer sequences of *ABCA7* primer set 2, indicates that none of the primers showed the tendency to form secondary structures. The difference in the melting temperature (T_m) between forward and reverse primer is only 0.3°C.

Table 15: Characteristics of the *ABCA7* primer set 2; F... forward primer, R… reverse primer, S… sequencing primer, [btn]-… biotin

Primer sequence [5'-3']	**Secondary structure**	**T_m [°C]**
F: TAGTGTTTGTTTTTGGATAAGTTGGA		60.1
R: [btn]-AAACCCAAATCTAAAATTAAATACTCTATA		59.8
S: GGTATTTTTAGAGGTAG	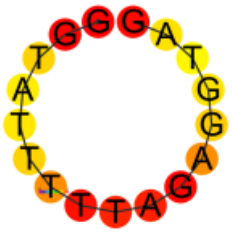	45.0

PCR was optimized using two different primer concentrations (0.2 µM and 0.4 µM) and four different annealing temperatures, namely 54.0, 57.5, 59.8 and 62.5°C.

Figure 30: Agarose gel showing the results of the PCR optimization experiments for *ABCA7* primer set 2; NTC… no template control, 0%... bisulfite converted *EpiTect human unmethylated control DNA*, 100%... bisulfite converted *CpGenome universal methylated DNA*

At the highest annealing temperature (62.5°C, lane 20-25 in Figure 30) no bands derived from the correct amplicon length of 164 bp were visible. At an annealing temperature of 59.8°C and a primer concentration of 0.2 µM (lane 14-15 in Figure 30) the band obtained for the 0% standard was less intense than the band obtained for the 100% standard. Annealing temperatures of 54°C and 57.5°C yielded similar results. With the higher primer concentration (0.4 µM), higher amounts of the specific PCR product but also a higher number of unspecific products were formed. The optimum annealing temperature was assumed to be between 54.0°C and 57.5°C. As a consequence, a further optimization experiment was performed in this temperature range using a primer concentration of 0.2 µM with the aim to minimize the formation of unspecific products.

Figure 31: Agarose gel showing the results of the second PCR optimization for *ABCA7* primer set 2; NTC… no template control, 0%... bisulfite converted *EpiTect human unmethylated control DNA*, 100%... bisulfite converted *CpGenome universal methylated DNA*

The gel showed intense bands at all tested annealing temperatures and the correct PCR product was obtained. At a temperature of 55.4°C almost no unspecific products were obtained. Thus, an annealing temperature of 55.4°C and a primer concentration of 0.2 µM were considered as optimal. The PCR reaction setup and the temperature program for *ABCA7* primer set 2 are listed in Table 16 and Table 17, respectively.

Table 16: PCR reaction setup for *ABCA7* primer set 2; modified from [114]

Component	**Volume per reaction [µL]**
PyroMark PCR Master Mix, 2x	12.5
CoralLoad concentrate, 10x	2.5
Forward primer (initial concentration 10 µM)	0.5
Reverse primer (initial concentration 10 µM)	0.5
RNase-free water	7
Template DNA (c=5 ng/µL)	2
Total volume	25

Table 17: PCR temperature program for *ABCA7* primer set 2; modified from [114]

Step	Time	Temperature [°C]	
Activation	15 min	95	
Denaturation	30 s	94	3 step cycling
Annealing	30 s	55.4	
Extension	30 s	72	
Final extension	10 min	72	
Number of cycles	50		

Figure 32 shows an example of a pyrogram. The analyzed sequence before bisulfite treatment was CCCTGGTGT**YGYG**GGCCCTGCAACTGCT**YGYG**GAACAT**YG**ATTCT GGGC**YG**G**YG**T**YG**. All CpGs are marked as **YG** (Y… variable position; either TG or CG after bisulfite treatment). The length of the analyzed region was 57 bases and the region contained 8 CpGs.

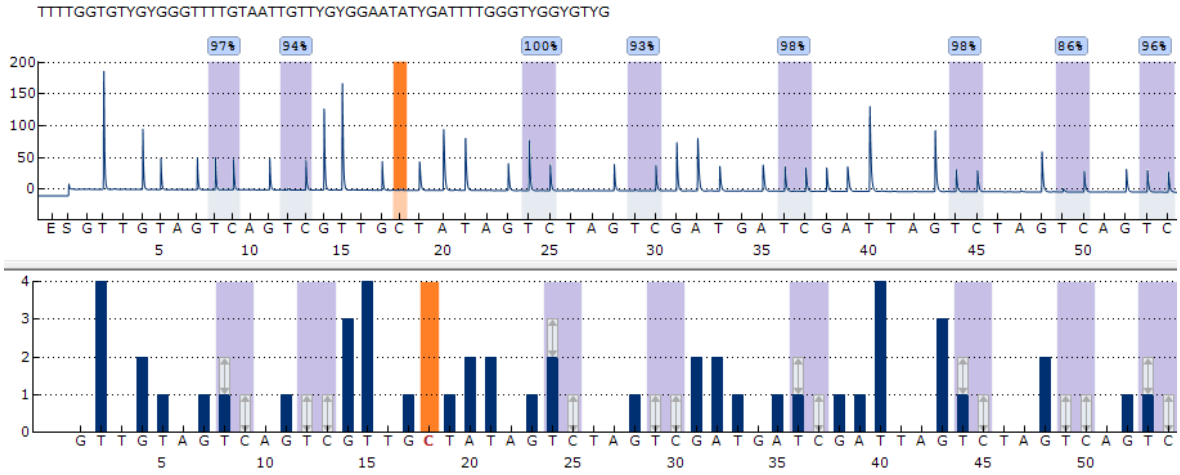

Figure 32: Representative pyrogram for *ABCA7* primer set 2 in comparison to the histogram showing the expected peak pattern; variable positions are highlighted in grey, position highlighted in orange shows the bisulfite control

5.2.3 Primer set 3

Primer set 3 was designed to target the promoter region of *ABCA7*. The promoter region was retrieved from TRED [120] and a section of the *ABCA7* promoter region is shown in Figure 33.

>gi|568815579:1041781-1042781 Homo sapiens chromosome 19, GRCh38.p2 Primary Assembly

TGGAGTCAGGCAGAGTCCACAGGGCCTCAGCACCAGGCGTCTCCCCGCAGGCCACTTCCCAAACAAGCCA
CTGCCATCGGCGGGCACCGTGCCCTGGCTCCAGGGTCTCATCTGTAATGTGAACAACACCTGCTTTCCGCA
GCTGACACCGGGCGAGGAGCCCGGGCGCCTGAGCAACTTCAACGACTCCCTGTGAGCCAGAGGCAGTGGG
TGCGGCCGGCCTGCAAACTCGGGGCTGCAGTGCCGGCCGGAACCCCGCCTCCTGCCCTCTCTCTGTCCCC
AGGGTCTCCCGGCTGCTAGCCGATGCCCGCACTGTGCTGGGAGGGGCCAGTGCCCACAGGACGCTGGCTG
GCCTAGGGAAGCTGATCG[1]CCACG[2]CTGAGGGCTGCACG[3]CAGCACG[4]GGTGAGGAGGCCG[5]GGGGGCCTCT
GGCAGGGCTGAGCTCTGAGCCTCAACTTGCCG[6]GGCCG[7]TGAAATGGGCACAGGGTGGGGGTGGGTGCCTC
AGACCAACGTCCCCCCAGCCCCATGCTCCCGTGCGCTCCTCCCCCAGCCCAGCCTCAACCAACCAAGCAGT
CTCCACTGGAACCACCCATGCTGGATGTCGCGGAGCTGCTGACGTCACTGCTGCGCACGGTAGGGTGTCG
GGGCGGGACCGCGCTGACTTCCTGGGACACTGCACTGGGGATGTCCTGGCACTGCCCCACCCCGGGCCAA
GGACCTCCCGTTCCAGGCATCCAGGCTGTCCCTGGTCTCTGCGGTGATGCTGCTTGTCCGTCTGGGCCCCC
AGACAGAGTGTGTCTGACCCAGTGAGGAAGACTCGTCTGTGAGATCTCCAATGAGTCCCTTTGCCTCTCAGA
GCCTCAGTTTCCCTATTTGTAAAGTGGGGGCTATGATAGTATGGTCTGCCTGGGAACTGGCCAGAGCGCTGG
ACCCCTAGTGAGTGTTCAAAATCATTGTCCCCCTTGTGGTCTTTCTCCCCAGGAATCCCTGGGGTTGGCACT
GGGCCAAGCCCAGGAG

Figure 33: Section of the sequence of *ABCA7* targeted by primer set 3; target region for PSQ DNA methylation analysis with primer set 3 is highlighted yellow, binding sites for forward and reverse primers are highlighted blue, binding site for the sequencing primer is highlighted blue and underlined twice, CpGs are highlighted green and the analyzed CpGs are numbered according to their order in the corresponding pyrogram

Figure 34 shows the applied settings for designing *ABCA7* primer set 3.

PCR Primer	
Min Primer Length [nt]	18
Max Primer Length [nt]	30
Optimal Amplicon Length From [nt]	50
Optimal Amplicon Length To [nt]	100
Max Amplicon Length [nt]	200
Allow Primer Over Variable Position	☐
Melting Temperature Algorithm	NN Mismatch
Primer Concentration [µM]	0.2
Min Melting Temperature [°C]	50.0
Max Melting Temperature [°C]	72.0
Max Allowed Tm Difference [°C]	15
Max GC Difference [%]	60

Sequencing Primer	
Min Primer Length [nt]	15
Max Primer Length [nt]	25
Min Distance From Target [nt]	0
Max Distance From Target [nt]	15
Allow Primer Over Variable Position	☐
Generate Forward Primers	☑
Generate Reverse Primers	☑
Melting Temperature Algorithm	NN Mismatch
Min Melting Temperature [°C]	29.0
Max Melting Temperature [°C]	59.0

Figure 34: Primer design settings for *ABCA7* primer set 3

Table 18 summarizes the most important characteristics of the primers. It indicates that none of the primers showed the tendency to form secondary structures.

Table 18: Characteristics of the *ABCA7* primer set 3; F... forward primer, R… reverse primer, S… sequencing primer, [btn]-… biotin

Primer sequence [5'-3']	**Secondary structure**	**T_m [°C]**
F: TTGGTTGGTTTAGGGAAGTTG	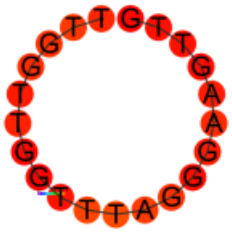	57.5
R: [btn]-CCCACCCTATACCCATTTC	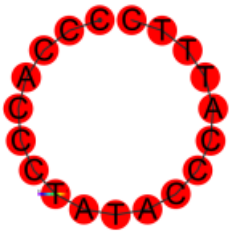	57.5
S: GGTTTAGGGAAGTTGAT	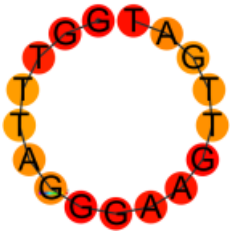	47.5

Four annealing temperatures (52.5, 56.0, 58.3 and 61.5°C) and two primer concentrations (0.2 µM and 0.4 µM) were used in PCR optimization experiments.

The results obtained by loading the PCR products onto an agarose gel are shown in Figure 35.

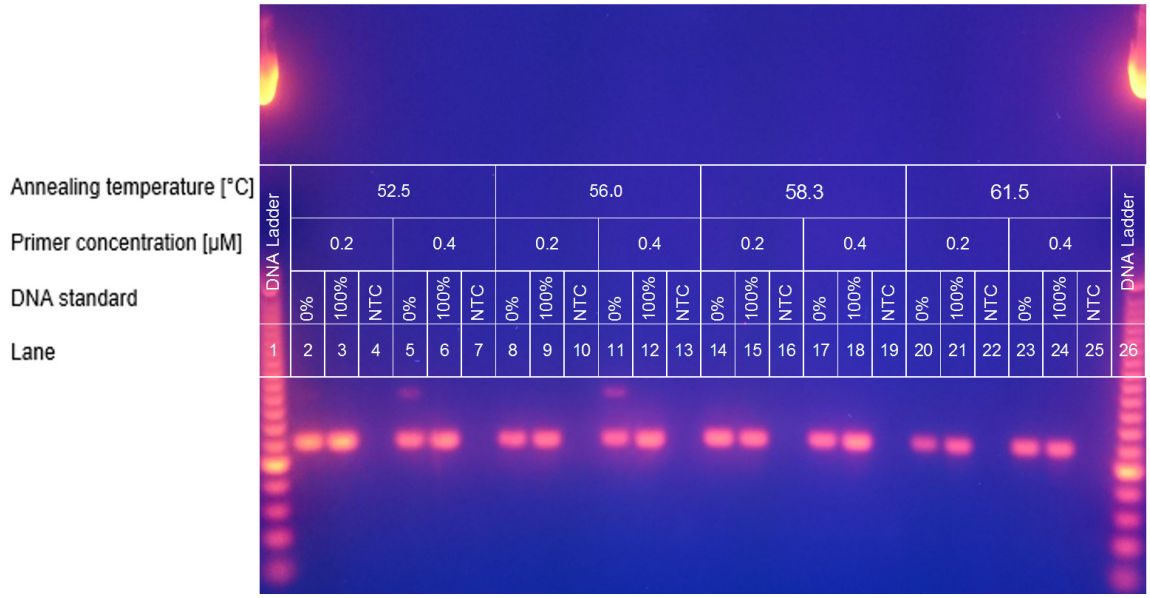

Figure 35: Agarose gel showing the results of the PCR optimization for *ABCA7* primer set 3; NTC… no template control, 0%... bisulfite converted *EpiTect human unmethylated control DNA*, 100%... bisulfite converted *CpGenome universal methylated DNA*

Figure 35 demonstrates that the specific PCR product (131 bp) was obtained under all conditions tested.

No unspecific products were formed at an annealing temperature of 58.3°C (lane 14-19 in Figure 35) and at an annealing temperature of 61.5°C (lane 20-25).

At an annealing temperature of 61.5°C, a lower amount of specific PCR product was obtained than at 58.3°C. Thus, an annealing temperature of 58.3°C and, to minimize the formation of unspecific products, a primer concentration of 0.2 µM were considered as optimal. Table 19 lists the PCR reaction setup for *ABCA7* primer set 3 and Table 20 shows the corresponding temperature program.

Table 19: PCR reaction setup for *ABCA7* primer set 3; modified from [114]

Component	Volume per reaction [µL]
PyroMark PCR Master Mix, 2x	12.5
CoralLoad concentrate, 10x	2.5
Forward primer (initial concentration 10 µM)	0.5
Reverse primer (initial concentration 10 µM)	0.5
RNase-free water	7
Template DNA (c=5 ng/µL)	2
Total volume	25

Table 20: PCR temperature program for ABCA7 primer set 3; modified from [114]

Step	Time	Temperature [°C]	
Activation	15 min	95	
Denaturation	30 s	94	3 step cycling
Annealing	30 s	58.3	
Extension	30 s	72	
Final extension	10 min	72	
Number of cycles	50		

Figure 36 shows an example of a pyrogram. The analyzed sequence before bisulfite treatment was **YG**CCA**YG**CTGAGGGCTGCA**YG**CAGCA**YG**GGTGAGGAGGC**YG** GGGGGCCTCTGGCAGGGCTGAGCTCTGAGCCTCAACTTGC**YG**GGC**YG**. All CpGs are marked as **YG** (Y… variable position; either TG or CG after bisulfite treatment). The analyzed region was 88 bp long and contained 7 CpGs.

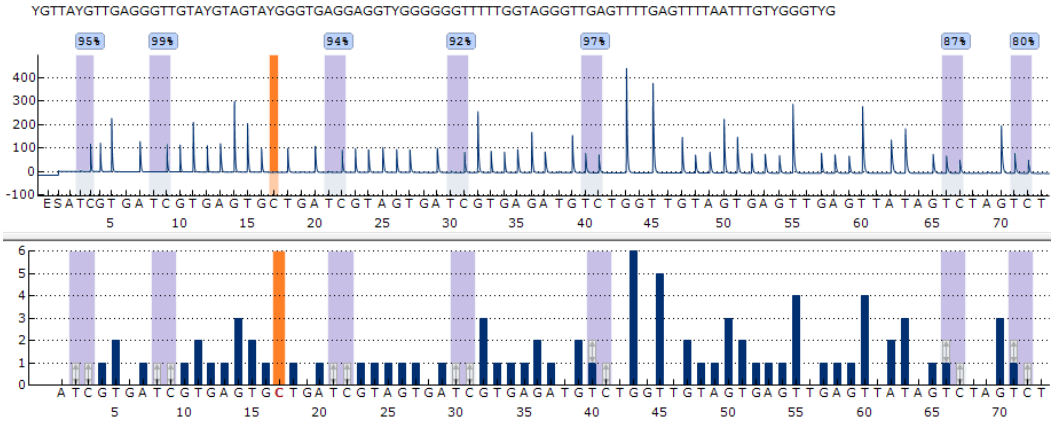

Figure 36: Representative pyrogram for *ABCA7* primer set 3 in comparison to the histogram showing the expected peak pattern; variable positions are highlighted in grey, position highlighted in orange shows the bisulfite control

6 Results and Discussion

The objective of the present study was to investigate whether the methylation levels of *PSEN1*, *ABCA7*, *ABCB1*, *ABCC1* and LINE-1 are potential biomarkers for the early diagnosis of late-onset Alzheimer's disease (LOAD). Whole blood DNA extracts from 39 Alzheimer's disease (AD) and 40 healthy control patients were provided by our co-operation partners Mag. Dr. Ellen Umlauf and Assoc. Prof. Dipl.-Ing. Dr. Maria Zellner, Institute of Physiology, Medical University of Vienna. Moreover, the DNA methylation levels of 9 pooled DNA extracts from AD patients and 9 pooled DNA extracts from controls were analyzed.

DNA of pooled extracts was converted in course of this diploma thesis, DNA of individual extracts had already been converted by Denana Avdic in course of her master thesis. Pools were created to reduce time and costs [108] and moreover to reduce the biological variation of samples which includes factors like lifestyle, age and genetic background [121].

Whole blood DNA amounts between 172 ng and 500 ng were bisulfite converted as described in section 4.2, amplified by PCR (see section 4.5 for details) and the DNA methylation status of *PSEN1*, *ABCA7*, *ABCB1* and *ABAC1* was determined by PSQ (see section 4.6 for details) and methylation levels of LINE-1 were analyzed by MS-HRM (see section 4.7 for details).

Values below 5% methylation were set as <LOQ and values above 95% were set as >ULOQ which was given by the manufacturer (Qiagen). For statistical calculations all values <LOQ were handled as $\frac{\mathrm{LOQ}}{2} = 2.5\%$ and all values >ULOQ were assumed as 97.5% [115].

6.1 Problems concerning the bisulfite conversion

The DNA methylation status in *ABCB1* promoter region was analyzed in whole blood extracts from 39 AD and 40 control patients, with a method developed in-house by Melanie Spitzwieser. A detailed description of the applied method is given in section 4 (experimental part) and section 7.8. The DNA methylation status of *ABCB1* ranged from <LOQ to 75%. It has to be considered that the values do not represent the actual methylation status of *ABCB1* due to the failed bisulfite conversion.

The bisulfite reaction was performed as described in section 4.2.

Bisulfite conversion of DNA from individual extracts had already been carried out by Denana Avdic in course of her master thesis. However, when the DNA was analyzed by

PSQ, bisulfite conversion turned out to be not complete. Most probably, the conversion failed because the kit had been stored inappropriately. All reagents were kept at -80°C. The required temperature for storage is, however, 2-8°C for the spin columns, *DNA Protect Buffer* (Qiagen) and *Buffer BD* (Qiagen). The *Bisulfite Solution* (Qiagen) and all other buffers should be stored at 15-25°C according to manufacturer's protocol (Qiagen). Pooled DNA extracts (P5, P6, P15, P16), *CpGenome universal methylated DNA* (Millipore) and *EpiTect human unmethylated control DNA* (Qiagen) were treated using the inappropriately stored kit at the beginning of the thesis. Inappropriate conversion was noticed during the bisulfite reaction setup, as well as in the pyrograms obtained by PSQ. After the bisulfite reaction set-up, it was striking that the solution did not turn blue. As a result, the bisulfite control during PSQ indicated a failed conversion with the incorrectly stored kit. Figure 37 shows the beginning of two pyrograms. The pyrogram at the top was obtained after using the kit that was stored at -80°C, that at the bottom after using a kit stored according to suggestions of the manufacturer. In contrast to the pyrogram at the bottom, the pyrogram at the top contains a peak at the position highlighted in orange (bisulfite control), indicating that the bisulfite conversion failed.

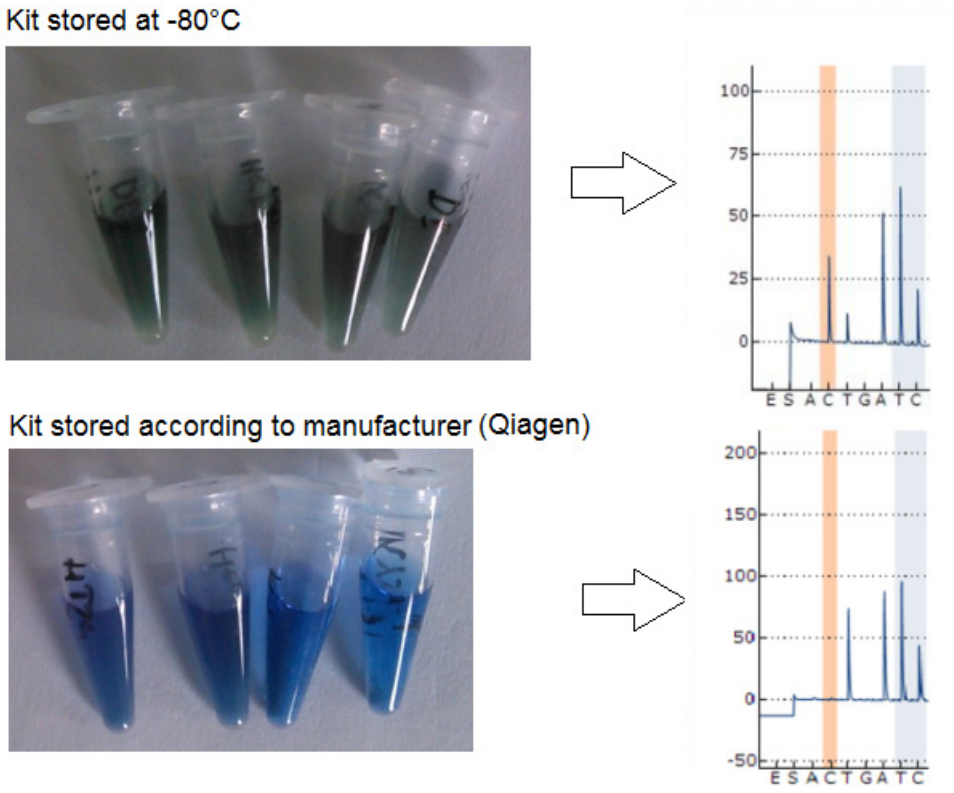

Figure 37: Influence of incorrect storage of the bisulfite kit on the color change during the bisulfite reaction and the bisulfite control in the pyrogram of *PSEN1* PSQ methylation analysis; PSQ bisulfite control shaded orange

However, not in all samples the bisulfite control indicated a failed conversion, but the results showed a failed conversion compared to samples that were converted with another kit. Table 21 lists the results for a comparison of the incorrectly stored kit and another kit for *ABCB1* and demonstrates the discrepancy between the methylation levels obtained with the two bisulfite kits.

Table 21: Comparison of the methylation status [%] of *ABCB1* obtained after bisulfite conversion with an incorrectly stored and a correctly stored bisulfite kit; standards (0% and 100% methylation), individual extracts K320 (control) and A214 (AD) and pooled extracts P5, P6 (AD) and P15, P16 (control)

Correct bisulfite conversion	**Methylation status [%]**						
Sample	**CpG1**	**CpG2**	**CpG3**	**CpG4**	**CpG5**	**CpG6**	**CpG7**
0% standard	<LOQ	<LOQ	<LOQ	<LOQ	<LOQ	<LOQ	<LOQ
100% standard	>ULOQ	>ULOQ	>ULOQ	93	87	78	88
K320	<LOQ	<LOQ	<LOQ	<LOQ	<LOQ	<LOQ	<LOQ
A214	<LOQ	<LOQ	<LOQ	<LOQ	<LOQ	<LOQ	<LOQ
P5	<LOQ	<LOQ	<LOQ	<LOQ	<LOQ	<LOQ	<LOQ
P6	<LOQ	<LOQ	<LOQ	6	<LOQ	<LOQ	<LOQ
P15	<LOQ	<LOQ	<LOQ	<LOQ	7	7	<LOQ
P16	<LOQ	<LOQ	<LOQ	5	<LOQ	<LOQ	<LOQ

Failed bisulfite conversion	**Methylation status [%]**						
Sample	**CpG1**	**CpG2**	**CpG3**	**CpG4**	**CpG5**	**CpG6**	**CpG7**
0% standard	<LOQ	<LOQ	>ULOQ	<LOQ	<LOQ	76	<LOQ
100% standard	69	>ULOQ	>ULOQ	88	63	57	43
K320	<LOQ	35	24	8	7	<LOQ	8
A214	<LOQ	7	7	11	<LOQ	17	<LOQ
P5	<LOQ	39	41	22	<LOQ	20	24
P6	16	73	22	79	17	6	34
P15	23	62	30	<LOQ	47	8	7
P16	6	55	31	26	8	9	10

Thus, DNA from pooled extracts was freshly converted with a bisulfite kit that had been stored correctly.

For further analyses, DNA from pooled extracts (P1-P9, AD and P11-P19, control), *CpGenome universal methylated DNA* (Millipore) and *EpiTect human unmethylated control DNA* (Qiagen) was freshly converted with a bisulfite kit that had been stored correctly and used for determination of the DNA methylation status.

6.2 Determination of the DNA methylation status of *PSEN1* in blood DNA extracts from AD and healthy control patients

Nine pooled DNA extracts from AD patients and nine pooled DNA extracts from controls were analyzed with a method (see section 5.1. for details) developed in-house.

DNA methylation status of *PSEN1* was analyzed in one to 12 replicates for each pooled sample. However, when we repeatedly analyzed pooled DNA extracts, we obtained rather scattering DNA methylation levels. In order to elucidate the reason for the low repeatability, we analyzed one sample (P12) eight times. In the first series, PCR amplification was carried out in four separate tubes and each of the PCR products was pyrosequenced once. In the second series, PCR amplification was carried out in a larger reaction setup and the PCR products were pyrosequenced four times. Table 22 demonstrates that DNA methylation levels obtained for CpG1 and CpG2 in series 1 were more scattering than DNA methylation levels obtained in series 2. These results indicate that the pyrosequencing reaction was highly repeatable. We assume that scattering of the DNA methylation levels was caused by the biological variability. Whole blood consists of various blood cell populations, and most probably, each of them has characteristic DNA methylation marks. Thus, instead of performing outlier tests, the medians of the methylation levels were used for statistic calculations.

Table 22: Comparison of DNA methylation status [%] of PSEN1 based on one or respectively four PCR amplifications on one day; pooled blood DNA extract P12 (control), n.a. … not available due to "high peak height deviation" in the pyrogram

Sample: P12	CpG1	CpG2	CpG3	CpG4	CpG5	CpG6	CpG7	CpG8	CpG9	CpG10
1 PCR amplification	8	10	<LOQ	8	<LOQ	<LOQ	<LOQ	<LOQ	<LOQ	<LOQ
	9	10	<LOQ	8	<LOQ	<LOQ	<LOQ	<LOQ	<LOQ	<LOQ
	9	11	<LOQ	8	<LOQ	<LOQ	<LOQ	<LOQ	<LOQ	<LOQ
	8	11	<LOQ	8	6	<LOQ	<LOQ	n.a.	n.a.	n.a.
4 PCR amplifications	9	9	<LOQ	<LOQ	<LOQ	<LOQ	<LOQ	<LOQ	<LOQ	<LOQ
	19	5	<LOQ	<LOQ	10	n.a.	n.a.	n.a.	n.a.	n.a.
	6	7	<LOQ	<LOQ	<LOQ	<LOQ	<LOQ	<LOQ	<LOQ	<LOQ
	11	7	5	7	<LOQ	<LOQ	n.a.	n.a.	n.a.	n.a.

The methylation levels obtained for the last 5-6 CpGs were frequently inaccurate (see section 5.1 for details, raw data see section 7.10) and excluded from further calculations.

The DNA methylation levels of *PSEN1* obtained for the pooled DNA extracts from AD patients and controls are summarized in a scatter plot in Figure 38. In AD patients, DNA methylation levels were in the range from <LOQ (<5%) to 15% (CpG1, AD), in controls from <LOQ to 9% (CpG1, control). In particular in AD patients, the DNA methylation status of CpG1 and CpG2 was higher than that of CpG3-CpG10.

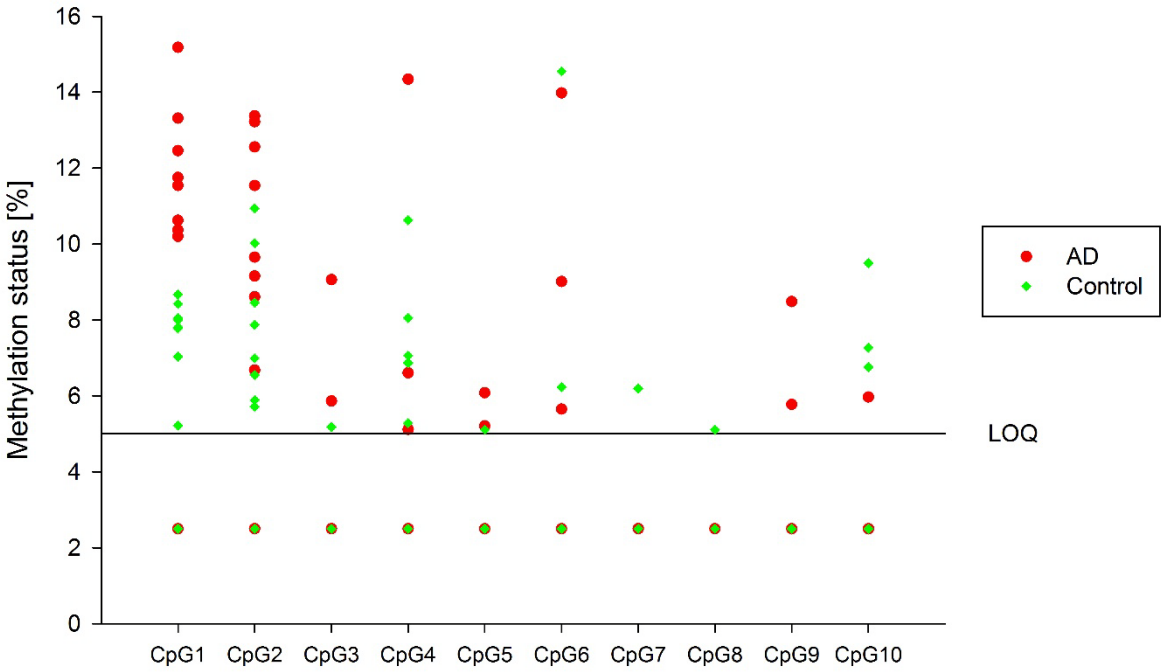

Figure 38: DNA methylation status [%] of *PSEN1* in pooled blood DNA extracts; median values of samples P1, P2, P4-P9 (AD, red) and P11-P19 (control, green) from at least 2 technical replicates and values from one analysis of P3

Table 23 summarizes statistical data of *PSEN1* methylation status in AD and control pooled blood DNA extracts showing the number (N) of valid values and values n.a. (not available), mean, median, standard deviation (SD), minimum (min) and maximum (max) of DNA methylation status.

Table 23: Statistical data of *PSEN1* methylation status [%]; mean and median of DNA methylation status of pooled blood DNA extracts from Alzheimer patients and controls, standard deviation (SD), minimum (min) and maximum (max) of DNA methylation levels; N valid… number of accurate values, N n.a. … number of values not available due to "high peak height deviation" in the pyrogram

Group		CpG1	CpG2	CpG3	CpG4	CpG5	CpG6	CpG7	CpG8	CpG9	CpG10
AD	N valid	9	9	9	9	9	9	7	5	5	5
	N n.a.	0	0	0	0	0	0	2	4	4	4
	Mean [%]	11	10	<LOQ	<LOQ	<LOQ	<LOQ	<LOQ	<LOQ	<LOQ	<LOQ
	Median [%]	12	10	<LOQ	<LOQ	<LOQ	<LOQ	<LOQ	<LOQ	<LOQ	<LOQ
	SD [%]	4	4	2	4	1	4	0	0	3	2
	Min [%]	<LOQ	<LOQ	<LOQ	<LOQ	<LOQ	<LOQ	<LOQ	<LOQ	<LOQ	<LOQ
	Max [%]	15	13	9	14	6	14	<LOQ	<LOQ	9	6
Control	N valid	9	9	9	9	9	9	9	9	5	6
	N missing	0	0	0	0	0	0	0	0	4	3
	Mean [%]	7	7	<LOQ	6	<LOQ	<LOQ	<LOQ	<LOQ	<LOQ	5
	Median [%]	8	7	<LOQ	7	<LOQ	<LOQ	<LOQ	<LOQ	<LOQ	<LOQ
	SD [%]	2	3	1	3	1	4	1	1	0	3
	Min [%]	<LOQ	<LOQ	<LOQ	<LOQ	<LOQ	<LOQ	<LOQ	<LOQ	<LOQ	<LOQ
	Max [%]	9	11	5	11	5	15	6	5	<LOQ	10

Mann–Whitney U test [117] was performed for CpGs 1, 2 and 4 to test if there was a significant difference in the methylation status of *PSEN1* between AD patients and controls and the results are shown in Table 24.

Table 24: Results of Mann-Whitney U test for DNA methylation status of *PSEN1*

	CpG1	CpG2	CpG4
Asymptotic significance (2-tailed)	0.005	0.064	0.143

A significant difference (p=0.005) was found for CpG1 (Figure 39).

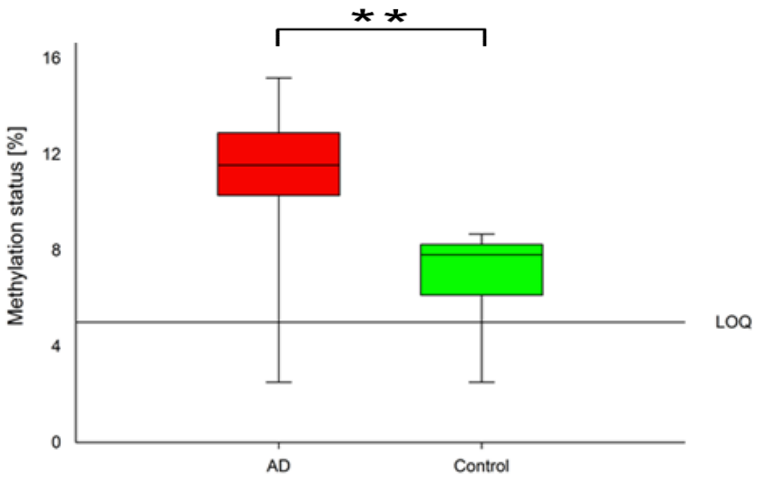

Figure 39: Box plots presenting the DNA methylation status [%] of *PSEN1* in CpG1 in pooled blood DNA extracts; median values of samples P1, P2, P4-P9 (AD, red) and P11-P19 (control, green) from at least 2 technical replicates and values from one analysis of P3, **p ≤ 0.010

6.3 Determination of the DNA methylation status of *ABCA7* in pooled blood DNA extracts from AD and control patients

The pooled blood DNA extracts were analyzed with methods developed in-house and described in detail in section 5.2. The DNA methylation status of three regions within the *ABCA7* gene was determined in two to four replicates.

6.3.1 DNA methylation of *ABCA7* analyzed with primer set 1

The results of the DNA methylation status of *ABCA7* (method *ABCA7* primer set 1, see section 5.2.1 for details) are summarized in a scatter plot in Figure 40 (raw data see section 7.10). Figure 40 shows that the pooled blood DNA extracts drastically differed in the median values of the methylation status in the targeted region, e.g. methylation levels ranging from <LOQ to >ULOQ in CpG4. Although the methylation levels in CpG3 and CpG6 were less variable, no difference was found between AD patients and controls.

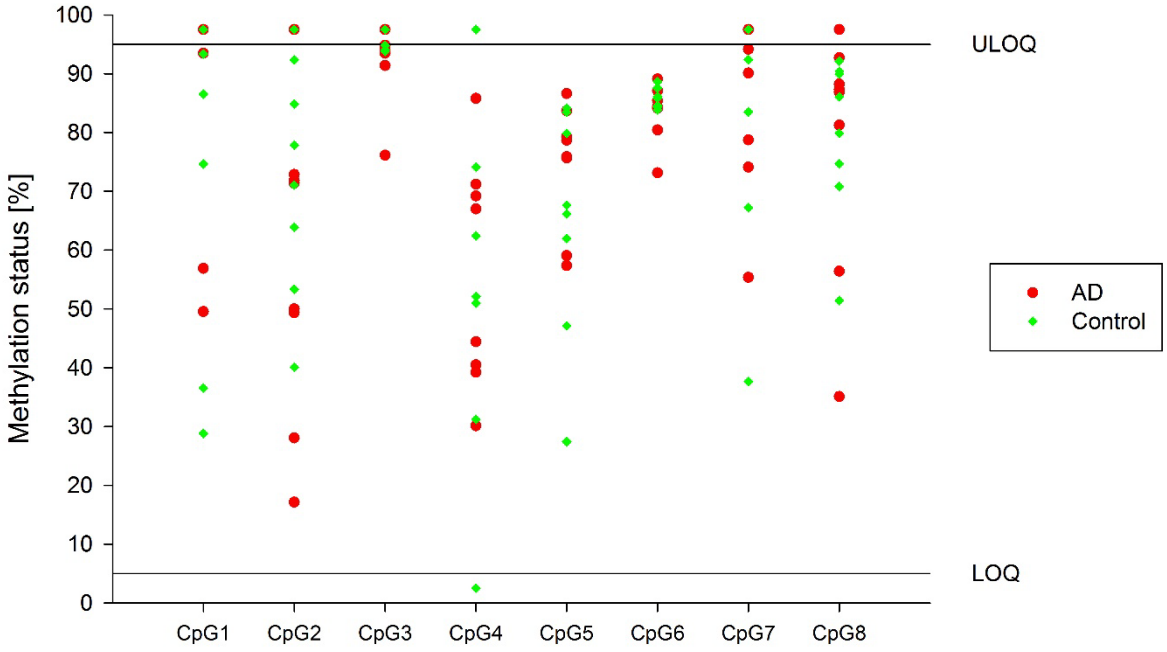

Figure 40: DNA methylation status [%] of *ABCA7* (analyzed with primer set 1) in pooled blood DNA extracts; median values of samples P1-P9 (AD, red) and P11-P19 (control, green) from at least 2 technical replicates

Table 25 summarizes the statistical data of *ABCA7* methylation levels analyzed with primer set 1 in AD patients and controls.

Table 25: Statistical data of *ABCA7* methylation status analyzed with primer set 1; mean and median of DNA methylation status of pooled blood DNA extracts from Alzheimer patients and controls, standard deviation (SD), minimum (min) and maximum (max) of DNA methylation levels

Group		**CpG1**	**CpG2**	**CpG3**	**CpG4**	**CpG5**	**CpG6**	**CpG7**	**CpG8**
AD	Mean [%]	86	57	92	56	75	84	86	78
	Median [%]	>ULOQ	61	94	56	77	84	92	87
	SD [%]	20	26	7	20	11	5	15	21
	Min [%]	50	17	78	30	57	73	55	35
	Max [%]	>ULOQ	>ULOQ	>ULOQ	86	87	89	>ULOQ	>ULOQ
Control	Mean [%]	77	73	>ULOQ	47	65	86	84	79
	Median [%]	90	75	>ULOQ	52	67	86	95	83
	SD [%]	28	20	2	33	20	2	21	14
	Min [%]	29	40	94	<LOQ	28	84	38	51
	Max [%]	>ULOQ	>ULOQ	>ULOQ	>ULOQ	84	89	>ULOQ	92

To evaluate a significant difference between the DNA methylation status in AD patients and controls, a Mann–Whitney U test [117] was performed for all CpGs. The results are summarized in Table 26.

Table 26: Results of Mann-Whitney U test for DNA methylation status of *ABCA7* (analyzed with primer set 1)

	CpG1	CpG2	CpG3	CpG4	CpG5	CpG6	CpG7	CpG8
Asymptotic significance (2-tailed), p-value	0.287	0.270	0.106	0.674	0.462	0.208	0.826	0.674

For none of the CpGs a significant difference was found.

6.3.2 DNA methylation of *ABCA7* analyzed with primer set 2

The DNA methylation levels obtained for ABCA7 with primer set 2 (see section 5.2.2 for details) are summarized in a scatter plot in Figure 41 (raw data see section 7.10). The target region is located 26046 bp upstream of the target region analyzed using primer set 1.

DNA methylation in pooled blood DNA extracts from AD patients and controls ranged from 70% to >ULOQ and showed a lower variability compared to DNA methylation of *ABCA7* analyzed with method *ABCA7* primer set 1.

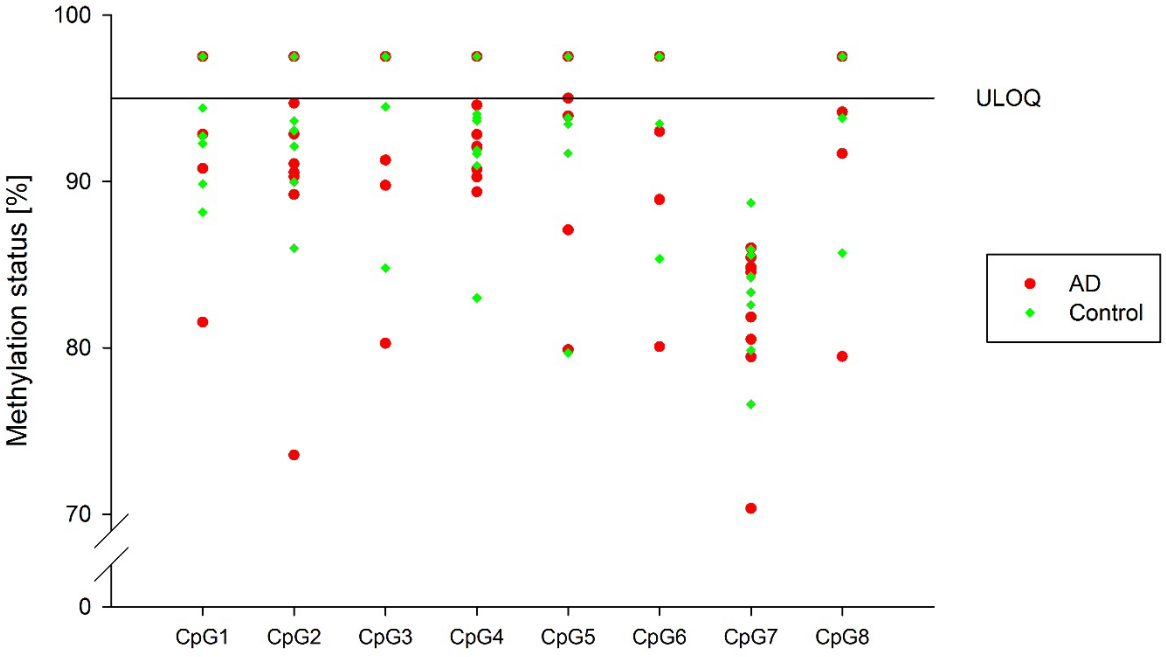

Figure 41: DNA methylation status [%] of *ABCA7* (analyzed with primer set 2) in pooled blood DNA extracts; median values of samples P1-P9 (AD, red) and P11-P19 (control, green) from at least 2 technical replicates

Table 27 summarizes the statistical data of DNA methylation levels of *ABCA7* (analyzed with primer set 2) in pooled blood DNA extracts from AD patients and controls.

Table 27: Statistical data of *ABCA7* methylation status analyzed with primer set 2; mean and median of DNA methylation status of pooled blood DNA extracts from Alzheimer patients and controls, standard deviation (SD), minimum (min) and maximum (max) of DNA methylation levels

Group		**CpG1**	**CpG2**	**CpG3**	**CpG4**	**CpG5**	**CpG6**	**CpG7**	**CpG8**
AD	Mean [%]	94	91	94	93	94	94	82	94
	Median [%]	>ULOQ	91	>ULOQ	92	>ULOQ	>ULOQ	85	>ULOQ
	SD [%]	5	7	6	3	6	6	5	6
	Min [%]	82	74	80	89	80	80	70	79
	Max [%]	>ULOQ	>ULOQ	>ULOQ	>ULOQ	>ULOQ	>ULOQ	86	>ULOQ
Control	Mean [%]	94	93	>ULOQ	93	94	>ULOQ	83	>ULOQ
	Median [%]	94	93	>ULOQ	94	>ULOQ	>ULOQ	84	>ULOQ
	SD [%]	4	4	4	4	6	4	4	4
	Min [%]	88	86	85	83	80	85	77	86
	Max [%]	>ULOQ	>ULOQ	>ULOQ	>ULOQ	>ULOQ	>ULOQ	89	>ULOQ

To test for a significant difference in the methylation levels in *ABCA7* (method *ABCA7* primer set 2) between AD patients and controls, Mann–Whitney U test [117] was performed for CpGs 1, 2, 4 and 7. The results are summarized in Table 28.

Table 28: Results of Mann-Whitney U test for DNA methylation status of *ABCA7* (analyzed with primer set 2)

	CpG1	CpG2	CpG4	CpG7
Asymptotic significance (2-tailed), p-value	0.467	0.756	0.824	0.757

No significant differences could be observed in the DNA methylation status of *ABCA7* between pooled blood DNA extracts from AD and control patients.

6.3.3 DNA methylation of *ABCA7* analyzed with primer set 3

The results of the analysis of the methylation status of 7 CpGs targeted by the method based on primer set 3 (see section 5.2.3 for details) are summarized in Figure 42 (raw data see section 7.10).

Repeated analysis of one and the same pooled DNA extract yielded similar results, indicating high technical repeatability. Methylation levels of the CpGs in the promoter region were in the range from 78% to >ULOQ.

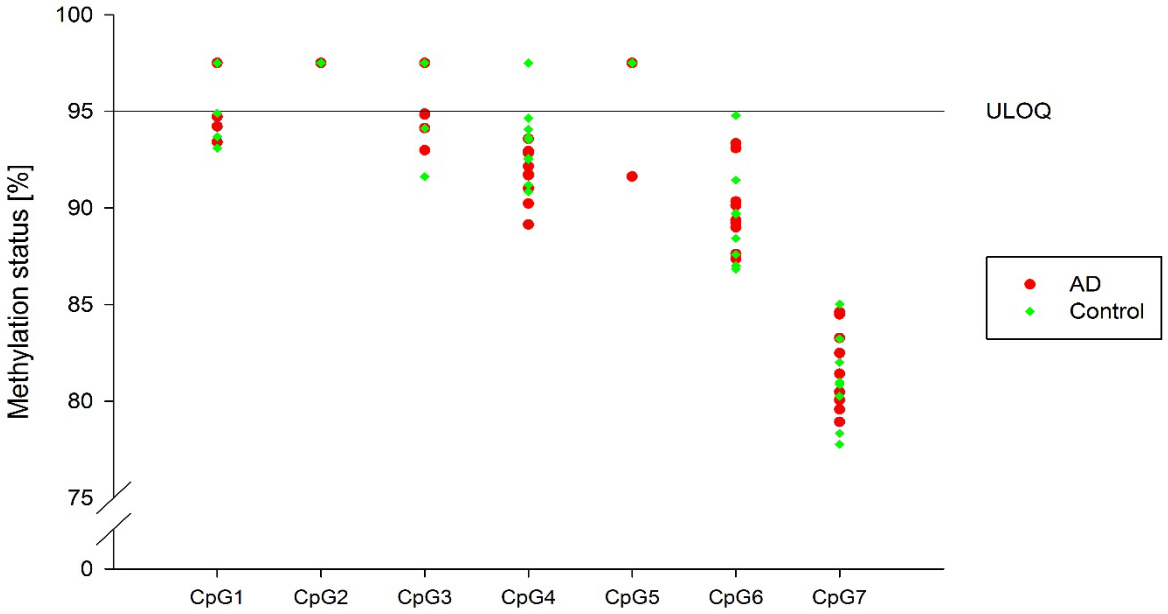

Figure 42: DNA methylation status [%] of *ABCA7* (analyzed with primer set 3) in pooled blood DNA extracts; median values of samples P1-P9 (AD, red) and P11-P19 (control, green) from at least 2 technical replicates

Table 29 summarizes the statistics of the DNA methylation status of *ABCA7* (method *ABCA7* primer set 3) in AD patients and controls showing mean, median, standard deviation (SD), minimum (min) and maximum (max) of DNA methylation levels.

Table 29: Statistical data of *ABCA7* promoter methylation status analyzed with primer set 3; mean and median of DNA methylation status of pooled blood DNA extracts from Alzheimer patients and controls, standard deviation (SD), minimum (min) and maximum (max) of DNA methylation levels

Group		CpG1	CpG2	CpG3	CpG4	CpG5	CpG6	CpG7
AD	Mean [%]	>ULOQ	>ULOQ	>ULOQ	92	>ULOQ	90	82
	Median [%]	>ULOQ	>ULOQ	>ULOQ	92	>ULOQ	89	81
	SD [%]	2	0	2	1	2	2	2
	Min [%]	93	>ULOQ	93	89	92	87	79
	Max [%]	>ULOQ	>ULOQ	>ULOQ	94	>ULOQ	93	85
Control	Mean [%]	>ULOQ	>ULOQ	>ULOQ	93	>ULOQ	89	81
	Median [%]	>ULOQ	>ULOQ	>ULOQ	94	>ULOQ	88	81
	SD [%]	2	0	2	2	0	3	2
	Min [%]	93	>ULOQ	92	91	>ULOQ	87	78
	Max [%]	>ULOQ	>ULOQ	>ULOQ	>ULOQ	>ULOQ	95	85

Due to the high technical repeatability, mean values (and not median values) of DNA methylation levels were used for statistic calculations. Student's t-test [117], based on the comparison of mean values, was performed for CpGs 4, 6 and 7 to evaluate a significant

difference in the DNA methylation status between AD patients and controls. The results are shown in Table 30.

Table 30: Results of Levene's test for equality of variances and Student's t-test for equality of means of DNA methylation status of *ABCA7* promoter (analyzed with primer set 3)

	Levene's test for equality of variances Significance, p-value	t-test for equality of means significance (2-tailed), p-value
CpG4	0.470	0.054 0.056
CpG6	0.550	0.499 0.499
CpG7	0.731	0.530 0.530

No significant differences in the DNA methylation status of the *ABCA7* promoter could be observed between pooled blood DNA extracts from AD and control patients.

6.4 Determination of the DNA methylation status of *ABCB1* in blood DNA extracts from AD and control patients

Seven pooled blood DNA extracts from AD patients (P1-P7) and seven pooled blood DNA extracts from control patients (P11-P17) were analyzed with a method developed in-house by Melanie Spitzwieser. A detailed description of the applied method is given in section 4 (experimental part) and section 7.8.

Determination of the DNA methylation status of the pooled blood DNA extracts mainly resulted in values <LOQ as seen in Table 31, thus no further measurements of pooled DNA extracts were performed.

Table 31: DNA methylation status of *ABCB1* in pooled blood DNA extracts; P1-7 (AD), P11-17 (control)

	Methylation status [%]						
Sample	**CpG1**	**CpG2**	**CpG3**	**CpG4**	**CpG5**	**CpG6**	**CpG7**
P1	<LOQ	<LOQ	<LOQ	<LOQ	<LOQ	<LOQ	<LOQ
P2	<LOQ	<LOQ	<LOQ	<LOQ	<LOQ	<LOQ	<LOQ
P3	<LOQ	<LOQ	<LOQ	<LOQ	<LOQ	<LOQ	<LOQ
P4	<LOQ	<LOQ	<LOQ	5	<LOQ	<LOQ	<LOQ
P5	<LOQ	<LOQ	<LOQ	<LOQ	<LOQ	<LOQ	<LOQ
P6	<LOQ	<LOQ	<LOQ	6	<LOQ	<LOQ	<LOQ
P7	<LOQ	<LOQ	<LOQ	<LOQ	<LOQ	<LOQ	<LOQ
P11	<LOQ	<LOQ	<LOQ	<LOQ	<LOQ	<LOQ	<LOQ
P12	<LOQ	<LOQ	<LOQ	<LOQ	<LOQ	<LOQ	<LOQ
P13	<LOQ	7	10	7	6	6	<LOQ
P14	<LOQ	<LOQ	<LOQ	<LOQ	<LOQ	<LOQ	<LOQ
P15	<LOQ	<LOQ	<LOQ	<LOQ	7	7	<LOQ
P16	<LOQ	<LOQ	<LOQ	5	<LOQ	<LOQ	<LOQ
P17	<LOQ	6	<LOQ	<LOQ	<LOQ	<LOQ	<LOQ

6.5 Determination of the DNA methylation status of *ABCC1* in blood DNA extracts from AD and control patients

Nine pooled blood DNA extracts from AD (P1-P9) patients and nine pooled blood DNA extracts from control patients (P11-P19) were analyzed with a method developed in-house by Melanie Spitzwieser. A detailed description of the applied method is given in section 4 (experimental part) and section 7.8.

In most pooled DNA extracts, the methylation status was found to be <LOQ as seen in Table 32. Thus, no further analyses were carried out.

Table 32: Methylation status of *ABCC1* in pooled blood DNA extracts; P1-9 (AD), P11-19 (control)

	Methylation status [%]							
Sample	**CpG1**	**CpG2**	**CpG3**	**CpG4**	**CpG5**	**CpG6**	**CpG7**	**CpG8**
P1	<LOQ	<LOQ	<LOQ	<LOQ	<LOQ	<LOQ	<LOQ	<LOQ
P2	<LOQ	<LOQ	<LOQ	5	<LOQ	<LOQ	<LOQ	10
P2	<LOQ	16	<LOQ	<LOQ	<LOQ	<LOQ	<LOQ	<LOQ
P3	<LOQ	16	<LOQ	<LOQ	<LOQ	<LOQ	<LOQ	<LOQ
P4	<LOQ	<LOQ	<LOQ	<LOQ	<LOQ	<LOQ	<LOQ	<LOQ
P5	<LOQ	<LOQ	<LOQ	<LOQ	<LOQ	<LOQ	<LOQ	<LOQ
P6	<LOQ	<LOQ	<LOQ	<LOQ	10	<LOQ	19	<LOQ
P7	<LOQ	6	<LOQ	<LOQ	<LOQ	<LOQ	<LOQ	<LOQ
P8	6	12	<LOQ	10	<LOQ	<LOQ	<LOQ	<LOQ
P9	<LOQ	<LOQ	<LOQ	9	<LOQ	<LOQ	10	<LOQ
P11	<LOQ	7	<LOQ	<LOQ	<LOQ	5	<LOQ	<LOQ
P12	<LOQ	<LOQ	<LOQ	<LOQ	<LOQ	<LOQ	<LOQ	<LOQ
P12	<LOQ	<LOQ	<LOQ	<LOQ	<LOQ	<LOQ	<LOQ	<LOQ
P13	<LOQ	38	<LOQ	<LOQ	<LOQ	<LOQ	9	<LOQ
P14	<LOQ	<LOQ	<LOQ	<LOQ	<LOQ	<LOQ	<LOQ	<LOQ
P15	<LOQ	<LOQ	<LOQ	<LOQ	<LOQ	<LOQ	<LOQ	<LOQ
P16	<LOQ	<LOQ	<LOQ	<LOQ	<LOQ	8	<LOQ	<LOQ
P17	<LOQ	<LOQ	<LOQ	<LOQ	<LOQ	<LOQ	<LOQ	<LOQ
P18	11	7	<LOQ	<LOQ	7	<LOQ	<LOQ	<LOQ
P19	<LOQ	<LOQ	<LOQ	<LOQ	<LOQ	<LOQ	<LOQ	<LOQ

6.6 HRM analysis of LINE-1

Nine pooled blood DNA extracts from AD (P1-P9) patients and nine pooled blood DNA extracts from control patients (P11-P19) were analyzed with a method developed in-house by Melanie Spitzwieser. A detailed description of the applied method is given in section 4.7 (experimental part). Standards were used to obtain a calibration curve as described in detail in section 4.7.

Figure 43 and Figure 44 show the normalized MS-HRM curves and the first negative derivative of the fluorescence for standards differing in the methylation status, respectively.

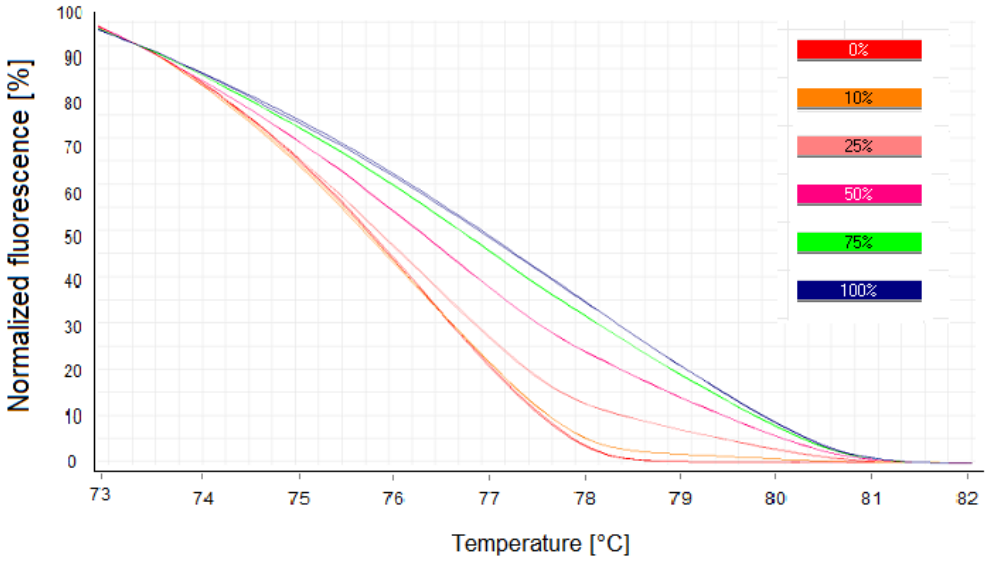

Figure 43: MS-HRM of LINE-1; normalized fluorescence against temperature for standards (0%, 10%, 25%, 50%, 75% and 100% methylated) produced by mixing bisulfite converted *EpiTect human unmethylated control DNA* and bisulfite converted *CpGenome universal methylated DNA*

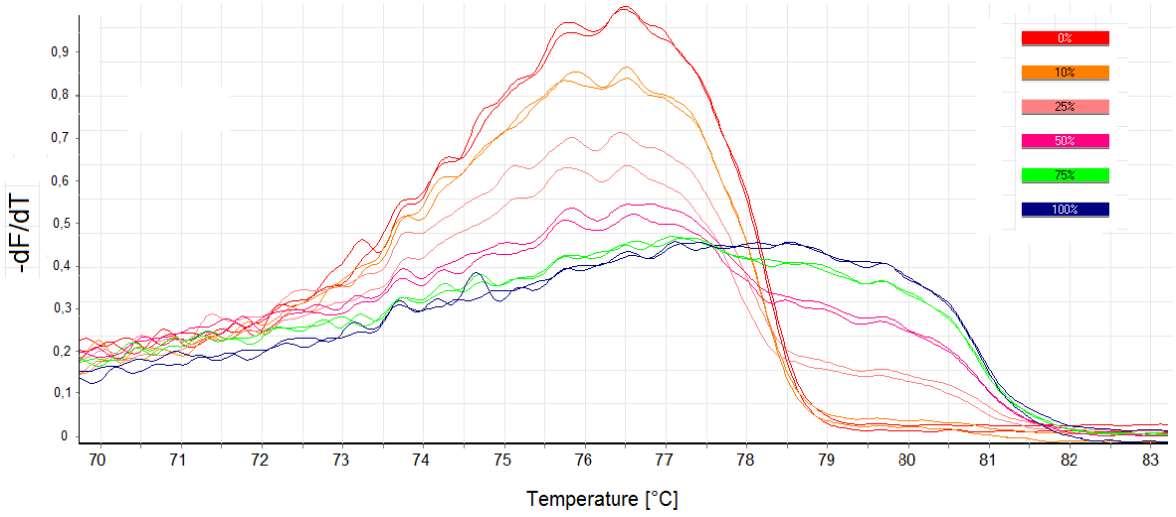

Figure 44: MS-HRM of LINE-1; first negative derivative of the normalized fluorescence over temperature (-dF/dT) against temperature for standards (0%, 10%, 25%, 50%, 75% and 100% methylated) produced by mixing bisulfite converted *EpiTect human unmethylated control DNA* and bisulfite converted *CpGenome universal methylated DNA*

A Four Parameter Logistic regression model was used for curve-fitting analysis. The equation describing the sigmoidal calibration curve was

$$y = y_0 + \frac{a}{1 + (\frac{x}{x_0})^b}$$

Equation 4: Equation for the model for the MS-HRM calibration curve

where y is the fluorescence, x is the methylation status and a, b, x_0 and y_0 being the four parameters.The calibration curve is shown in Figure 45.

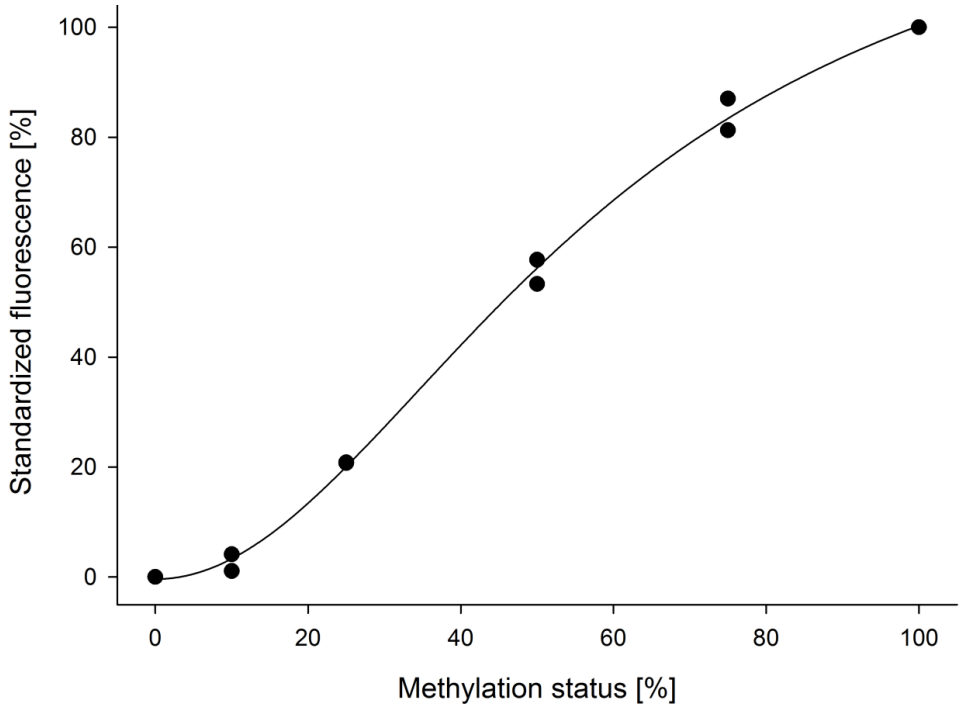

Figure 45: MS-HRM calibration curve for LINE-1; bisulfite converted standards with methylation status of 0, 10, 25, 50, 75 and 100% were analyzed in duplicates

Pooled blood DNA extracts were analyzed in four replicates (raw data see section 7.10). DNA methylation levels were determined to be close to 100%. Standards (bisulfite converted *EpiTect human unmethylated control DNA*, Qiagen and bisulfite converted *CpGenome Universal methylated DNA*, Millipore) were declared to have a methylation status of either 0% or 100%. However, our result indicated that the commercially available methylated standard was not completely methylated in the targeted region. It was described previously that commercial standards may not be fully methylated or unmethylated [100].

Table 33 summarizes the statistical data of LINE-1 methylation status in AD and control pooled blood DNA extracts, showing mean, median, standard deviation (SD), minimum (min) and maximum (max) of DNA methylation status in LINE-1.

Table 33: Statistical data of LINE-1 methylation status; mean, median, standard deviation (SD), minimum (min) and maximum (max) of DNA methylation levels in AD and control pooled DNA extracts

	AD	Control
Mean [%]	102	98
Median [%]	101	97
SD [%]	4	3
Min [%]	99	93
Max [%]	110	102

Mann–Whitney U test [117] was performed to test for a significant difference in the methylation status of LINE-1 between AD and control patients. Figure 46 indicates that the methylation status of LINE-1 was found to be significantly higher (p=0.015) in AD patients compared to controls. However, since the methylated standard used for establishing the calibration curve was not fully methylated (as described above), the methylation levels determined are systematically too high.

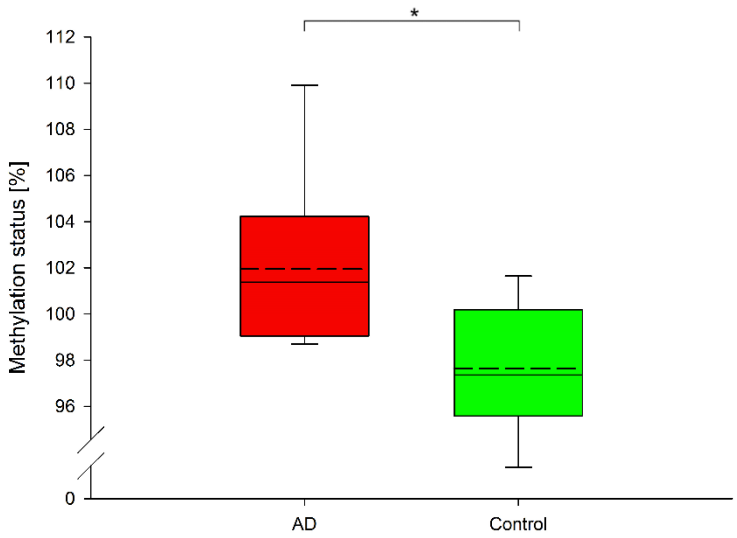

Figure 46: DNA methylation status of LINE-1 in pooled blood DNA extracts of AD (red) and control (green) patients; mean values from 4 technical replicates, *p ≤ 0.050, dashed line: mean, solid line: median

6.7 Analysis of cancer cell lines

Since data on the methylation status of *ABCA7* in cancer cells has not been published so far, in a preliminary experiment we determined methylation levels of *ABCA7* (method *ABCA7* primer set 3, see section 5.2.3 for details) in various drug sensitive and drug resistant cancer cell lines of different origin. The methylation levels are summarized in Figure 47.

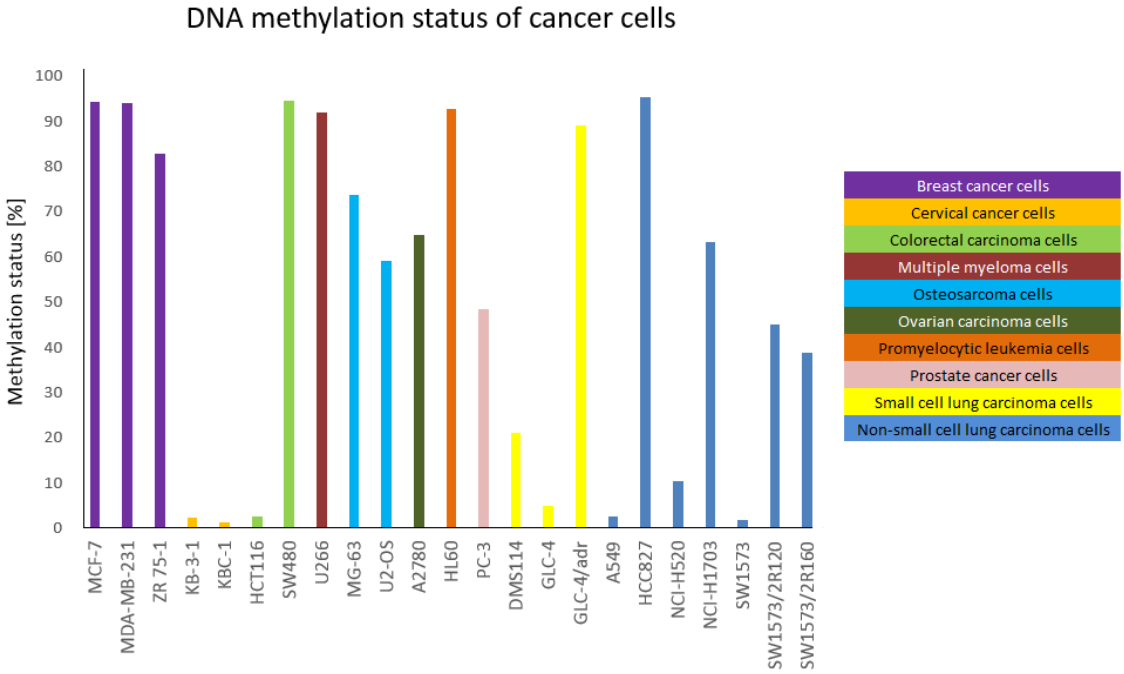

Figure 47: DNA methylation status of ABCA7 primer set 3 in cancer cell lines

The screening experiment showed that the cancer cell lines showed very different methylation levels. These findings should be confirmed in further analyses. In addition, it would be interested to investigate if DNA methylation plays a role in regulation of gene expression of *ABCA7*.

6.8 Discussion and conclusion

Alzheimer's disease is a polygenic and complex disease. In this thesis the methylation levels of *PSEN1*, *ABCA7*, *ABCB1* and *ABCC1* were analyzed by PSQ whereas the global DNA methylation status was analyzed by MS-HRM targeting LINE-1 in order to investigate if the DNA methylation status is a potential biomarker for early diagnosis of AD.

39 DNA extracts from whole blood of AD patients and 40 from healthy controls as well as nine pooled blood DNA extracts from AD patients and nine pooled blood DNA extracts from control patients were analyzed with methods developed in-house.

The multi-pass transmembrane protein *PSEN1* is part of the machinery involved in the cleavage of amyloid precursor protein and therefore plays a role in the pathophysiology of AD [19, 47].

Methylation levels determined in this study showed a high variability, meaning that values, obtained for the DNA methylation status of the analyzed CpGs, differed within the repeated measurements of one pooled DNA extract and one CpG. Methylation levels ranged from <LOQ (<5%) to 15%. Due to the high biological variability (heterogeneity due to the presence of methylated and unmethylated DNA strands in one and the same extract), medians of the methylation levels determined in replicates were used for statistical analyses.

A significant difference (p=0.005) between pooled AD and pooled control DNA extracts could be observed for one CpG (CpG1) in the *PSEN1* promoter region.

Tannorella *et al.* (2015) [122] analyzed blood DNA from 120 LOAD patients and 115 healthy controls by MS-HRM and did not find any difference in DNA methylation levels in *PSEN1* promoter region (methylation levels 0.54% ± 0.14, AD and 0.67% ± 0.15, controls) between AD cases and controls. The region analyzed by Tannorella *et al.* overlaps with the region analyzed during this thesis. These findings are in line with results published by Carboni *et al.* (2015) [123], who determined peripheral blood DNA methylation of *PSEN1* in 20 AD patients and 19 healthy controls by methylation-specific real-time PCR. The region investigated by Carboni *et al.* overlaps with the last 6 CpGs analyzed in this thesis. However, methylation levels obtained for the last 5-6 CpGs were frequently highlighted in yellow (or red) in the pyrogram, most frequently due to "high peak height deviation" or due to "high peak height deviation in variable position", indicating that the methylation status given was inaccurate. Thus, these values were excluded from statistical analyses. Nevertheless, the DNA methylation status of *PSEN1* was <LOQ in most samples, which is in line with results of Carboni *et al.* Moreover the DNA methylation status of *PSEN1* showed a large variability in each group (AD and control) [123] which is in line with our findings. In contrast, low methylation levels (AD 1.6%; control 2.7%) but significant

differences were determined by Bakulski *et al.* (2012) in post mortem frontal cortex samples of 12 LOAD patients and 12 controls using a *Infinium HumanMethylation27 BeadArray* (Illumina) [124]. Even if brain tissue samples collected post mortem may provide more accurate information and help understanding the underlying mechanisms, these samples give only information about the end-stage of the disease, neither about disease development nor possible diagnostics [81]. Blood is easier to collect compared to brain tissue samples and therefore more appropriate for future diagnostic procedures. However, it has to be considered that different types of biological specimens may show different methylation levels. Wang *et al.* (2008) did not observe any tissue specific differences in methylation levels but they found differences in methylation levels between lymphocytes and brain samples [36]. The discrepancies between the mentioned studies could be a result of methodological differences, the complexity of the analysis of human samples or the analysis of different tissues (brain tissue vs. blood DNA) [123]. The total variability between samples is the sum of biological variability and technical variability. The biological variability is the sum of differences in age, genetic background, lifestyle and health status. Of course sex plays an important role too but in this study only blood obtained from female patients was investigated.

ABC transporters, the largest group of active transporters [60], are associated with multidrug resistance [62] but their role in the CNS has not been deciphered so far [61].

ATP-binding cassette sub-family A member 7 (ABCA7) plays a major role in phagocytosis of neuronal debris [65] and is involved in the transport of phospholipids and thus could influence Aβ accumulation and lipid metabolism [63, 66]. Recent genome-wide association studies have shown an association of ABCA7 with LOAD. In this study we could not confirm the hypomethylation in LOAD at a CGI shore, located in a non-coding region of *ABCA7*, reported by Humphries et al. (2015) [70]. Humphries *et al.* [70] identified differences in the DNA methylation status of *ABCA7* between post mortem human brain samples of eight LOAD and eight control samples using a *Infinium HumanMethylation450* bead chip (Illumina).

Yu *et al.* (2015) [69] analyzed the DNA methylation at loci associated with AD using an *InfiniumHumanMethylation450* bead assay (Illumina). They analyzed DNA extracts from grey matter of the dorsolateral prefrontal cortex in 740 patients, 60.4% suffering from AD. Three CpGs were associated with AD and two of them were close to the 3' untranslated region of *ABCA7*. Yu *et al.* (2015) showed that an increased burden of AD pathologies goes along with increased DNA methylation of *ABCA7* [69].

In the current thesis two different primer sets were designed for *ABCA7* based on regions analyzed by Yu *et al.* (2015) [69] and Humphries *et al.* (2015) [70]. Another primer set was designed to analyze the methylation status in the promoter region of *ABCA7*.
The region analyzed with primer set 2 is located 2818 bp downstream from the promoter region (analyzed with primer set 3) of *ABCA7.* The region based on Yu *et al.* (2015) [69] is located 26046 bp downstream of the region analyzed with primer set 2.

The methylation status determined with primer set 1 showed a high variability among all subjects (AD as well as controls) and even ranged from <LOQ to >ULOQ (>95%) in one CpG (CpG4, control). Only two out of eight CpGs showed a narrow distribution, e.g. methylation levels of 84% ± 5 (AD) and 86% ± 2 (control) in CpG6. The methylation status determined with primer set 2 also showed a variability among the subjects but not as drastically as it did with primer set 1. The methylation degrees ranged from 70% to >ULOQ. Analysis with primer set 3 resulted in a high technical repeatability and methylation degrees were high, ranging from 78 to >ULOQ. Three of the seven analyzed CpGs showed mean methylation levels >ULOQ.
However, no significant differences could be observed in the methylation status of *ABCA7* between pooled AD and pooled control extracts.

ABCB1 as well as *ABCC1* play a role in the blood-brain barrier [78]. ABCB1 is an important transporter with a broad specificity for various drugs [71] as well as lipids. Therefore, it is characterized as a drug pump and associated with multidrug resistance. Currently, there is no direct evidence for special pathways by which AD could be influenced by ABCB1 [61].
The *ABCC1* gene is also associated with multidrug resistance [76]. Krohn *et al.* (2011) showed that Aβ accumulated with a deficiency of ABCC1 in a mouse model for AD. Moreover activation of *ABCC1* led to reduced Aβ levels [77]. Aβ leads to histopathological characteristics of AD [12].

The methylation status of *ABCB1* and *ABCC1* was investigated with methods developed in-house by Melanie Spitzwieser. The methylation level in 18 (9 AD, 9 controls) pooled blood DNA extracts was mainly <LOQ, therefore no further analyses of pooled blood DNA extracts were performed for *ABCB1* and *ABCC1*.
For *ABCB1* 39 DNA extracts from whole blood of AD patients and 40 DNA extracts of healthy controls were analyzed. However, no comparison of the DNA methylation levels of *ABCB1* between DNA extracts and pooled DNA extracts was possible because of the failed bisulfite conversion.

LINE-1 is a repetitive element that accounts for about 17% of the human genome [79] and can be analyzed to estimate global DNA methylation [46].

Bollati *et al.* (2011) showed an increase of LINE-1 methylation status in AD compared to a control group [81]. They investigated whole blood DNA of 43 AD patients and 38 controls using quantitative bisulfite-PCR pyrosequencing. In contrast, Hernández et al. (2014) did not find any difference in DNA methylation status in peripheral blood samples between 28 LOAD samples and 30 control samples using MS-HRM [125].

In this study nine pooled blood DNA extracts from AD patients and nine pooled blood DNA extracts from control patients were analyzed with a method developed in-house by Melanie Spitzwieser. A slight but significant ($p=0.015$) difference in the DNA methylation status was observed between AD patients and controls. The methylation status of LINE-1 was higher in pooled blood DNA extracts from AD patients compared to pooled blood DNA extracts from healthy controls. However, no statement can be made about the exact methylation degree of LINE-1 because the commercial methylated standard, required for calibration, was found to be not completely methylated.

Analyzing human samples is complex and can cause discrepancies between studies [123]. In this study, DNA was derived from blood cells. Blood contains various blood cell populations and one cannot exclude that different types of cells are analyzed. The composition of cells can vary in its subpopulations. Because of this fact the high variability in the results for methylation status is comprehensible.

A potential way to reduce this variability would be isolating for example white blood cells before extracting DNA. This procedure is time-consuming and also cost-intensive but could be an approach for future investigations and reliable explanations of the variability.

7 Appendix

7.1 List of utensils

7.1.1 Chemicals and kits

25 bp DNA ladder	Thermo Fisher Scientific (Austria, Vienna)
Agarose	Sigma-Aldrich Handels Gmbh (Austria, Vienna)
CpGenome universal methylated DNA	Millipore, part of Merck (Austria, Vienna)
DNA electrophoresis sample loading dye	Bio-Rad Laboratories (Austria, Vienna)
DNA exitus plus IF	AppliChem (Germany, Darmstadt)
EpiTect fast DNA bisulfite kit	Qiagen (Germany, Hilden)
EpiTect human unmethylated control DNA	Qiagen (Germany, Hilden)
EpiTect MS-HRM PCR kit	Qiagen (Germany, Hilden)
Ethanol (absolute)	VWR International (Austria, Vienna)
GelRed nucleic acid stain	Biotium, distributor VWR International (Austria, Vienna)
Milli-Q water	
Nucleic acid sample loading buffer, 5x	Bio-Rad Laboratories (Austria, Vienna)
Primer	Sigma-Aldrich Handels Gmbh (Austria, Vienna)
PyroMark denaturation solution	Qiagen (Germany, Hilden)
PyroMark PCR kit	Qiagen (Germany, Hilden)
PyroMark Q24 advanced CpG reagents	Qiagen (Germany, Hilden)
PyroMark wash buffer, 10x	Qiagen (Germany, Hilden)
RNase-free water (ultra-filtered and autoclaved)	Sigma-Aldrich Handels Gmbh (Austria, Vienna)
Streptavidin sepharose high performance	GE Healthcare (Austria, Vienna)
TAE buffer	40 mM Tris, 20 mM acetic acid, 1 mM EDTA

7.1.2 Consumables

Centrifuge tubes, 15 mL	VWR International (Austria, Vienna)
Centrifuge tubes, 50 mL	VWR International (Austria, Vienna)
iQ 96-Well PCR plate	Bio-Rad Laboratories (Austria, Vienna)
Microseal 'B' adhesive seals	Bio-Rad Laboratories (Austria, Vienna)
PCR tubes, 0.2 mL, sterile	Qiagen (Germany, Hilden)
Pipette tips TipBox, steril, BIO-CERT (50-1000 µL)	VWR International (Austria, Vienna)
Pipette tips TipBox, steril, BIO-CERT (5-200 µL)	VWR International (Austria, Vienna)
Pipette tips: Biosphere fil. tip (0.5-20 µL)	Sarstedt (Austria, Wiener Neudorf)
PyroMark Q24 cartridge	Qiagen (Germany, Hilden)

PyroMark Q24 plate	Qiagen (Germany, Hilden)
PyroMark vacuum prep filter probe	Qiagen (Germany, Hilden)
Reaction tubes, 0.6 mL, sterile	VWR International (Austria, Vienna)
Reaction tubes, 1.5 mL, sterile	VWR International (Austria, Vienna)
Strip tubes and caps, 0.1 mL	Qiagen (Germany, Hilden)
Thermo strips and caps, 0.2 mL	Thermo Fisher Scientific (Austria, Vienna)

7.1.3 Equipment

Analytical balance TE2144S	Sartorius (Austria, Vienna)
Centrifuge 5424 (rotor: FA-45-24-11)	Eppendorf (Germany, Wesseling-Berzdorf)
Centrifuge MiniStar Silverline	VWR International (Austria, Vienna)
PCR workstation pro	VWR International (Austria, Vienna) former Peqlab
Pipettes 0,5-10 µL, 20-200 µL, 100-1000 µL	Eppendorf (Germany, Wesseling-Berzdorf)
Pipettes 2-20 µL, 20-200 µL	Bio-Rad (USA, California); Bio-Rad Laboratories (Austria, Vienna)
Power supply power pac HV	Bio-Rad Laboratories (Austria, Vienna)
PyroMark Q24 advanced instrument	Qiagen (Germany, Hilden)
PyroMark Q24 vacuum workstation	Qiagen (Germany, Hilden)
Thermocycler iQ 5 real-time PCR detection system	Bio-Rad Laboratories (Austria, Vienna)
Thermocycler Rotor-Gene Q	Qiagen (Germany, Hilden)
Thermomixer comfort	Eppendorf (Germany, Wesseling-Berzdorf)
Transilluminator UVT-20M	Herolab (Germany, Wiesloch)
Vortexmixer classic advanced	VELP Scientifica GJM HANDEL & SERVICE (Austria, Vienna)
Vortexmixer VF2	IKA (Germany, Staufen)
Vortexmixer VV3	VWR International (Austria, Vienna)
Wide mini-subcell GT	Bio-Rad Laboratories (Austria, Vienna)

7.1.4 Webservers and databases

Creating Structural Formula
http://www.strukturformelzeichner.de/

National Center for Biotechnology Information (NCBI)
http://www.ncbi.nlm.nih.gov/

OligoAnalyzer 3.1
http://eu.idtdna.com/calc/analyzer

OligoCalc: Oligonucleotide Properties Calculator
http://biotools.nubic.northwestern.edu/OligoCalc.html

Promoter-Database: Transcriptional Regulatory Element Database (TRED)
https://cb.utdallas.edu/Yi-bin/TRED/tred.Yi?process=searchPromForm

RNAfold Web Server
http://rna.tbi.univie.ac.at/Yi-bin/RNAfold.Yi

7.1.5 Software

Citavi 5.2.0.8	Swiss Academic Software (Switzerland, Wädenswil)
Excel 2010	Microsoft (USA, Redmond)
iQ 5 Optical System Software 2.1	Bio-Rad Laboratories (Austria, Vienna)
Paint	Microsoft (USA, Redmond)
PyroMark Assay Design 2.0	Qiagen (Germany, Hilden)
PyroMark Q24 Advanced 3.0.0	Qiagen (Germany, Hilden)
Rotor-Gene Q Series Software 2.3.1	Qiagen (Germany, Hilden)
SigmaPlot 11.0	Systat Software (USA, San Jose)
SPSS 21.0	IBM (USA, Armonk)
Word 2010	Microsoft (USA, Redmond)

7.2 Abstract

Alzheimer's disease (AD) is complex and the most common neurodegenerative disorder. AD inevitably leads to need for long-term care and death. Diagnosis of AD is one of the major problems scientists are currently struggling with because the only way to ensure that a patient suffered from AD is to investigate its brain post mortem. The establishment of accurate biomarkers especially for the most common form of AD, late-onset AD (LOAD), is important not only because of early diagnosis, but also because of gaining information about the processes and mechanisms of the disease. Even though research aimed at finding biomarkers, currently no accurate biomarkers are available for LOAD. Previous investigations showed promising but also contradictory results regarding differences in methylation status between AD and control patients. The discrepancies between findings could be a result of methodological differences, the complexity of the analysis of human samples or the analysis of different types of samples (brain tissue vs. blood DNA).

The aim of this study was to look for differences in DNA methylation between AD patients and a control group to find potential biomarkers for correct and early diagnosis of LOAD.

The DNA methylation status of various regions of the genome was determined in whole blood by pyrosequencing and methylation-sensitive high resolution melting analysis. In both methodologies, bisulfite converted DNA is used.

The methylation status of *PSEN1, ABCA7, ABCB1* and *ABCC1* was determined by PSQ, the methods for *PSEN1* and *ABCA7* were developed as part of this thesis.
Inspite high variability of methylation levels determined for *PSEN1*, a significant difference was found for one CpG (CpG1) between AD patients and controls. In pooled blood DNA extracts from AD patients, CpG1 was higher methylated than in pooled blood DNA extracts from controls.

In both groups, the methylation levels of *ABCB1* and *ABCC1* were generally below the limit of quantification. In contrast, methylation levels of CpGs in the promoter and in a non-coding region of *ABCA7* were mainly above the upper limit of quantification in AD patients and controls. In both groups, investigated CpGs close to the 3' untranslated region of *ABCA7* showed high DNA methylation levels of pooled blood DNA extracts and a high variability within individual CpGs. No differences between the DNA methylation status of pooled blood DNA extracts from AD patients and controls could be detected.

Additionally, LINE-1 methylation levels were determined to obtain information about the global DNA methylation status. LINE-1 methylation levels were significantly higher in extracts from AD patients compared to the control group.

7.3 Kurzzusammenfassung

Alzheimer ist eine komplexe Erkrankung und die häufigste neurodegenerative Krankheit. Sie führt unweigerlich zu einem langfristigen Pflegebedarf und letztendlich zum Tod. Die Diagnose von Alzheimer ist eine der größten Herausforderungen für die Wissenschaft, da momentan eine eindeutige Diagnose nur durch eine Obduktion des Gehirns gestellt werden kann. Die Entwicklung von Biomarkern für Alzheimer, vor allem für die häufigste Form - LOAD (Late-onset Alzheimer's disease) – ist von entscheidender Bedeutung. Biomarker sind nicht nur bedeutsam für eine frühe Diagnose, sondern sie liefern auch Informationen über die Prozesse und Mechanismen, die der Krankheit zu Grunde liegen. Obwohl sich die Forschung seit einiger Zeit mit der Suche nach Biomarkern beschäftigt, sind noch keine akkuraten Biomarker für LOAD verfügbar. Frühere Untersuchungen zeigten vielversprechende aber auch widersprüchliche Ergebnisse in Bezug auf Unterschiede in dem DNA Methylierungsgrad zwischen Alzheimer Patienten und Kontrollen. Die Unstimmigkeit zwischen verschiedenen Studien könnte in der Anwendung unterschiedlicher Methoden, der Komplexität biologischer Proben oder der Analyse von unterschiedlichen Probentypen (Hirngewebe vs. Blut DNA) begründet liegen.

Das Ziel dieser Arbeit war die Suche nach Unterschieden im Methylierungsgrad zwischen einer Alzheimer- und einer Kontrollgruppe, um einen potentiellen Biomarker zur frühen Diagnose von Alzheimer zu finden.

Die Bestimmung des Methylierungsgrades erfolgte in gepoolten DNA Extrakten aus Blut von Alzheimerpatienten beziehungsweise einer Kontrollgruppe. Der Methylierungsgrad der Gene *PSEN1*, *ABCA7*, *ABCB1* und *ABCC1* wurde mittels Pyrosequenzierung bestimmt. LINE-1 wurde mittels methylierungs-sensitiver hochauflösender Schmelzkurvenanalyse untersucht. Bei beiden Methoden wird Bisulfit-konvertierte DNA eingesetzt. Neue Pyrosequenziermethoden für *PSEN1* und *ABCA7* wurden im Rahmen dieser Arbeit entwickelt.

Trotz hoher Variabilität der Methylierungsgrad in der Promotor-Region von *PSEN1*, konnte ein signifikanter Unterschied an einem CpG (CpG1) festgestellt werden. Der Methylierungsgrad in Alzheimer Proben war geringfügig höher als der Methylierungsgrad in der Kontrollgruppe.

Für *ABCB1* und *ABCC1* wurden Methylierungsgrade unterhalb der Bestimmungsgrenze ermittelt. Im Gegensatz dazu war der Methylierungsgrad der untersuchten CpGs der Promotor-Region und einer nicht-kodierenden Region in *ABCA7* großteils über der oberen Bestimmungsgrenze.

Die Analyse von CpGs im 3‘ untranslatierten Bereich in *ABCA7* zeigte in beiden Gruppen hohe Methylierungsgrade und eine hohe Variabilität zwischen einzelnen CpGs. Es konnte jedoch kein signifikanter Unterschied im Methylierungsgrad von *ABCA7* festgestellt werden.

Der Methylierungsgrad von LINE-1 wurde ermittelt, um den globalen Methylierungsgrad abschätzen zu können. Für Alzheimerpatienten wurde ein signikant höherer Methylierungsgrad von LINE-1 erhalten als für die Kontrollgruppe.

7.4 List of abbreviations

[btn]-	Biotin modification
°C	Temperature in degree Celsius
µg	Microgram
µL	Microliter
µM	Micromolar
A	Adenine
ABCA7	ATP binding cassette subfamily A member 7
ABCB1	ATP binding cassette subfamily B member 1
ABCC1	ATP binding cassette subfamily C member 1
ABC-transporter	ATP-binding cassette transporter
AD	Alzheimer’s disease
APP	Amyloid precursor protein
APS	Adenosine 5´-phosphate
ATP	Adenosine triphosphate
Aβ	Amyloid-β-protein
bp	Base pair
C	Cytosine
c	Concentration
CGI	CpG island
CNS	Central nervous system
CpG	Cytosine-phosphate-guanine dinucleotide
dATP	Deoxyadenosine triphosphate
dATPαS	Deoxyadenosine α-thio triphosphate
dCTP	Deoxycytidine triphosphate
dGTP	Deoxyguanosine triphosphate
DNA	Deoxyribonucleic acid
DNMT	DNA methyltransferase
dNTP	Deoxynucleoside triphosphate
dTTP	Deoxythymidine triphosphate
EOAD	Early-onset Alzheimer's disease
FMR	Fully methylated regions
G	Guanine
g	Gram
kb	Kilo bases
L	Liter
LINE	Long interspersed element
LMR	Low methylated regions

LOAD	Late-onset Alzheimer's disease
LOQ	Limit of quantification
MBD	Methyl-CpG-specific binding domain
min	Minute
mL	Milliliter
mM	Millimolar
MS-HRM	Methylation-sensitive high resolution melting analysis
N	Number
NCBI	National Center for Biotechnology Information
NFT	Neurofibrillary tangles
ng	Nanogram
nM	Nanomolar
NTC	No template control
PCR	Polymerase chain reaction
PPi	Pyrophosphate
PSEN1	Presenilin 1
PSEN2	Presenilin 2
PSQ	Pyrosequencing
RNA	Ribonucleic acid
rpm	Revolutions per minute
s	Second
SAM	S-adenosylmethionine
SD	Standard deviation
SF	Standardized fluorescence
SP	Senile plaques
T	Thymine
T_a	Annealing temperature
TAE	Tris-acetate-EDTA
Taq	*Thermus aquaticus*
T_m	Melting temperature
U	Uracil
ULOQ	Upper limit of quantification
UMR	Unmethylated regions
UV	Ultraviolet
V	Volt
YG	Variable position (either TG or CG after bisulfite treatment)

7.5 List of tables

Table 1: Bisulfite reaction setup; modified from [109] 28
Table 2: Temperature program for bisulfite reaction; modified from [109] 29
Table 3: General scheme for PCR reaction setup; modified from [114] 32
Table 4: PCR temperature program; modified from [114] 32
Table 5: PSQ reaction setup; modified from [97] 33
Table 6: MS-HRM analysis setup for LINE-1; modified from [101] 34
Table 7: Pipetting scheme for MS-HRM standards using bisulfite converted commercial standards 35
Table 8: General scheme for the MS-HRM temperature program; modified from [114] 35
Table 9: Characteristics of the *PSEN1* primers 39
Table 10: PCR reaction setup for *PSEN1*; modified from [114] 41
Table 11: PCR temperature program for *PSEN1*; modified from [114] 41
Table 12: Characteristics of the *ABCA7* primer set 1 44
Table 13: PCR reaction setup for *ABCA7* primer set 1; modified from [114] 46
Table 14: PCR temperature program for *ABCA7* primer set 1; modified from [114] 46
Table 15: Characteristics of the *ABCA7* primer set 2 48
Table 16: PCR reaction setup for *ABCA7* primer set 2; modified from [114] 50
Table 17: PCR temperature program for *ABCA7* primer set 2; modified from [114] 51
Table 18: Characteristics of the *ABCA7* primer set 3 53
Table 19: PCR reaction setup for *ABCA7* primer set 3; modified from [114] 55
Table 20: PCR temperature program for ABCA7 primer set 3; modified from [114] 55
Table 21: Comparison of the methylation status [%] of *ABCB1* obtained after bisulfite conversion with an incorrectly stored and a correctly stored bisulfite kit 58
Table 22: Comparison of DNA methylation status [%] of PSEN1 based on one or respectively four PCR amplifications on one day 59
Table 23: Statistical data of *PSEN1* methylation status [%] 61
Table 24: Results of Mann-Whitney U test for DNA methylation status of *PSEN1* 61
Table 25: Statistical data of *ABCA7* methylation status analyzed with primer set 1 63
Table 26: Results of Mann-Whitney U test for DNA methylation status of *ABCA7* (analyzed with primer set 1) 64
Table 27: Statistical data of *ABCA7* methylation status analyzed with primer set 2 65
Table 28: Results of Mann-Whitney U test for DNA methylation status of *ABCA7* (analyzed with primer set 2) 65
Table 29: Statistical data of *ABCA7* promoter methylation status analyzed with primer set 3 66
Table 30: Results of Levene's test for equality of variances and Student's t-test for equality of means of DNA methylation status of *ABCA7* promoter (analyzed with primer set 3) 67
Table 31: DNA methylation status of *ABCB1* in pooled blood DNA extracts 68
Table 32: Methylation status of *ABCC1* in pooled blood DNA extracts 69
Table 33: Statistical data of LINE-1 methylation status 72

7.6 List of figures

Figure 1: Macroscopical and microscopical changes in AD; modified from [9, 10] 3
Figure 2: Bases of DNA and RNA; cytosine, uracil, thymine, adenine and guanine 5
Figure 3: Base pair rules; modified from [25, 26] 5
Figure 4: 5-methylcytosine 7
Figure 5: DNA methylation patterns 7
Figure 6: Bisulfite conversion of cytosine and 5-methylcytosine; modified from [83] 13
Figure 7: Bisulfite conversion and amplification 14
Figure 8: Principle of PCR 15
Figure 9: Kinetics of PCR; modified from [24] 16
Figure 10: C_T value; modified from [86] 16
Figure 11: PCR temperature profile; modified from [24] 17
Figure 12: Luciferase-based enzymatic PSQ system; modified from [95, 96] 20
Figure 13: Example of a pyrogram and the corresponding histogram 21
Figure 14: MS-HRM methylation profile of methylated and unmethylated DNA; modified from [98, 99] 22
Figure 15: MS-HRM; first negative derivative of the normalized fluorescence over temperature for differently methylated samples; modified from [102] 23
Figure 16: 25 bp DNA ladder 26
Figure 17: Summary of PSQ and MS-HRM workflow 27
Figure 18: Bisufite reaction procedure; modified from [110] 30
Figure 19: Section of the promoter region of *PSEN1* 38
Figure 20: Settings for designing *PSEN1* primers 38
Figure 21: Agarose gel showing the results of PCR optimization for *PSEN1* 40
Figure 22: Agarose gel showing the results of the second PCR optimization for *PSEN1* 40
Figure 23: Representative pyrogram for *PSEN1* in comparison to the histogram showing the expected peak pattern 42
Figure 24: Section of the sequence of *ABCA7* targeted by primer set 1 43
Figure 25: Primer design settings for *ABCA7* primer set 1 44
Figure 26: Agarose gel showing the results of the PCR optimization experiments for *ABCA7* primer set 1 45
Figure 27: Representative pyrogram for *ABCA7* primer set 1 in comparison to the histogram showing the expected peak pattern 46
Figure 28: Section of the sequence of *ABCA7* targeted by primer set 2 47
Figure 29: Primer design settings for *ABCA7* primer set 2 47
Figure 30: Agarose gel showing the results of the PCR optimization experiments for *ABCA7* primer set 2 49
Figure 31: Agarose gel showing the results of the second PCR optimization for *ABCA7* primer set 2 50
Figure 32: Representative pyrogram for *ABCA7* primer set 2 in comparison to the histogram showing the expected peak pattern 51
Figure 33: Section of the sequence of *ABCA7* targeted by primer set 3 52
Figure 34: Primer design settings for *ABCA7* primer set 3 52
Figure 35: Agarose gel showing the results of the PCR optimization for *ABCA7* primer set 3 54
Figure 36: Representative pyrogram for *ABCA7* primer set 3 in comparison to the histogram showing the expected peak pattern 55
Figure 37: Influence of incorrect storage of the bisulfite kit on the color change during the bisulfite reaction and the bisulfite control in the pyrogram of *PSEN1* PSQ methylation analysis 57
Figure 38: DNA methylation status [%] of *PSEN1* in pooled blood DNA extracts 60
Figure 39: Box plots presenting the DNA methylation status [%] of *PSEN1* in CpG1 in pooled blood DNA extracts 62
Figure 40: DNA methylation status [%] of *ABCA7* (analyzed with primer set 1) in pooled blood DNA extracts 63
Figure 41: DNA methylation status [%] of *ABCA7* (analyzed with primer set 2) in pooled blood DNA extracts 64
Figure 42: DNA methylation status [%] of *ABCA7* (analyzed with primer set 3) in pooled blood DNA extracts 66
Figure 43: MS-HRM of LINE-1; normalized fluorescence against temperature for standards 70
Figure 44: MS-HRM of LINE-1; first negative derivative 70

Figure 45: MS-HRM calibration curve for LINE-1 71
Figure 46: DNA methylation status of LINE-1 in pooled blood DNA extracts of AD (red) and control (green) patients 72
Figure 47: DNA methylation status of ABCA7 primer set 3 in cancer cell lines 73

7.7 List of equations

Equation 1: Standard calculation of T_m; based on [85, 103] 24
Equation 2: Salt adjusted T_m calculation; based on [103] 24
Equation 3: Standard fluorescence calculation 36
Equation 4: Equation for the model for the MS-HRM calibration curve 71

7.8 Overview of methods

Region	Primer sequence (5'-3')	T_a [°C]	c_{Primer} [µM]	Method and reference
PSEN1	F: TGGTGGGAGAGGGTAGAGA R: [btn]-CCAAAACTCCACCTAACCTTC S: GTGTTAAATTTAGGATGGT	58.9	0.4	PSQ In-house
ABCB1	F: GTTGGAGGTGAGATTAATTTT R: [btn]-AAACCCCCAACTCTACCT S: GAGAGTAGTAAGAGGGA	58.3	0.2	PSQ In-house developed by M. Spitzwieser [126]
ABCC1	F: TTTATAGGATGAAATGAGGGTATAGT R: [btn]-AACAACCCAACCAACCACCTCT S: GTGTGTGGTTTTAAAGATT	59.8	0.4	PSQ In-house developed by M. Spitzwieser
ABCA7 (primer set 1)	F: AGGTAGTTAGGAGGGGATTTATAT R: [btn]- ACACCTATCCCCTCACCTC S: AGGAAGGATTTAGGTTG	60.2	0.2	PSQ In-house
ABCA7 (primer set 2)	F: TAGTGTTTGTTTTTGGATAAGTTGGA R: [btn]-AAACCCAAATCTAAAATTAAATACTCTATA S: GGTATTTTTAGAGGTAG	55.4	0.2	PSQ In-house
ABCA7 (primer set 3)	F: TTGGTTGGTTTAGGGAAGTTG R: [btn]-CCCACCCTATACCCATTTC S: GGTTTAGGGAAGTTGAT	58.3	0.2	PSQ In-house
LINE-1	F: TGTTAGATAGTGGGTGTAGGTT R: AAATACATCCGTCACCCCTTT	57.0	0.25	HRM In-house developed by M. Spitzwieser

F… forward primer, R… reverse primer, S… sequencing primer, T_a… annealing temperature, c_{Primer}… primer concentration

7.9 Pooled DNA extracts from AD patients and controls

Pool	DNA extract	Class	Age [y]
P1	A033	AD	65
	A172	AD	68
	A184	AD	68
	A055	AD	69
	A214	AD	70
	A041	AD	71
	A070	AD	74
	A163	AD	76
	A044	AD	77
	A111	AD	78
P2	A161	AD	79
	A174	AD	79
	A032	AD	80
	A038	AD	80
	A064	AD	80
	A148	AD	80
	A081	AD	81
	A187	AD	81
	A199	AD	82
	A249	AD	82
P3	A042	AD	83
	A043	AD	84
	A155	AD	84
	A159	AD	84
	A192	AD	85
	A069	AD	86
	A060	AD	87
	A117	AD	87
	A134	AD	87
	A175	AD	87
P4	A179	AD	87
	A114	AD	89
	A031	AD	90
	A034	AD	91
	A072	AD	91
	A066	AD	94
P5	A268	AD	67
	A138	AD	70
	A276	AD	70
	A167	AD	74
	A091	AD	79
	A245	AD	79
	A135	AD	80
	A256	AD	80
	A258	AD	80
	A101	AD	81
P6	A129	AD	81
	A197	AD	81
	A133	AD	82
	A124	AD	83
	A132	AD	84
	A173	AD	84
	A190	AD	84
	A202	AD	84
	A203	AD	84
	K343	AD	84
P7	A141	AD	85
	K246	AD	85
	K264	AD	85
	A106	AD	86
	A145	AD	86
	A195	AD	86
	A198	AD	86
	A205	AD	86
	A131	AD	87
	A176	AD	87
P8	A103	AD	88
	A105	AD	88
	A119	AD	88
	A125	AD	88
	A126	AD	88
	A193	AD	88
	K287	AD	88
	A152	AD	89
	A165	AD	89
	A169	AD	89
P9	A201	AD	89
	A104	AD	90
	A266	AD	90
	A118	AD	91
	A186	AD	91
	A241	AD	94
	A248	AD	94
	K331	AD	94
	A098	AD	95
	A157	AD	95
P11	K158	Control	66
	K263	Control	66
	K378	Control	68
	K348	Control	69
	K336	Control	70

	K185	Control	72
	K200	Control	73
	K210	Control	74
	K177	Control	75
	K357	Control	75
P12	K307	Control	77
	K230	Control	79
	K337	Control	79
	K152	Control	80
	K268	Control	80
	K319	Control	80
	K447	Control	80
	K159	Control	81
	K214	Control	81
	K221	Control	82
P13	K305	Control	82
	K361	Control	82
	K257	Control	83
	K374	Control	83
	K153	Control	84
	K157	Control	85
	K203	Control	85
	K206	Control	86
	K320	Control	86
	K329	Control	86
P14	K146	Control	87
	K149	Control	87
	K155	Control	87
	K293	Control	87
	K148	Control	88
	K150	Control	88
	K317	Control	88
	K324	Control	89
	K184	Control	90
	K217	Control	90
P15	K371	Control	67
	K493	Control	74
	K344	Control	75
	K464	Control	75
	K500	Control	76
	K312	Control	77
	K402	Control	77
	K509	Control	77
	K323	Control	78
	K366	Control	78
P16	K219	Control	79
	K351	Control	79
	K454	Control	79
	K284	Control	80
	K376	Control	81
	K242	Control	82
	K367	Control	82
	K373	Control	82
	K259	Control	83
	K261	Control	83
P17	K277	Control	83
	K291	Control	83
	K283	Control	84
	K227	Control	85
	K309	Control	85
	K345	Control	85
	K453	Control	85
	K235	Control	86
	K244	Control	86
	K273	Control	86
P18	K299	Control	86
	K353	Control	86
	K386	Control	86
	K397	Control	86
	K205	Control	87
	K365	Control	87
	K387	Control	87
	K404	Control	87
	K431	Control	87
	K321	Control	88
P19	K201	Control	86
	K303	Control	89
	K340	Control	89
	K245	Control	90
	K318	Control	90
	K308	Control	91
	K310	Control	91
	K384	Control	91
	K278	Control	92
	K372	Control	95

7.10 Raw data

The following section lists the raw data obtained by PSQ analyses of pooled blood DNA extracts after correct bisulfite conversion; Values n.a. (not available) were excluded from calculations due to inaccurate methylation levels indicated by the internal color code in the pyrogram. According to the manufacturer of the pyrosequencing instrument (Qiagen), the LOQ and ULOQ of pyrosequencing is 5% and 95%, respectively. For statistical analyses, values below the LOQ (5%) were treated as LOQ/2 (2.5%), values above ULOQ as 97.5%.

PSEN1	AD samples

	DNA methylation status [%]												
	CpG1	**CpG2**	**CpG3**	**CpG4**	**CpG5**	**CpG6**	**CpG7**	**CpG8**	**CpG9**	**CpG10**	**Mean (all CpGs)**	**SD**	**rel. SD**
P1	17	18	6	<LOQ	5	9	<LOQ	n.a.	n.a.	n.a.	9	6	71
	8	7	<LOQ	n.a.	n.a.	n.a.	n.a.	n.a.	n.a.	n.a.	6	2	40
Mean	12	13	4										
Median	12	13	4										
SD	5	6	2										
rel. SD	37	46	39										
P2	13	14	<LOQ	8	<LOQ	n.a.	n.a.	n.a.	n.a.	n.a.	8	5	61
	10	9	<LOQ	5	<LOQ	<LOQ	n.a.	n.a.	n.a.	n.a.	5	3	61
Mean	12	12	<LOQ	7	<LOQ								
Median	12	12	<LOQ	7	<LOQ								
SD	1	2	-	2	-								
rel. SD	13	21	-	27	-								
P3	15	13	9	14	<LOQ	<LOQ	<LOQ	<LOQ	<LOQ	<LOQ	7	5	80

P4	26	n.a.	n.a.	n.a.	n.a.	n.a.	n.a.	n.a.	n.a.	n.a.			
	11	7	<LOQ	<LOQ	<LOQ	n.a.	n.a.	n.a.	n.a.	n.a.	5	3	69
	10	20	<LOQ	<LOQ	<LOQ	<LOQ	n.a.	n.a.	n.a.	n.a.	7	7	99
	<LOQ	<LOQ	7	9	<LOQ	<LOQ	<LOQ	n.a.	n.a.	n.a.	<LOQ	3	63
Mean	12	10	4	5	<LOQ	<LOQ	<LOQ						
Median	11	7	<LOQ	<LOQ	<LOQ	<LOQ	<LOQ						
SD	9	8	2	3	-	-	-						
rel. SD	69	77	53	67	-	-	-						

P5	11	<LOQ	<LOQ	<LOQ	<LOQ	10	<LOQ	<LOQ	n.a.	n.a.	<LOQ	3	76
	10	13	7	9	<LOQ	<LOQ	<LOQ	<LOQ	n.a.	<LOQ	6	4	69
	11	10	8	7	n.a.	n.a.	n.a.	n.a.	n.a.	n.a.	9	1	14
	<LOQ	<LOQ	6	<LOQ	<LOQ	<LOQ	<LOQ	<LOQ	9	<LOQ	<LOQ	2	61
	<LOQ	20	<LOQ	<LOQ	<LOQ	<LOQ	16	<LOQ	<LOQ	<LOQ	6	6	111
	16	8	<LOQ	<LOQ	<LOQ	n.a.	n.a.	n.a.	n.a.	n.a.	6	5	84
Mean	9	9	5	4	<LOQ	4	6	<LOQ	6	<LOQ			
Median	10	9	4	<LOQ	<LOQ	<LOQ	<LOQ	<LOQ	6	<LOQ			
SD	5	6	2	3	-	3	6	-	3	-			
rel. SD	56	64	49	62	-	74	99	-	57	-			

P6	<LOQ	<LOQ	<LOQ	<LOQ	<LOQ	<LOQ	n.a.	n.a.	n.a.	n.a.	<LOQ	-	-
	21	12	<LOQ	6	<LOQ	n.a.	<LOQ	<LOQ	n.a.	n.a.	7	7	95
	<LOQ	<LOQ	20	<LOQ	<LOQ	<LOQ	n.a.	<LOQ	14	<LOQ	6	6	108
	<LOQ	<LOQ	<LOQ	<LOQ	<LOQ	<LOQ	<LOQ	<LOQ	<LOQ	9	<LOQ	2	65
	31	6	<LOQ	<LOQ	n.a.	n.a.	n.a.	n.a.	n.a.	n.a.	10	12	114
Mean	12	5	6	<LOQ	<LOQ	<LOQ	<LOQ	<LOQ	8	6			
Median	<LOQ	<LOQ	<LOQ	<LOQ	<LOQ	<LOQ	<LOQ	<LOQ	8	6			
SD	12	4	7	1	-	-	-	-	6	3			
rel. SD	100	72	116	44	-	-	-	-	71	58			

P7	13	8	<LOQ	<LOQ	n.a.	n.a.	n.a.	n.a.	n.a.	n.a.	6	4	67
	8	11	9	<LOQ	6	<LOQ	<LOQ	<LOQ	5	5	5	3	56
Mean	10	10	6	<LOQ									
Median	10	10	6	<LOQ									
SD	3	2	3	-									
rel. SD	26	18	57	-									

P8	20	20	<LOQ	<LOQ	<LOQ	14	n.a.	n.a.	n.a.	n.a.	10	8	78
	7	7	4	n.a.	n.a.	n.a.	n.a.	n.a.	n.a.	n.a.	6	1	24
Mean	13	13	<LOQ										
Median	13	13	<LOQ										
SD	6	6	1										
rel. SD	48	48	22										

P9	8	8	<LOQ	<LOQ	<LOQ	7	<LOQ	<LOQ	<LOQ	<LOQ	<LOQ	2	58
	15	9	<LOQ	8	5	4	n.a.	n.a.	n.a.	n.a.	7	4	58
Mean	12	9	<LOQ	5	4	6							
Median	12	9	<LOQ	5	4	6							
SD	4	1	-	3	1	1							
rel. SD	33	7	-	51	30	25							

PSEN1	Control samples

DNA methylation status [%]

	CpG1	**CpG2**	**CpG3**	**CpG4**	**CpG5**	**CpG6**	**CpG7**	**CpG8**	**CpG9**	**CpG10**	**Mean (all CpGs)**	**SD**	**rel. SD**
P11	12	9	<LOQ	<LOQ	<LOQ	7	<LOQ	<LOQ	n.a.	10	6	4	64
	<LOQ	<LOQ	5	11	<LOQ	<LOQ	n.a.	n.a.	n.a.	n.a.	<LOQ	3	72
Mean	7	6	4	7	<LOQ	5							
Median	7	6	4	7	<LOQ	5							
SD	5	3	1	4	-	2							
rel. SD	64	58	37	64	-	47							

P12	12	11	<LOQ	7	<LOQ	12	<LOQ	<LOQ	<LOQ	9	6	4	63
	14	<LOQ	7	10	<LOQ	<LOQ	<LOQ	<LOQ	6	n.a.	5	4	73
	9	9	<LOQ	<LOQ	<LOQ	<LOQ	<LOQ	<LOQ	<LOQ	<LOQ	<LOQ	3	67
	19	5	<LOQ	<LOQ	10	n.a.	n.a.	n.a.	n.a.	n.a.	8	6	79
	6	7	<LOQ	<LOQ	<LOQ	<LOQ	<LOQ	<LOQ	<LOQ	<LOQ	<LOQ	2	50
	11	7	5	7	<LOQ	<LOQ	n.a.	n.a.	n.a.	n.a.	6	3	52
	8	10	<LOQ	8	<LOQ	<LOQ	<LOQ	<LOQ	<LOQ	<LOQ	<LOQ	3	66
	10	11	<LOQ	<LOQ	n.a.	n.a.	n.a.	n.a.	n.a.	n.a.	6	4	62
	8	10	<LOQ	7	<LOQ	<LOQ	n.a.	n.a.	n.a.	n.a.	5	3	56
	9	10	<LOQ	8	<LOQ	<LOQ	<LOQ	<LOQ	<LOQ	5	5	3	63
	9	11	<LOQ	8	<LOQ	<LOQ	<LOQ	<LOQ	<LOQ	<LOQ	<LOQ	3	68
	8	11	<LOQ	8	6	<LOQ	<LOQ				6	3	53
Mean	10	9	<LOQ	6	4	<LOQ	<LOQ	<LOQ	<LOQ	4			
Median	9	10	<LOQ	7	<LOQ	<LOQ	<LOQ	<LOQ	<LOQ	<LOQ			
SD	3	3	1	2	2	3	-	-	1	2			
rel. SD	34	29	44	42	65	80	-	-	40	59			

P13	20	21	<LOQ	n.a.	n.a.	n.a.	n.a.	n.a.	n.a.	n.a.	15	9	59
	<LOQ	<LOQ	<LOQ	8	<LOQ	5	n.a.	n.a.	n.a.	n.a.	<LOQ	2	53
	8	8	<LOQ	6	5	<LOQ	<LOQ	<LOQ	n.a.	n.a.	5	2	50
Mean	10	11	<LOQ	7	4	4							
Median	8	8	<LOQ	7	4	4							
SD	7	8	-	1	1	1							
rel. SD	72	75	-	14	35	32							

P14	12	9	5	<LOQ	<LOQ	8	n.a.	n.a.	n.a.	n.a.	6	3	52
	8	7	5	<LOQ	<LOQ	5	<LOQ	8	n.a.	n.a.	5	2	44
	8	4	<LOQ	5	<LOQ	6	<LOQ	<LOQ	<LOQ	<LOQ	<LOQ	2	48
Mean	9	7	4	<LOQ	<LOQ	6	<LOQ	5					
Median	8	7	5	<LOQ	<LOQ	6	<LOQ	5					
SD	2	2	1	1	-	1	-	3					
rel. SD	20	30	29	38	-	20	-	51					

P15	<LOQ	<LOQ	<LOQ	26	<LOQ	5	<LOQ	<LOQ	n.a.	n.a.	6	8	134
	<LOQ	<LOQ	<LOQ	<LOQ	<LOQ	<LOQ	<LOQ	<LOQ	<LOQ	<LOQ	<LOQ	-	-
	<LOQ	7	<LOQ	<LOQ	10	6	<LOQ	<LOQ	<LOQ	<LOQ	<LOQ	3	64
Mean	<LOQ	4	<LOQ	10	5	4	<LOQ	<LOQ	<LOQ	<LOQ			
Median	<LOQ	<LOQ	<LOQ	<LOQ	<LOQ	5	<LOQ	<LOQ	<LOQ	<LOQ			
SD	-	2	-	11	4	2	-	-	-	-			
rel. SD	-	50	-	107	73	34	-	-	-	-			

P16	5	11	<LOQ	10	6	15	<LOQ	<LOQ	<LOQ	8	7	4	62
	8	<LOQ	8	<LOQ	<LOQ	13	<LOQ	<LOQ	<LOQ	6	5	4	71
	19	11	<LOQ	<LOQ	<LOQ	29	<LOQ	5	n.a.	n.a.	9	9	100
Mean	11	8	4	5	4	19	<LOQ	<LOQ	<LOQ	7			
Median	8	11	<LOQ	<LOQ	<LOQ	15	<LOQ	<LOQ	<LOQ	7			
SD	6	4	3	4	2	7	-	1	-	1			
rel. SD	56	49	61	72	47	38	-	38	-	16			

P17	6	8	<LOQ	6	8	<LOQ	<LOQ	<LOQ	n.a.	n.a.	5	2	49
	10	9	<LOQ	15	<LOQ	n.a.	n.a.	n.a.	n.a.	n.a.	8	5	61
Mean	8	8	<LOQ	11	5								
Median	8	8	<LOQ	11	5								
SD	2	1	-	4	3								
rel. SD	23	8	-	39	51								

P18	5	8	<LOQ	n.a.	<LOQ	<LOQ	<LOQ	<LOQ	<LOQ	5	<LOQ	2	52
	12	6	5	8	<LOQ	n.a.	n.a.	<LOQ	n.a.	8	6	3	50
Mean	8	7	4		<LOQ			<LOQ		7			
Median	8	7	4		<LOQ			<LOQ		7			
SD	4	1	1		-			-		2			
rel. SD	43	18	36		-			-		25			

P19	8	9	<LOQ	5	<LOQ	<LOQ	10	<LOQ	n.a.	n.a.	5	3	58
	<LOQ	<LOQ	7	6	<LOQ	<LOQ	<LOQ	<LOQ	n.a.	n.a.	<LOQ	2	51
Mean	5	6	5	5	<LOQ	<LOQ	6	<LOQ					
Median	5	6	5	5	<LOQ	<LOQ	6	<LOQ					
SD	3	3	2	1	-	-	4	-					
rel. SD	52	56	49	11	-	-	60	-					

***ABCA7* primer set 1**	AD samples

	DNA methylation status [%]										
	CpG1	**CpG2**	**CpG3**	**CpG4**	**CpG5**	**CpG6**	**CpG7**	**CpG8**	**Mean (all CpGs)**	**SD**	**rel. SD**
P1	>ULOQ	22	94	47	76	73	>ULOQ	89	74	25	34
	>ULOQ	>ULOQ	91	5	35	39	61	88	64	33	51
	62	28	76	39	82	85	79	81	66	20	30
Mean	86	49	87	30	64	66	79	86			
Median	>ULOQ	28	91	39	76	73	79	88			
SD	17	34	8	18	21	19	15	4			
rel. SD	20	69	9	60	33	29	19	4			
P2	>ULOQ	32	93	17	78	80	>ULOQ	35	66	31	46
	82	72	92	30	76	32	74	25	60	25	41
	>ULOQ	81	94	49	60	85	59	76	75	16	22
Mean	92	62	93	32	71	66	77	45			
Median	>ULOQ	72	93	30	76	80	74	35			
SD	7	21	1	13	8	24	16	22			
rel. SD	8	34	1	41	11	36	21	49			
P3	>ULOQ	>ULOQ	>ULOQ	80	84	87	>ULOQ	94	92	7	7
	>ULOQ	60	>ULOQ	>ULOQ	53	87	62	60	77	19	24
	>ULOQ	83	95	63	84	86	>ULOQ	93	87	11	12
	>ULOQ	46	>ULOQ	56	85	88	>ULOQ	92	83	19	23
Mean	>ULOQ	72	>ULOQ	74	76	87	89	85			
Median	>ULOQ	71	>ULOQ	71	84	87	>ULOQ	93			
SD	-	20	1	16	14	1	15	14			
rel. SD	-	28	1	22	18	1	17	17			

P4	19	<LOQ	75	n.a.	78	84	>ULOQ	24	54	35	65
	95	>ULOQ	77	81	81	85	>ULOQ	89	88	7	9
Mean	57	50	76		79	84	>ULOQ	56			
Median	57	50	76		79	84	>ULOQ	56			
SD	38	48	1		2	1	-	33			
rel. SD	67	95	2		2	1	-	58			
P6	89	>ULOQ	>ULOQ	86	83	88	13	>ULOQ	82	26	32
	>ULOQ	>ULOQ	>ULOQ	<LOQ	90	90	>ULOQ	>ULOQ	84	31	37
Mean	93	>ULOQ	>ULOQ	44	87	89	55	>ULOQ			
Median	93	>ULOQ	>ULOQ	44	87	89	55	>ULOQ			
SD	4	-	-	42	3	1	42	-			
rel. SD	4	-	-	94	4	1	76	-			
P7	>ULOQ	77	87	86	20	84	65	87	76	23	30
	49	49	94	7	79	84	>ULOQ	52	64	28	44
	>ULOQ	38	>ULOQ	94	86	89	>ULOQ	92	86	19	22
Mean	81	55	93	62	62	85	87	77			
Median	>ULOQ	49	94	86	79	84	>ULOQ	87			
SD	23	16	4	39	30	2	15	18			
rel. SD	28	30	4	63	48	3	17	23			
P8	>ULOQ	15	>ULOQ	92	54	85	>ULOQ	87	78	27	35
	>ULOQ	73	93	30	57	37	94	87	71	25	35
	>ULOQ	91	95	67	84	87	45	91	82	17	20
Mean	>ULOQ	60	95	63	65	70	79	88			
Median	>ULOQ	73	95	67	57	85	94	87			
SD	-	33	2	25	13	23	24	2			
rel. SD	-	55	2	40	20	33	31	2			
P9	81	27	93	55	43	84	83	74	67	22	33
	18	8	95	83	76	85	>ULOQ	89	69	33	48
Mean	50	17	94	69	59	84	90	81			
Median	50	17	94	69	59	84	90	81			
SD	32	9	1	14	16	1	7	8			
rel. SD	64	55	1	20	28	1	8	9			

ABCA7 primer set 1	Control samples

	DNA methylation status [%]										
	CpG1	CpG2	CpG3	CpG4	CpG5	CpG6	CpG7	CpG8	Mean (all CpGs)	SD	rel. SD
P11	65	55	94	21	80	84	82	90	71	22	31
	75	85	>ULOQ	82	88	90	92	75	86	8	9
	>ULOQ	87	>ULOQ	31	83	86	>ULOQ	92	84	21	25
Mean	79	76	>ULOQ	45	84	87	91	86			
Median	75	85	>ULOQ	31	83	86	92	90			
SD	14	15	2	27	3	2	6	7			
rel. SD	17	19	2	59	4	3	7	9			
P12	>ULOQ	>ULOQ	80	<LOQ	62	76	83	71	71	28	40
	>ULOQ	>ULOQ	95	<LOQ	80	85	7	90	69	38	54
	>ULOQ	>ULOQ	>ULOQ	>ULOQ	<LOQ	89	>ULOQ	95	84	31	37
Mean	>ULOQ	>ULOQ	91	34	48	83	63	85			
Median	>ULOQ	>ULOQ	95	<LOQ	62	85	83	90			
SD	-	-	8	45	33	5	40	10			
rel. SD	-	-	9	131	69	6	63	12			
P13	29	71	95	<LOQ	27	88	>ULOQ	71	60	33	56
P14	89	50	>ULOQ	50	82	85	58	66	72	17	24
	>ULOQ	78	89	45	45	81	76	55	71	19	27
	69	23	>ULOQ	54	53	86	58	94	67	23	35
	>ULOQ	>ULOQ	>ULOQ	58	86	89	>ULOQ	94	90	13	14
Mean	88	62	95	52	67	86	72	77			
Median	93	64	>ULOQ	52	68	86	67	80			
SD	12	28	4	5	18	3	16	17			
rel. SD	13	45	4	10	27	3	22	22			
P16	>ULOQ	>ULOQ	>ULOQ	>ULOQ	84	88	>ULOQ	92	94	5	5
	85	92	88	84	63	80	90	83	83	8	10
	>ULOQ	<LOQ	>ULOQ	>ULOQ	87	89	>ULOQ	94	83	31	37
Mean	93	64	94	93	78	86	95	90			
Median	>ULOQ	92	>ULOQ	>ULOQ	84	88	>ULOQ	92			
SD	6	44	4	7	11	4	3	5			
rel. SD	6	68	5	7	13	5	4	5			

P17	>ULOQ	>ULOQ	94	62	62	84	>ULOQ	61	82	16	20
	87	78	74	39	35	74	78	90	69	19	28
	77	77	>ULOQ	70	47	88	>ULOQ	86	80	16	19
Mean	87	84	88	57	48	82	91	79			
Median	87	78	94	62	47	84	>ULOQ	86			
SD	9	10	11	13	11	6	9	13			
rel. SD	10	11	12	23	23	7	10	16			

P18	<LOQ	<LOQ	>ULOQ	>ULOQ	88	88	<LOQ	5	48	45	94
	71	78	>ULOQ	51	45	89	73	>ULOQ	75	19	25
Mean	37	40	>ULOQ	74	66	89	38	51			
Median	37	40	>ULOQ	74	66	89	38	51			
SD	34	38	-	23	22	1	35	46			
rel. SD	93	94	-	32	33	1	93	90			

P19	>ULOQ	53	95	50	80	85	>ULOQ	90	81	18	22
	>ULOQ	24	94	>ULOQ	80	84	>ULOQ	29	75	29	38
	>ULOQ	77	77	51	75	67	>ULOQ	75	77	14	18
Mean	>ULOQ	51	88	66	78	79	>ULOQ	65			
Median	>ULOQ	53	94	51	80	84	>ULOQ	75			
SD	-	22	8	22	2	8	-	26			
rel. SD	-	42	9	33	3	11	-	40			

***ABCA7* primer set 2**	AD samples

DNA methylation status [%]

	CpG1	**CpG2**	**CpG3**	**CpG4**	**CpG5**	**CpG6**	**CpG7**	**CpG8**	**Mean (all CpGs)**	**SD**	**rel. SD**
P1	95	95	92	92	>ULOQ	>ULOQ	86	>ULOQ	94	4	4
	>ULOQ	95	>ULOQ	94	>ULOQ	>ULOQ	80	94	94	6	6
	>ULOQ	93	>ULOQ	91	94	95	81	94	93	5	5
Mean	>ULOQ	94	>ULOQ	92	>ULOQ	>ULOQ	82	95			
Median	>ULOQ	95	>ULOQ	92	>ULOQ	>ULOQ	81	94			
SD	1	1	3	1	2	1	2	2			
rel. SD	1	1	3	1	2	1	3	2			

P2	>ULOQ	88	>ULOQ	88	90	93	77	>ULOQ	91	7	7
	>ULOQ	93	>ULOQ	94	>ULOQ	>ULOQ	82	>ULOQ	94	5	5
	80	80	83	82	78	77	68	80	79	4	6
	>ULOQ	>ULOQ	>ULOQ	>ULOQ	>ULOQ	>ULOQ	84	>ULOQ	>ULOQ	5	5
Mean	93	90	94	90	91	91	78	93			
Median	>ULOQ	91	>ULOQ	91	94	95	79	>ULOQ			
SD	7	7	6	6	8	8	6	8			
rel. SD	8	7	6	7	9	9	8	8			

P3	>ULOQ	>ULOQ	>ULOQ	94	>ULOQ	>ULOQ	87	>ULOQ	>ULOQ	4	4
	>ULOQ	>ULOQ	>ULOQ	92	94	>ULOQ	88	>ULOQ	95	3	3
	88	85	82	88	80	80	77	86	83	4	5
	74	71	70	82	71	73	63	72	72	5	7
Mean	89	88	87	89	86	87	79	88			
Median	93	91	90	90	87	89	82	92			
SD	10	11	12	4	11	11	10	10			
rel. SD	11	13	13	5	12	12	13	12			

P4	>ULOQ	>ULOQ	91	95	>ULOQ	>ULOQ	85	>ULOQ	95	4	5
	>ULOQ	90	>ULOQ	>ULOQ	>ULOQ	93	88	>ULOQ	95	4	4
	79	71	80	73	77	78	68	76	75	4	5
Mean	91	86	90	88	91	90	80	90			
Median	>ULOQ	90	91	95	>ULOQ	93	85	>ULOQ			
SD	9	11	7	11	10	8	9	10			
rel. SD	10	13	8	12	11	9	11	11			

P5	>ULOQ	93	>ULOQ	>ULOQ	>ULOQ	>ULOQ	89	>ULOQ	>ULOQ	3	3
	>ULOQ	>ULOQ	>ULOQ	>ULOQ	>ULOQ	>ULOQ	89	>ULOQ	>ULOQ	3	3
	67	57	70	71	66	66	58	66	65	5	7
	>ULOQ	85	>ULOQ	>ULOQ	>ULOQ	>ULOQ	82	>ULOQ	94	6	6
Mean	90	83	91	91	90	90	79	90			
Median	>ULOQ	89	>ULOQ	>ULOQ	>ULOQ	>ULOQ	85	>ULOQ			
SD	13	16	12	11	14	14	13	13			
rel. SD	15	19	13	13	15	15	16	15			

P6	>ULOQ	86	>ULOQ	>ULOQ	>ULOQ	>ULOQ	86	>ULOQ	95	5	5
	>ULOQ	>ULOQ	>ULOQ	>ULOQ	>ULOQ	>ULOQ	89	>ULOQ	>ULOQ	3	3
	35	33	36	70	34	34	30	18	36	14	39
	66	61	63	81	62	63	54	61	64	7	11
Mean	74	69	73	87	73	73	65	69			
Median	82	74	80	89	80	80	70	79			
SD	26	25	26	11	27	27	24	33			
rel. SD	35	36	35	13	36	36	37	48			

P7	>ULOQ	>ULOQ	>ULOQ	91	>ULOQ	>ULOQ	86	>ULOQ	95	4	4
	>ULOQ	94	>ULOQ	93	>ULOQ	>ULOQ	86	>ULOQ	95	4	4
	>ULOQ	>ULOQ	>ULOQ	93	>ULOQ	>ULOQ	88	>ULOQ	>ULOQ	3	3
Mean	>ULOQ	>ULOQ	>ULOQ	92	>ULOQ	>ULOQ	87	>ULOQ			
Median	>ULOQ	>ULOQ	>ULOQ	93	>ULOQ	>ULOQ	86	>ULOQ			
SD	-	1	-	1	-	-	1	-			
rel. SD	-	1	-	1	-	-	1	-			

P8	>ULOQ	>ULOQ	>ULOQ	92	>ULOQ	94	86	>ULOQ	95	4	4
	>ULOQ	>ULOQ	94	79	95	>ULOQ	70	91	90	10	11
	>ULOQ	>ULOQ	>ULOQ	92	>ULOQ	>ULOQ	83	>ULOQ	95	5	5
	>ULOQ	93	>ULOQ	>ULOQ	>ULOQ	>ULOQ	87	>ULOQ	>ULOQ	4	4
Mean	>ULOQ	>ULOQ	>ULOQ	90	>ULOQ	>ULOQ	82	>ULOQ			
Median	>ULOQ	>ULOQ	>ULOQ	92	>ULOQ	>ULOQ	85	>ULOQ			
SD	-	2	1	7	1	1	7	3			
rel. SD	-	2	1	8	1	1	9	3			

P9	84	88	>ULOQ	>ULOQ	93	>ULOQ	87	>ULOQ	93	5	6
	>ULOQ	>ULOQ	>ULOQ	93	>ULOQ	>ULOQ	89	>ULOQ	>ULOQ	3	3
	83	77	85	87	80	84	72	78	81	5	6
	>ULOQ	>ULOQ	>ULOQ	>ULOQ	>ULOQ	>ULOQ	83	>ULOQ	>ULOQ	5	5
Mean	90	90	94	94	92	94	83	93			
Median	91	93	>ULOQ	95	95	>ULOQ	85	>ULOQ			
SD	7	8	6	4	7	6	7	8			
rel. SD	8	9	6	4	8	6	8	9			

ABCA7 primer set 2	Control samples

	DNA methylation status [%]										
	CpG1	**CpG2**	**CpG3**	**CpG4**	**CpG5**	**CpG6**	**CpG7**	**CpG8**	**Mean (all CpGs)**	**SD**	**rel. SD**
P11	>ULOQ	88	>ULOQ	94	95	>ULOQ	82	>ULOQ	94	5	6
	>ULOQ	92	>ULOQ	95	>ULOQ	95	83	>ULOQ	94	5	5
	87	82	87	84	83	83	73	84	83	4	5
	>ULOQ	92	>ULOQ	94	89	>ULOQ	85	90	93	5	5
Mean	95	88	95	92	91	93	81	92			
Median	>ULOQ	90	>ULOQ	94	92	>ULOQ	83	94			
SD	5	4	4	4	6	6	5	6			
rel. SD	5	4	5	5	6	7	6	6			
P12	>ULOQ	93	>ULOQ	94	n.a.	>ULOQ	88	91	94	3	4
	>ULOQ	>ULOQ	>ULOQ	>ULOQ	>ULOQ	>ULOQ	85	92	95	4	5
	50	48	51	71	49	49	42	46	51	8	16
	82	79	72	72	80	73	69	80	76	5	6
Mean	82	79	80	84	75	79	71	77			
Median	90	86	85	83	80	85	77	86			
SD	20	19	19	12	20	20	18	19			
rel. SD	24	25	24	15	26	26	26	24			
P13	>ULOQ	90	>ULOQ	94	>ULOQ	>ULOQ	87	>ULOQ	95	4	4
	>ULOQ	>ULOQ	>ULOQ	90	>ULOQ	>ULOQ	89	93	95	4	4
	63	60	67	75	63	63	55	63	64	6	9
	87	90	>ULOQ	>ULOQ	93	>ULOQ	84	>ULOQ	93	5	5
Mean	86	84	90	89	88	89	79	88			
Median	92	90	>ULOQ	92	95	>ULOQ	86	95			
SD	14	14	13	8	15	15	14	14			
rel. SD	16	17	15	9	17	17	18	16			

P14	>ULOQ	89	>ULOQ	94	>ULOQ	>ULOQ	80	>ULOQ	94	6	6
	91	>ULOQ	>ULOQ	>ULOQ	93	>ULOQ	87	n.a.	94	4	4
	94	92	>ULOQ	92	90	94	83	93	92	4	4
Mean	94	93	>ULOQ	94	94	>ULOQ	83	95			
Median	94	92	>ULOQ	94	93	>ULOQ	83	95			
SD	3	3	-	2	3	2	3	2			
rel. SD	3	4	-	3	3	2	3	3			

P15	>ULOQ	>ULOQ	>ULOQ	>ULOQ	>ULOQ	>ULOQ	87	>ULOQ	>ULOQ	4	4
	>ULOQ	80	>ULOQ	>ULOQ	>ULOQ	82	89	82	90	8	8
	>ULOQ	>ULOQ	>ULOQ	>ULOQ	>ULOQ	>ULOQ	92	>ULOQ	>ULOQ	2	2
Mean	>ULOQ	92	>ULOQ	>ULOQ	>ULOQ	92	89	92			
Median	>ULOQ	>ULOQ	>ULOQ	>ULOQ	>ULOQ	>ULOQ	89	>ULOQ			
SD	-	8	-	-	-	8	2	7			
rel. SD	-	9	-	-	-	8	3	8			

P16	91	>ULOQ	>ULOQ	>ULOQ	85	>ULOQ	86	>ULOQ	94	5	6
	84	89	>ULOQ	>ULOQ	>ULOQ	94	89	94	93	5	5
	86	88	91	84	93	>ULOQ	74	93	88	7	8
	>ULOQ	>ULOQ	91	>ULOQ	>ULOQ	>ULOQ	85	>ULOQ	95	4	4
Mean	90	93	94	94	93	>ULOQ	84	95			
Median	88	93	94	>ULOQ	95	>ULOQ	86	>ULOQ			
SD	5	5	3	6	5	1	6	2			
rel. SD	6	5	3	6	6	1	7	2			

P17	>ULOQ	93	>ULOQ	95	>ULOQ	>ULOQ	84	>ULOQ	95	4	5
	92	91	>ULOQ	91	>ULOQ	>ULOQ	86	>ULOQ	94	4	4
	>ULOQ	>ULOQ	>ULOQ	90	>ULOQ	>ULOQ	83	>ULOQ	95	5	6
Mean	>ULOQ	94	>ULOQ	92	>ULOQ	>ULOQ	84	>ULOQ			
Median	>ULOQ	93	>ULOQ	91	>ULOQ	>ULOQ	84	>ULOQ			
SD	2	3	-	2	-	-	1	-			
rel. SD	3	3	-	2	-	-	2	-			

P18	>ULOQ	93	>ULOQ	91	>ULOQ	>ULOQ	84	>ULOQ	94	5	5
	>ULOQ	94	>ULOQ	>ULOQ	>ULOQ	>ULOQ	85	>ULOQ	>ULOQ	4	4
	80	78	84	85	84	86	69	90	82	6	7
	>ULOQ	95	>ULOQ	92	>ULOQ	>ULOQ	87	>ULOQ	95	4	4
Mean	93	90	94	92	94	95	81	>ULOQ			
Median	>ULOQ	94	>ULOQ	92	>ULOQ	>ULOQ	84	>ULOQ			
SD	8	7	6	4	6	5	7	3			
rel. SD	8	8	6	5	6	5	9	3			

P19	93	>ULOQ	>ULOQ	>ULOQ	>ULOQ	93	80	>ULOQ	94	6	6
	>ULOQ	>ULOQ	>ULOQ	93	93	>ULOQ	86	>ULOQ	95	4	4
	93	91	95	94	94	87	77	92	90	6	6
Mean	94	95	>ULOQ	95	95	93	81	>ULOQ			
Median	93	>ULOQ	>ULOQ	94	94	93	80	>ULOQ			
SD	2	3	1	2	2	4	4	3			
rel. SD	2	3	1	2	2	4	5	3			

***ABCA7* primer set 3**	AD samples

DNA methylation status [%]

	CpG1	**CpG2**	**CpG3**	**CpG4**	**CpG5**	**CpG6**	**CpG7**	**Mean (all CpGs)**	**SD**	**rel. SD**
P1	>ULOQ	>ULOQ	>ULOQ	89	>ULOQ	89	77	92	7	8
	>ULOQ	>ULOQ	94	92	>ULOQ	87	80	92	6	6
	92	>ULOQ	>ULOQ	91	>ULOQ	86	80	92	6	7
Mean	>ULOQ	>ULOQ	>ULOQ	91	>ULOQ	88	79			
Median	>ULOQ	>ULOQ	>ULOQ	91	>ULOQ	87	80			
SD	2	-	1	1	-	1	2			
rel. SD	3	-	1	1	-	1	2			

P2	>ULOQ	>ULOQ	94	90	>ULOQ	88	83	92	5	6
	>ULOQ	>ULOQ	94	93	>ULOQ	88	83	93	5	5
	>ULOQ	>ULOQ	>ULOQ	94	>ULOQ	85	81	93	7	7
Mean	>ULOQ	>ULOQ	95	92	>ULOQ	87	82			
Median	>ULOQ	>ULOQ	94	93	>ULOQ	88	83			
SD	-	-	2	2	-	2	1			
rel. SD	-	-	2	2	-	2	1			

P3	>ULOQ	>ULOQ	95	95	>ULOQ	89	80	93	6	7
	94	>ULOQ	>ULOQ	92	>ULOQ	89	80	93	6	6
	>ULOQ	>ULOQ	93	91	>ULOQ	89	84	93	5	5
Mean	>ULOQ	>ULOQ	95	92	>ULOQ	89	81			
Median	>ULOQ	>ULOQ	95	92	>ULOQ	89	80			
SD	2	-	2	2	-	0	2			
rel. SD	2	-	2	2	-	0	2			

P4	93	>ULOQ	>ULOQ	88	>ULOQ	93	79	92	6	7
	89	>ULOQ	>ULOQ	>ULOQ	>ULOQ	>ULOQ	79	94	7	7
	>ULOQ	>ULOQ	>ULOQ	89	>ULOQ	92	79	93	6	7
Mean	93	>ULOQ	>ULOQ	91	>ULOQ	94	79			
Median	93	>ULOQ	>ULOQ	89	>ULOQ	93	79			
SD	4	-	-	4	-	2	0			
rel. SD	4	-	-	5	-	2	0			

P5	>ULOQ	>ULOQ	>ULOQ	>ULOQ	>ULOQ	94	86	95	4	4
	>ULOQ	95	94	93	90	89	85	92	4	4
	94	>ULOQ	>ULOQ	91	92	93	80	92	6	6
Mean	>ULOQ	>ULOQ	>ULOQ	94	93	92	84			
Median	>ULOQ	>ULOQ	>ULOQ	93	92	93	85			
SD	2	1	2	3	3	2	3			
rel. SD	2	1	2	3	4	2	3			

P6	>ULOQ	>ULOQ	95	90	>ULOQ	90	84	93	5	5
	92	>ULOQ	>ULOQ	90	>ULOQ	90	86	93	4	5
	>ULOQ	>ULOQ	>ULOQ	>ULOQ	>ULOQ	92	84	95	5	5
Mean	>ULOQ	>ULOQ	>ULOQ	93	>ULOQ	91	85			
Median	>ULOQ	>ULOQ	>ULOQ	90	>ULOQ	90	84			
SD	3	-	1	4	-	1	1			
rel. SD	3	-	1	4	-	1	1			

P7	>ULOQ	>ULOQ	93	92	>ULOQ	92	80	93	6	6
	>ULOQ	>ULOQ	>ULOQ	95	>ULOQ	88	82	94	6	6
	93	>ULOQ	>ULOQ	91	>ULOQ	89	81	93	5	6
Mean	>ULOQ	>ULOQ	>ULOQ	93	>ULOQ	90	81			
Median	>ULOQ	>ULOQ	>ULOQ	92	>ULOQ	89	81			
SD	2	-	2	2	-	2	1			
rel. SD	2	-	2	2	-	2	1			

P8	94	>ULOQ	92	93	>ULOQ	89	80	92	6	6
	>ULOQ	>ULOQ	93	94	>ULOQ	88	81	93	6	6
	94	>ULOQ	>ULOQ	94	>ULOQ	91	78	93	6	7
Mean	95	>ULOQ	94	93	>ULOQ	89	80			
Median	94	>ULOQ	93	94	>ULOQ	89	80			
SD	2	-	2	0	-	1	1			
rel. SD	2	-	3	0	-	2	1			

P9	94	>ULOQ	95	90	>ULOQ	90	81	92	5	6
	>ULOQ	>ULOQ	>ULOQ	94	>ULOQ	88	84	94	5	6
	95	>ULOQ	95	92	>ULOQ	94	82	93	5	5
Mean	95	>ULOQ	>ULOQ	92	>ULOQ	91	82			
Median	95	>ULOQ	95	92	>ULOQ	90	82			
SD	2	-	1	2	-	3	1			
rel. SD	2	-	1	2	-	3	1			

***ABCA7* primer set 3**	Control samples

DNA methylation status [%]

	CpG1	**CpG2**	**CpG3**	**CpG4**	**CpG5**	**CpG6**	**CpG7**	**Mean (all CpGs)**	**SD**	**rel. SD**
P11	>ULOQ	>ULOQ	94	92	>ULOQ	89	77	92	7	7
	>ULOQ	>ULOQ	>ULOQ	>ULOQ	>ULOQ	87	81	94	6	7
	93	>ULOQ	>ULOQ	94	>ULOQ	86	83	93	5	6
Mean	>ULOQ	>ULOQ	>ULOQ	94	>ULOQ	87	81			
Median	>ULOQ	>ULOQ	>ULOQ	94	>ULOQ	87	81			
SD	2	-	1	2	-	1	2			
rel. SD	2	-	2	3	-	2	3			

P12	92	>ULOQ	92	90	>ULOQ	93	81	92	5	6
	>ULOQ	>ULOQ	90	95	>ULOQ	90	82	93	5	6
	93	>ULOQ	93	>ULOQ	>ULOQ	88	83	93	5	6
Mean	94	>ULOQ	91	94	>ULOQ	90	82			
Median	93	>ULOQ	92	95	>ULOQ	90	82			
SD	2	-	1	3	-	2	1			
rel. SD	2	-	1	3	-	3	1			

P13	>ULOQ	>ULOQ	92	>ULOQ	>ULOQ	90	76	93	7	8
	91	>ULOQ	>ULOQ	93	>ULOQ	93	83	93	5	5
	>ULOQ	>ULOQ	94	94	>ULOQ	88	87	94	4	4
Mean	95	>ULOQ	95	95	>ULOQ	90	82			
Median	>ULOQ	>ULOQ	94	94	>ULOQ	90	83			
SD	3	-	2	2	-	2	5			
rel. SD	3	-	2	2	-	2	6			

P14	>ULOQ	>ULOQ	>ULOQ	88	>ULOQ	95	81	93	6	6
	>ULOQ	>ULOQ	>ULOQ	91	>ULOQ	89	82	93	6	6
	>ULOQ	>ULOQ	>ULOQ	94	>ULOQ	91	81	94	6	6
Mean	>ULOQ	>ULOQ	>ULOQ	91	>ULOQ	92	81			
Median	>ULOQ	>ULOQ	>ULOQ	91	>ULOQ	91	81			
SD	-	-	-	2	-	3	1			
rel. SD	-	-	-	2	-	3	1			

P15	>ULOQ	>ULOQ	>ULOQ	>ULOQ	>ULOQ	92	86	95	4	4
	>ULOQ	94	>ULOQ	>ULOQ	>ULOQ	95	85	95	4	4
	>ULOQ	>ULOQ	>ULOQ	>ULOQ	>ULOQ	95	80	95	6	6
Mean	>ULOQ	>ULOQ	>ULOQ	>ULOQ	>ULOQ	94	84			
Median	>ULOQ	>ULOQ	>ULOQ	>ULOQ	>ULOQ	95	85			
SD	-	2	-	-	-	1	3			
rel. SD	-	2	-	-	-	2	3			

P16	93	>ULOQ	>ULOQ	91	>ULOQ	87	76	91	7	8
	>ULOQ	>ULOQ	91	91	>ULOQ	87	78	91	7	7
	94	>ULOQ	>ULOQ	91	>ULOQ	83	85	92	6	6
Mean	95	>ULOQ	95	91	>ULOQ	86	80			
Median	94	>ULOQ	>ULOQ	91	>ULOQ	87	78			
SD	2	-	3	0	-	2	4			
rel. SD	2	-	3	0	-	2	5			

P17	91	>ULOQ	>ULOQ	94	>ULOQ	91	81	93	6	6
	>ULOQ	>ULOQ	>ULOQ	92	>ULOQ	88	81	93	6	6
	>ULOQ	>ULOQ	>ULOQ	93	>ULOQ	88	83	93	6	6
Mean	95	>ULOQ	>ULOQ	93	>ULOQ	89	81			
Median	>ULOQ	>ULOQ	>ULOQ	93	>ULOQ	88	81			
SD	3	-	-	1	-	1	1			
rel. SD	3	-	-	1	-	2	1			

P18	92	>ULOQ	>ULOQ	95	>ULOQ	88	77	92	7	8
	95	>ULOQ	95	89	91	91	78	91	6	6
	>ULOQ	95	>ULOQ	93	>ULOQ	85	83	93	6	6
Mean	95	>ULOQ	>ULOQ	92	95	88	79			
Median	95	>ULOQ	>ULOQ	93	>ULOQ	88	78			
SD	2	1	1	2	3	2	3			
rel. SD	2	1	1	2	3	3	3			

P19	94	>ULOQ	>ULOQ	94	>ULOQ	84	79	92	7	8
	>ULOQ	>ULOQ	>ULOQ	94	>ULOQ	91	82	94	5	6
	>ULOQ	>ULOQ	>ULOQ	91	>ULOQ	87	80	93	6	7
Mean	>ULOQ	>ULOQ	>ULOQ	93	>ULOQ	87	80			
Median	>ULOQ	>ULOQ	>ULOQ	94	>ULOQ	87	80			
SD	2	-	-	1	-	3	1			
rel. SD	2	-	-	1	-	3	2			

The following section lists the raw data of all MS-HRM analyses of pooled blood DNA extracts after a correct bisulfite conversion.

LINE-1	AD samples

DNA methylation status [%]

					Mean	**Median**	**SD**	**rel. SD**
P1	96	96	102	103	99	99	3	4
P2	98	96	98	104	99	98	3	3
P3	113	109	113	106	110	111	3	3
P4	104	97	96	98	99	97	3	3
P5	102	105	94	97	99	100	4	4
P6	105	110	91	99	101	102	7	7
P7	101	103	100	102	102	102	1	1
P8	102	102	104	105	103	103	1	1
P9	111	102	107	101	105	105	4	4

LINE-1	Control samples

DNA methylation status [%]

					Mean	**Median**	**SD**	**rel. SD**
P11	93	96	96	94	95	95	1	1
P12	98	100	96	96	97	97	2	2
P13	98	95	95	98	96	96	1	1
P14	104	101	100	101	102	101	1	1
P15	108	95	100	93	99	98	6	6
P16	108	90	104	102	101	103	7	7
P17	92	94	92	95	93	93	1	2
P18	99	96	102	97	99	98	2	2
P19	99	92	98	96	96	97	2	3

8 References

[1] Alzheimer's Disease International. 2009. *World Alzheimer Report 2009*. http://www.alz.co.uk/research/files/WorldAlzheimerReport.pdf. Accessed 12 October 2015.

[2] Prince, M., Wimo, A., Guerchet, M., Ali, G., Wu, Y., and Prina, M. 2015. World Alzheimer Report 2015. *The global impact of dementia: an analysis of prevalence, incidence, cost & trends*, 10–28.

[3] Ferri, C. P., Prince, M., Brayne, C., Brodaty, H., Fratiglioni, L., Ganguli, M. *et al.* 2005. Global prevalence of dementia. A Delphi consensus study. *The Lancet* 366 (9503) 2112–2117.

[4] Jellinger, K., Ed. 2006. *Alzheimer: Meilensteine aus hundert Jahren wissenschaftlicher und klinischer Forschung*. Akademische Verlagsgesellschaft Aka, Berlin, 1-15.

[5] Francis, P. T., Palmer, A. M., Snape, M., and Wilcock, G. K. 1999. The cholinergic hypothesis of Alzheimer's disease: a review of progress. *Journal of Neurology, Neurosurgery & Psychiatry* 66, 2, 137–147.

[6] Alzheimer, A. 2006. Über eine eigenartige Erkrankung der Hirnrinde. In *Alzheimer: Meilensteine aus hundert Jahren wissenschaftlicher und klinischer Forschung*, K. Jellinger, Ed. Akademische Verlagsgesellschaft Aka, Berlin, 146–148.

[7] World Health Organization. 1993. *The ICD-10 classification of mental and behavioural disorders*. *Diagnostic criteria for research*. World Health Organization, Geneva.

[8] Wright, M. T., McSweeny, A. J., and Kieswetter, A. 2004. Aging and Dementia. In *Textbook of Biological Psychiatry*, J. Panksepp, Ed. John Wiley & Sons, 437–487.

[9] Alzheimer's Association. *Brain tour (10. under the microscope)*. https://www.alz.org/braintour/healthy_vs_alzheimers.asp. Accessed 14.03.16.

[10] Alzheimer's Association. *Brain tour (9. more brain changes)*. https://www.alz.org/braintour/healthy_vs_alzheimers.asp. Accessed 14.03.16.

[11] Lu, H., Liu, X., Deng, Y., and Qing, H. 2013. DNA methylation, a hand behind neurodegenerative diseases. *Frontiers in Aging Neuroscience* 5, 85.

[12] Hardy, J. A. and Higgins, G. A. 1992. Alzheimer's disease: the amyloid cascade hypothesis. *Science* 256 (5054) 184–185.

[13] Hardy, J. and Selkoe, D. J. 2002. The amyloid hypothesis of Alzheimer's disease: Progress and problems on the road to therapeutics. *Science* 297 (5580) 353–356.

[14] Finckh, U. 2006. Genetische Faktoren bei Alzheimer-Demenz. *Deutsches Ärzteblatt* 103, 15, A1010-A1016.

[15] Kuperstein, I., Broersen, K., Benilova, I., Rozenski, J., Jonckheere, W., Debulpaep *et al.* 2010. Neurotoxicity of Alzheimer's disease Aβ peptides is induced by small changes in the Aβ42 to Aβ40 ratio. *EMBO Journal* 29 (19) 3408–3420.

[16] Wang, R., Wang, B., He, W., and Zheng, H. 2006. Wild-type presenilin 1 protects against Alzheimer disease mutation-induced amyloid pathology. *Journal of Biological Chemistry* 281, 22, 15330–15336.

[17] Kim, J., Onstead, L., Randle, S., Price, R., Smithson, L., Zwizinski *et al*. 2007. Aβ40 inhibits amyloid deposition in vivo. *Journal of Neuroscience* 27, 3, 627–633.

[18] Haass, C. and Selkoe, D. J. 2007. Soluble protein oligomers in neurodegeneration: Lessons from the Alzheimer's amyloid β-peptide. *Nature Reviews Molecular Cell Biology* 8, 2, 101–112.

[19] Haass, C., Kaether, C., Thinakaran, G., and Sisodia, S. 2012. Trafficking and proteolytic processing of APP. *Cold Spring Harbor Perspectives in Medicine* 2, 5, a006270.

[20] Eschweiler, G. W., Leyhe, T., Klöppel, S., and Hüll, M. 2010. New developments in the diagnosis of dementia. *Deutsches Ärzteblatt International* 107, 39, 677.

[21] Khachaturian, Z. S. 2006. Diagnose der Alzheimer-Krankheit. In *Alzheimer: Meilensteine aus hundert Jahren wissenschaftlicher und klinischer Forschung*, K. Jellinger, Ed. Akademische Verlagsgesellschaft Aka, Berlin, 101–122.

[22] Henry, M. S., Passmore, A. P., Todd, S., McGuinness, B., Craig, D., and Johnston, J. A. 2013. The development of effective biomarkers for Alzheimer's disease: a review. *International Journal of Geriatric Psychiatry* 28 (4) 331–340.

[23] Alberts, B., Johnson, A., Lewis, J., Raff, M., Roberts, K., Walter, P. 2015. *Molecular Biology of the Cell*. (Sixth Edition). Garland Science, New York, 173-183, 404-413.

[24] McPherson, M. and Møller, S. 2007. *PCR*. Garland Science, 1-17, 23-36.

[25] Department of Industry, Innovation, Science, Research and Tertiary Education Website Archive. http://archive.industry.gov.au/Biotechnologyonline.gov.au/popups/img_helix.html. Accessed 23.02.16.

[26] MCAT Review and MCAT Prep Online. http://mcat-review.org/molecular-biology-dna.php. Accessed 23.02.16.

[27] Robertson, K. D. 2001. DNA methylation, methyltransferases, and cancer. *Oncogene* 20 (24) 3139–3155.

[28] Waddington, C. H. 2012. The epigenotype. 1942. *International Journal of Epidemiology* 41 (1) 10–13.

[29] Wu, C.-T. and Morris, J. R. 2001. Genes, genetics, and epigenetics: A correspondence. *Science* 293 (5532) 1103–1105.

[30] Fraga M.F., Ballestar E., Paz M.F., Ropero S., Setien F., Ballestar M.L. *et al*. 2005. Epigenetic differences arise during the lifetime of monozygotic twins. *Proceedings of the National Academy of Sciences of the United States of America* 102 (30) 10604–10609.

[31] Szulwach, K. E. and Jin, P. 2014. Integrating DNA methylation dynamics into a framework for understanding epigenetic codes. *BioEssays: News and Reviews in Molecular, Cellular and Developmental Biology* 36 (1) 107–117.

[32] Dupont, C., Armant, D. R., and Brenner, C. A. 2009. Epigenetics: definition, mechanisms and clinical perspective. *Seminars in Reproductive Medicine* 27 (5) 351–357.

[33] Griffith, J. S. and Mahler, H. R. 1969. DNA ticketing theory of memory. *Nature* 223 (5206) 580–582.

[34] Struhl, K. 1999. Fundamentally different logic of gene regulation in eukaryotes and prokaryotes. *Cell* 98 (1) 1–4.

[35] Cacabelos, R., Torrellas, C., and López-Muñoz, F. 2014. Epigenomics of Alzheimer's Disease. *Journal of Experimental & Clinical Medicine* 6 (3) 75–82.

[36] Wang, S.-C., Oelze, B., and Schumacher, A. 2008. Age-specific epigenetic drift in late-onset Alzheimer's disease. *PLoS One* 3 (7) e2698.

[37] Hotchkiss, R. D. 1948. The quantitative separation of purines, pyrimidines, and nucleosides by paper chromatography. *The Journal of Biological Chemistry* 175 (1) 315–332.

[38] Bird, A. 2002. DNA methylation patterns and epigenetic memory. *Genes and Development* 16 (1) 6–21.

[39] Ehrlich, M., Gama-Sosa, M. A., Huang, L.-H., Midgett, R. M., Kuo, K. C., Mccune, R. A., and Gehrke, C. 1982. Amount and distribution of 5-methylcytosine in human DNA from different types of tissues or cells. *Nucleic Acids Research* 10 (8) 2709–2721.

[40] Bird, A. P. 1986. CpG-rich islands and the function of DNA methylation. *Nature* 321 (6067) 209–213.

[41] Watt, F. and Molloy, P. L. 1988. Cytosine methylation prevents binding to DNA of a HeLa cell transcription factor required for optimal expression of the adenovirus major late promoter. *Genes and Development* 2 (9) 1136–1143.

[42] Sado, T., Fenner, M. H., Tan, S. S., Tam, P., Shioda, T., and Li, E. 2000. X inactivation in the mouse embryo deficient for Dnmt1: distinct effect of hypomethylation on imprinted and random X inactivation. *Developmental Biology* 225 (2) 294–303.

[43] Bradley-Whitman, M. A. and Lovell, M. A. 2013. Epigenetic changes in the progression of Alzheimer's disease. *Mechanisms of Ageing and Development* 134 (10) 486–495.

[44] Joo, J.-H. E., Andronikos, R. H., and Saffery, R. 2010. Metabolic regulation of DNA methylation in mammals. In *Handbook of Epigenetics: The New Molecular and Medical Genetics*, T. Tollefsbol, Ed. Elsevier Science, 281-294.

[45] Wu, J. C. and Santi, D. V. 1987. Kinetic and catalytic mechanism of HhaI methyltransferase. *Journal of Biological Chemistry* 262 (10) 4778–4786.

[46] Yang, A. S., Estécio, M. R. H., Doshi, K., Kondo, Y., Tajara, E. H., and Issa, J. J. 2004. A simple method for estimating global DNA methylation using bisulfite PCR of repetitive DNA elements. *Nucleic Acids Research* 32 (3) e38-e38.

[47] George-Hyslop, S. and Fraser, P. E. 2012. Assembly of the presenilin γ-/ε-secretase complex. *Journal of Neurochemistry* 120, s1, 84–88.

[48] Mirnics, Z. K., Calafat, J., Udby, L., Lovelock, J., Kjeldsen, L., Rothermund, K., Sisodia, S. S., Borregaard, N., and Corey, S. J. 2002. Identification of the presenilins in hematopoietic cells with localization of presenilin 1 to neutrophil and platelet granules. *Blood Cells, Molecules, and Diseases* 28 (1) 28–38.

[49] Delvaux, E., Bentley, K., Stubbs, V., Sabbagh, M., and Coleman, P. D. 2013. Differential processing of amyloid precursor protein in brain and in peripheral blood leukocytes. *Neurobiology of Aging* 34 (6) 1680–1686.

[50] Sherrington, R., Rogaev, E. I., Liang, Y., Rogaeva, E. A., Levesque, G., Ikeda, M. *et al*. 1995. Cloning of a gene bearing missense mutations in early-onset familial Alzheimer's disease. *Nature* 375 (6534) 754–760.

[51] Rogaev, E. I., Sherrington, R., Rogaeva, E. A., Levesque, G., Ikeda, M., Liang, Y. *et al*. 1995. Familial Alzheimer's disease in kindreds with missense mutations in a gene on chromosome 1 related to the Alzheimer's disease type 3 gene. *Nature* 376, 6543, 775–778.

[52] Lleó, A., Blesa, R., Queralt, R., Ezquerra, M., Molinuevo, J. L., Peña-Casanova, J., *et al*. 2002. Frequency of mutations in the presenilin and amyloid precursor protein genes in early-onset Alzheimer disease in Spain. *Archives of Neurology* 59 (11) 1759–1763.

[53] Strooper, B. de, Iwatsubo, T., and Wolfe, M. S. 2012. Presenilins and γ-secretase: structure, function, and role in Alzheimer disease. *Cold Spring Harbor Perspectives in Medicine* 2 (1) a006304.

[54] Fuso, A., Seminara, L., Cavallaro, R. A., D'Anselmi, F., and Scarpa, S. 2005. S-adenosylmethionine/homocysteine cycle alterations modify DNA methylation status with consequent deregulation of PS1 and BACE and beta-amyloid production. *Molecular and Cellular Neuroscience* 28 (1) 195–204.

[55] Wong, P. C., Zheng, H., Chen, H., Becher, M. W., Sirinathsinghji, D. J. S., Trumbauer, M. E. *et al*. 1997. Presenilin 1 is required for Notch 1 and Dll1 expression in the paraxial mesoderm. *Nature* 387 (6630) 288–292.

[56] Scarpa, S., Fuso, A., D'Anselmi, F., and Cavallaro, R. A. 2003. Presenilin 1 gene silencing by S-adenosylmethionine: A treatment for Alzheimer disease? *FEBS Letters* 541 (1-3) 145–148.

[57] Fuso, A., Nicolia, V., Pasqualato, A., Fiorenza, M. T., Cavallaro, R. A., and Scarpa, S. 2011. Changes in Presenilin 1 gene methylation pattern in diet-induced B vitamin deficiency. *Neurobiology of Aging* 32 (2) 187–199.

[58] Fuso, A., Nicolia, V., Cavallaro, R. A., Ricceri, L., D'Anselmi, F., Coluccia, P. *et al*. 2008. B-vitamin deprivation induces hyperhomocysteinemia and brain S-adenosylhomocysteine, depletes brain S-adenosylmethionine, and enhances PS1 and BACE expression and amyloid-β deposition in mice. *Molecular and Cellular Neuroscience* 37 (4) 731–746.

[59] Higgins, C. F. and Linton, K. J. 2003. ABC transporters: An introduction and overview. In *ABC proteins: from Bacteria to Man*, I. B. Holland, S. P. C. Cole, K. Kuchler and C. F. Higgins, Eds. Academic Press, XVII-XXIII.

[60] Higgins, C. F. and Linton, K. J. 2004. The ATP switch model for ABC transporters. *Nature Structural and Molecular Biology* 11 (10) 918–926.

[61] Kim, W. S., Weickert, C. S., and Garner, B. 2008. Role of ATP-binding cassette transporters in brain lipid transport and neurological disease. *Journal of Neurochemistry* 104 (5) 1145–1166.

[62] Borowski, E., Bontemps-Gracz, M. M., and Piwkowska, A. 2005. Strategies for overcoming ABC-transporters-mediated multidrug resistance (MDR) of tumor cells. *Acta Biochimica Polonica* 52 (3) 609–627.

[63] Zhao, Q.-F., Yu, J.-T., Tan, M.-S., and Tan, L. 2015. ABCA7 in Alzheimer's Disease. *Molecular Neurobiology* 51 (3) 1008–1016.

[64] Vasquez, J. B., Fardo, D. W., and Estus, S. 2013. ABCA7 expression is associated with Alzheimer's disease polymorphism and disease status. *Neuroscience Letters* 556, 58–62.

[65] Jehle, A. W., Gardai, S. J., Li, S., Linsel-Nitschke, P., Morimoto, K., Janssen, W. J., Vandivier, R. W. *et al*. 2006. ATP-binding cassette transporter A7 enhances phagocytosis of apoptotic cells and associated ERK signaling in macrophages. *The Journal of Cell Biology* 174 (4) 547–556.

[66] Quazi, F. and Molday, R. S. 2013. Differential phospholipid substrates and directional transport by ATP-binding cassette proteins ABCA1, ABCA7, and ABCA4 and disease-causing mutants. *Journal of Biological Chemistry* 288 (48) 34414–34426.

[67] Satoh, K., Abe-Dohmae, S., Yokoyama, S., St. George-Hyslop, P., and Fraser, P. E. 2015. ATP-binding cassette transporter A7 (ABCA7) loss of function alters Alzheimer amyloid processing. *Journal of Biological Chemistry* 290 (40) 24152–24165.

[68] Karch, C. M., Jeng, A. T., Nowotny, P., Cady, J., Cruchaga, C., and Goate, A. M. 2012. Expression of novel Alzheimer's disease risk genes in control and Alzheimer's disease brains. *PLoS One* 7, 11.

[69] Yu, L., Chibnik, L. B., Srivastava, G. P., Pochet, N., Yang, J., Xu, J. *et al*. 2015. Association of brain DNA methylation in SORL1, ABCA7, HLA-DRB5, SLC24A4, and BIN1 with pathological diagnosis of Alzheimer disease. *JAMA Neurology* 72 (1) 15–24.

[70] Humphries, C., Kohli, M. A., Whitehead, P., Mash, D. C., Pericak-Vance, M. A., and Gilbert, J. 2015. Alzheimer disease (AD) specific transcription, DNA methylation and splicing in twenty AD associated loci. *Molecular and Cellular Neuroscience* 67, 37–45.

[71] Schinkel, A. H., Wagenaar, E., Mol, C., and van Deemter, L. 1996. P-glycoprotein in the blood-brain barrier of mice influences the brain penetration and pharmacological activity of many drugs. *Journal of Clinical Investigation* 97 (11) 2517–2524.

[72] Langmann, T., Mauerer, R., Zahn, A., Moehle, C., Probst, M., Stremmel, W., and Schmitz, G. 2003. Real-time reverse transcription-PCR expression profiling of the complete human ATP-binding cassette transporter superfamily in various tissues. *Clinical Chemistry* 49 (2) 230–238.

[73] Lam, F. C., Liu, R., Lu, P., Shapiro, A. B., Renoir, J. M., Sharom, F. J., and Reiner, P. B. 2001. beta-Amyloid efflux mediated by p-glycoprotein. *Journal of Neurochemistry* 76 (4)1121–1128.

[74] Cirrito, J. R., Deane, R., Fagan, A. M., Spinner, M. L., Parsadanian, M., Finn, M. B., Jiang, H., Prior, J. L., Sagare, A., Bales, K. R., Paul, S. M., Zlokovic, B. V., Piwnica-Worms, D., and Holtzman, D. M. 2005. P-glycoprotein deficiency at the blood-brain barrier increases amyloid-beta deposition in an Alzheimer disease mouse model. *The Journal of Clinical Investigation* 115 (11) 3285–3290.

[75] Kuhnke, D., Jedlitschky, G., Grube, M., Krohn, M., Jucker, M., Mosyagin, I., Cascorbi, I., Walker, L. C., Kroemer, H. K., Warzok, R. W., and Vogelgesang, S. 2007. MDR1-P-glycoprotein (ABCB1) mediates transport of Alzheimer's amyloid-β peptides - Implications for the mechanisms of Aβ clearance at the blood-brain barrier. *Brain Pathology* 17 (4) 347–353.

[76] Cole, S., Bhardwaj, G., Gerlach, J. H., Mackie, J. E., Grant, C. E., Almquist, K. C., *et al*. 1992. Overexpression of a transporter gene in a multidrug-resistant human lung cancer cell line. *Science* 258 (5088) 1650–1654.

[77] Krohn, M., Lange, C., Hofrichter, J., Scheffler, K., Stenzel, J., Steffen, J. *et al*. 2011. Cerebral amyloid-β proteostasis is regulated by the membrane transport protein ABCC1 in mice. *Journal of Clinical Investigation* 121(10) 3924–3931.

[78] Schumacher, T., Krohn, M., Hofrichter, J., Lange, C., Stenzel, J., Steffen, J. *et al*. 2012. ABC transporters B1, C1 and G2 differentially regulate neuroregeneration in mice. *PLoS One* 7, 4.

[79] Lander, E. S., Linton, L. M., Birren, B., Nusbaum, C., Zody, M. C., Baldwin, J. *et al.* 2001. Initial sequencing and analysis of the human genome. *Nature* 409 (6822) 860–921.

[80] Halusková, J. 2010. Epigenetic studies in human diseases. *Folia biologica* 56 (3) 83–96.

[81] Bollati, V., Galimberti, D., Pergoli, L., Dalla Valle, E., Barretta, F., Cortini, F. *et al*. 2011. DNA methylation in repetitive elements and Alzheimer disease. *Brain, Behavior, and Immunity* 25 (6) 1078–1083.

[82] Ass.-Prof. Dipl.-Ing. Dr. Maria Zellner. *LOAD Profile*. *Development of a late-onset-Alzheimer´s disease (LOAD) profile for accurate diagnosis and identification of potential therapeutic approaches.* https:// www.meduniwien.ac.at/homepage/content/wissenschaft-forschung/drittmittelfinanzierte-projekte/eu-projekte/load-maria-zellner. Accessed 24.08.16.

[83] Clark, S. J., Harrison, J., Paul, C. L., and Frommer, M. 1994. High sensitivity mapping of methylated cytosines. *Nucleic Acids Research* 22 (15) 2990–2997.

[84] Wang, R.-H., Gehrke, C. W., and Ehrlich, M. 1980. Comparison of bisulfite modification of 5-methyldeoxycytidine and deoxycytidine residues. *Nucleic Acids Research* 8 (20) 4777–4790.

[85] Müller, H.-J. and Prange, D. R. 2016. *PCR - Polymerase-Kettenreaktion*. Springer Berlin Heidelberg, Berlin, Heidelberg, V, 1-8, 65-76, 97-100.

[86] Bio-Rad. *What is Real-Time PCR (qPCR)?* http://www.bio-rad.com/de-at/applications-technologies/what-real-time-pcr-qpcr. Accessed 14.03.16.

[87] QIAGEN. https://www.qiagen.com/at/resources/faq?id=783d4566-9ad9-4fab-9936-182beda65617&lang=en. Accessed 13.03.16.

[88] Don, R. H., Cox, P. T., Wainwright, B. J., Baker, K., and Mattick, J. S. 1991. 'Touchdown' PCR to circumvent spurious priming during gene amplification. *Nucleic Acids Research* 19 (14) 4008.

[89] Korbie, D. J. and Mattick, J. S. 2008. Touchdown PCR for increased specificity and sensitivity in PCR amplification. *Nature Protocols* 3 (9) 1452–1456.

[90] Sanger, F., Nicklen, S., and Coulson, A. R. 1977. DNA sequencing with chain-terminating inhibitors. *Proceedings of the National Academy of Sciences of the United States of America* 74 (12) 5463–5467.

[91] Ronaghi, M., Karamohamed, S., Pettersson, B., Uhlén, M., and Nyrén, P. 1996. Real-time DNA sequencing using detection of pyrophosphate release. *Analytical Biochemistry* 242 (1) 84–89.

[92] Mikeska, T., Felsberg, J., Hewitt, C. A., and Dobrovic, A. 2011. Analysing DNA methylation using bisulphite pyrosequencing. *Epigenetics Protocols*, 33–53.

[93] Gharizadeh, B., Nordström, T., Ahmadian, A., Ronaghi, M., and Nyrén, P. 2002. Long-read pyrosequencing using pure 2′-deoxyadenosine-5′-o′-(1-thiotriphosphate) Sp-isomer. *Analytical Biochemistry* 301 (1) 82–90.

[94] Harrington, C. T., Lin, E. I., Olson, M. T., and Eshleman, J. R. 2013. Fundamentals of pyrosequencing. *Archives of Pathology and Laboratory Medicine* 137 (9) 1296–1303.

[95] Ronaghi, M. 1998. DNA sequencing. A sequencing method based on real-time pyrophosphate. *Science* 281, (5375) 363–365.

[96] Sun, Y. and Xi, Y. 2014. Human leucocyte antigen matching strategy. In *HLA and Associated Important Diseases*, Y. Xi, Ed. InTech. DOI=10.5772/57500.

[97] QIAGEN. 2016. *PyroMark Q24 user manual*. https://www.qiagen.com/at/resources/resourcedetail?id=59f0275d-e60f-4517-b786-b0e0ca13952e&lang=en. Accessed 29.02.16.

[98] Reed, G. H., Kent, J. O., and Wittwer, C. T. 2007. High-resolution DNA melting analysis for simple and efficient molecular diagnostics. *Pharmacogenomics* 8 (6) 597–608.

[99] Wojdacz, T. K. and Dobrovic, A. 2007. Methylation-sensitive high resolution melting (MS-HRM): A new approach for sensitive and high-throughput assessment of methylation. *Nucleic Acids Research* 35, 6.

[100] Wojdacz, T. K., Dobrovic, A., and Hansen, L. L. 2008. Methylation-sensitive high-resolution melting. *Nature Protocols* 3 (12) 1903–1908.

[101] QIAGEN. 2009. *EpiTect HRM PCR Handbook*. https://www.qiagen.com/at/resources/resourcedetail?id=ecc4658f-5fdf-42f2-ac15-29ee25cab2a6&lang=en. Accessed 01.03.16.

[102] Kristensen, L. S. and Hansen, L. L. 2009. PCR-based methods for detecting single-locus DNA methylation biomarkers in cancer diagnostics, prognostics, and response to treatment. *Clinical Chemistry* 55 (8) 1471–1483.

[103] Northwestern University. *OligoCalc*. http://biotools.nubic.northwestern.edu/OligoCalc.html. Accessed 14.03.16.

[104] King, C. R. and Scott-Horton, T. 2007. Pyrosequencing®. *Pyrosequencing® Protocols*, 39–55.

[105] Warnecke, P. M., Stirzaker, C., Melki, J. R., Millar, D. S., Paul, C. L., and Clark, S. J. 1997. Detection and measurement of PCR bias in quantitative methylation analysis of bisulphite-treated DNA. *Nucleic Acids Research* 25 (21) 4422–4426.

[106] Mülhardt, C. 2009. *Der Experimentator: Molekularbiologie, Genomics*. Springer, 58-60.

[107] Mikkelsen, S. R. and Corton, E. *Bioanalytical Chemistry. 2004*. New Jersey, USA: John Wiley & Sons, Inc, 167, 177.

[108] Sham, P., Bader, J. S., Craig, I., O'Donovan, M., and Owen, M. 2002. DNA pooling: A tool for large-scale association studies. *Nature Reviews Genetics* 3 (11) 862–871.

[109] QIAGEN. 2012. *EpiTect Fast Bisulfite Conversion Handbook*. https://www.qiagen.com/at/resources/resourcedetail?id=15863f2d-9d1c-4f12-b2e8-a0c6a82b2b1e&lang=en. Accessed 11.12.15.

[110] QIAGEN. *EpiTect Fast DNA Bisufite Kit procedure*. https://www.qiagen.com/at/shop/epigenetics/epitect-fast-bisulfite-conversion-kits/. Accessed 02.03.16.

[111] Institute for Theoretical Chemistry, University of Vienna. *RNAfold*. http://rna.tbi.univie.ac.at/cgi-bin/RNAfold.cgi. Accessed 25.03.16.

[112] Integrated DNA Technologies. *OligoAnalyzer 3.1*. http://eu.idtdna.com/calc/analyzer. Accessed 25.03.16.

[113] Holmstrom, K. and Rasmussen, O. F. 1990. An easy method to check the efficiency of biotin end-labelling of DNA-fragments. *Nucleic Acids Research* 18 (15) 4632.

[114] QIAGEN. 2009. *PyroMark PCR Handbook*. https://www.qiagen.com/at/resources/resourcedetail?id=b8cdb9f4-c1ec-4045-83dd-468f4bf5b8fa&lang=en. Accessed 02.03.16.

[115] Environmental Protection Agency, Office of Pesticide Programs. 2000. *Assigning Values to Non-Detected/Non-Quantified Pesticide Residues in Human Health Food Exposure Assessments*.

[116] QIAGEN. 2012. *Rotor-Gene Q User Manual*. https://www.qiagen.com/at/resources/resourcedetail?id=58d4a7d9-287f-4b01-85c3-5cb83db2228b&lang=en. Accessed 02.03.16.

[117] Köhler, W., Schachtel, G., Voleske, P. 2012. *Biostatistik*. *Eine Einführung für Biologen und Agrarwissenschaftler*. Springer, Berlin, Heidelberg, 88-103.

[118] Haan, M. N., Miller, J. W., Aiello, A. E., Whitmer, R. A., Jagust, W. J., Mungas, D. *et al*. 2007. Homocysteine, B vitamins, and the incidence of dementia and cognitive impairment: Results from the Sacramento area Latino study on aging. *American Journal of Clinical Nutrition* 85 (2) 511–517.

[119] National Center for Biotechnology Information. http://www.ncbi.nlm.nih.gov/. Accessed 25.03.16.

[120] Michael Zhang Lab. 26.03.16. *Transcriptional Regulatory Element Database (TRED)*. https://cb.utdallas.edu/cgi-bin/TRED/tred.cgi?process=home.

[121] Winkler, W., Zellner, M., Diestinger, M., Babeluk, R., Marchetti, M., Goll, A. *et al*. 2008. Biological variation of the platelet proteome in the elderly population and its implication for biomarker research. *Molecular and Cellular Proteomics* 7 (1) 193–203.

[122] Tannorella, P., Stoccoro, A., Tognoni, G., Petrozzi, L., Salluzzo, M. G., Ragalmuto, A. *et al*. 2015. Methylation analysis of multiple genes in blood DNA of Alzheimer's disease and healthy individuals. *Neuroscience Letters* 600, 143–147.

[123] Carboni, L., Lattanzio, F., Candeletti, S., Porcellini, E., Raschi, E., Licastro, F., and Romualdi, P. 2015. Peripheral leukocyte expression of the potential biomarker proteins Bdnf, Sirt1, and Psen1 is not regulated by promoter methylation in Alzheimer's disease patients. *Neuroscience Letters* 605, 44–48.

[124] Bakulski, K. M., Dolinoy, D. C., Sartor, M. A., Paulson, H. L., Konen, J. R., Lieberman, A. P. *et al.* 2012. Genome-wide DNA methylation differences between late-onset Alzheimer's disease and cognitively normal controls in human frontal cortex. *Journal of Alzheimer's Disease* 29 (3) 571–588.

[125] Hernández, H. G., Mahecha, M. F., Mejía, A., Arboleda, H., and Forero, D. A. 2014. Global long interspersed nuclear element 1 DNA methylation in a Colombian sample of patients with late-onset Alzheimer's disease. *American Journal of Alzheimer's Disease and other Dementias* 29 (1) 50–53.

[126] Miklos, W., Pelivan, K., Kowol, C. R., Pirker, C., Dornetshuber-Fleiss, R., Spitzwieser, M. *et al*. 2015. beiTriapine-mediated ABCB1 induction via PKC induces widespread therapy unresponsiveness but is not underlying acquired triapine resistance. *Cancer Letters* 361 (1) 112–120.